

**Finite Element Modelling of Rheological and Penetration
Characteristics of Curing PMMA Bone Cement in Total Hip
Replacement**

By

Mohammad Mafizur Rahman, BSc Eng.

**This thesis is submitted to Dublin City University as the fulfillment of the
requirement for the award of the degree of
Doctor of Philosophy**

Supervisors

Dr. Abdul Ghani Olabi, Ph.D.

Dr. Nicholas Dunne, Ph.D.

and

Professor M.S.J Hashmi, Ph.D, D.Sc.

School of Mechanical and Manufacturing Engineering

Dublin City University

July 2006



DECLARATION

I hereby certify that this material, which I now submit for assessment on the programme of study leading to the award of *Doctor of Philosophy*, is entirely my own work and has not been taken from the work of others and to the extent that such work has been cited and acknowledged within the text of my work.

Signed: _____



Mohammad Mafizur Rahman

ID No.: 51185431

Date: _____

26/05/2006

Dedicated to my Mother, Father and Brother

ACKNOWLEDMENTS

I would like to thank to Professor M S J Hashmi for his supervision and guidance during this research work. Thanks are also expressed to Dr A G Olabi and Dr Nicholas Dunne for their supervision during this research work.

I would like to express my thanks to Mr Liam Domican, Mr Christopher Crouch, Mr Michael May and Mr Keith Hickey for their technical assistance at various stages of this work.

Finally, the encouragement of my mother, father, brothers and sisters deserve greater acknowledgement than words can express.

At last not least, all praises to almighty Creator for enabling me to complete this work.

Mohammad Mafizur Rahman

Abstract

**Finite Element Modelling of Rheological and Penetration
Characteristics of Curing PMMA Bone Cement in
Total Hip Replacement**

By
Mohammad Mafizur Rahman

This thesis is concerned with the study of the rheological properties of PMMA bone cement that is used as a grout for bone and prosthesis in THR and TKR. Interdigitation of bone cement through porous cancellous bone depends on the rheological characteristics of bone cement and porosity of the cancellous bone. The rheological characteristics of the bone cement are thus an important factor effecting the optimum penetration of bone cement through cancellous bone.

In this project the rheological properties of commercial bone cement were collected from other researchers and used in this study as the input for the finite element simulation (FIDAP simulation software) to determine the flow patterns and degree of penetration of the cement. The thermal properties of curing PMMA bone cement were measured using a standard mould at different vacuum pressures. The changes in the rheological properties with respect to time were used as the inputs to the finite element software.

The maximum temperature of bone cement was found to decrease with increasing cement mixing vacuum level for pseudoplastic bone cements. Each of the bone cements investigated has a minimum setting time at maximum vacuum mixing. The average penetration increased by increasing the prosthesis insertion velocity for pseudoplastic bone cement. The maximum pressure developed in the bone cement can be decreased significantly for pseudoplastic bone cement by increasing the prosthesis insertion velocity. No significant difference was found in the bone cement penetration when the duration of applied pressure used prior to prosthesis insertion for cement was altered. The increase in bone cement penetration was high for cement with pseudoplastic behaviour as the time of prosthesis insertion was increased from 0.5 minute to 1.5 minutes. The maximum pressure developed in the bone cement was found to decrease significantly for bone cement with pseudoplastic behaviour when the prosthesis insertion time was increased. For bone cements with pseudoplastic behaviour decreasing the amount of bone cement increases the penetration.

Definition and Nomenclature

Symbol	Definition	Dimension
Dough Time	The time after commencement of mixing at which the mixing ceases to adhere to a standard probe	s
FDA	Food and drug administration	-
IMP	Intramedullary pressure	Pa
PMMA	Polymethyl- methacrylate	-
Set time	The time at which the acrylic bone cement reaches 90-100% cure	s
THP	Total Hip Prosthesis	-
THR	Total Hip Replacement	-
τ	Shear stress	Pa
γ	Velocity gradient or shear rate	s^{-1}
η	Viscosity	Pa s
n	Power law index or flow behaviour index	-
K	Consistency coefficient	Pa s
τ_w	Shear stress at capillary wall	Pa
γ_w	Shear rate $d\gamma/dt$ at wall	s^{-1}

Contents

DECLARATION	i
DEDICATION	ii
ACKNOWLEDGMENTS	iii
ABSTRACT	iv
NOMENCLATURE	v
CONTENTS	vi
LIST OF FIGURES	x
LIST OF TABLES	xv

Chapter one Background and Introductory Materials

1 1 Total hip joint replacement (THR)	1
1 2 Commonly used implant biomaterials	4
1 2 1 Metals	4
1 2 2 Ceramics	7
1 2 3 Polymers	7
1 3 Human bone	8
1 3 1 Bone properties	8
1 3 2 Cancellous bone anisotropic permeability	11
1 4 Fixation of the stem	12
1 4 1 Cemented fixation	13
1 5 Cement/Prosthesis Interface	15
1 6 Strength of interface among bone, cement and prosthesis	16
1 7 Bone implant interface mechanics	17
1 8 Commercially available bone cements	18
1 8 1 Properties of bone cement	21
1 8 2 Polymerisation of bone cement	22
1 8 2 1 Elementary kinetics of free radical addition polymerization	25
1 8 3 Setting time of self-curing cement	26
1 8 4 Desired characteristics of bone cement	26
1 9 Hip replacement prostheses	26
1 10 Cementing technique	27

1 11 Bone cement mixing	28
1 12 Femoral pressuriser	29
1 13 Surgical technique	29
1 14 Bleeding pressure	31
1 15 Rheology of bone cement	32
1 16 Flow through porous media	35
1 17 Brief objective of the project	38
1 18 Structure of thesis	38

Chapter two Literature Review and Objective

2 1 Literature review	41
2 1 1 Mixing of bone cement	41
2 1 2 Thermal characteristics of curing acrylic bone cement	42
2 1 3 Polymerisation of bone cement	43
2 1 4 Rheological properties of bone cements	43
2 1 5 Cement pressurization and flow through cancellous bone	46
2 2 Objective and outline of the project work	51

Chapter three Experimental method and procedure

3 1 Experimental determination of thermal property	53
3 1 1 Materials	53
3 1 2 Methods	53
3 1 2 1 Mixing at different vacuum level	53
3 1 2 2 Measurement of setting properties	53
3 2 Experimental procedure for comparison of simulation	55
3 2 1 Materials and accessories	55
3 2 2 Experimental works	60
3 2 2 1 Procedure of hip replacement surgery	60
3 2 2 2 Measurement of the depth of penetration	62

Chapter four FEA of bone cement penetration in total hip replacement

4 1 Brief introduction of Finite Element Analysis	64
4 2 Model for simulation	65
4 3 Defining material properties	66

4 3 1 Material properties of bone cement	66
4 3 2 Material properties of cancellous bone	68
4 4 Boundary Condition	68
4 5 Study parameter of this project	70
4 6 Finite element analysis software	71
4 7 Solution parameters of the simulation	71
Chapter five Results, comparison and discussion	
5 1 Polymerisation study	74
5 1 1 Maximum temperature	76
5 1 2 Setting temperature	77
5 1 3 Setting time	78
5 2 2D Simulation of bone cement flow in total hip replacement	80
5 2 1 Effect of prosthesis insertion velocity	82
5 2 1 1 Penetration of bone cement through porous cancellous bone	83
5 2 1 2 Trends of penetration with respect to prosthesis insertion velocity	87
5 2 1 3 Maximum pressure developed in the bone cement	88
5 2 2 Effect of prosthesis insertion time duration	89
5 2 2 1 Penetration of bone cement through porous cancellous bone	90
5 2 2 2 Trends of penetration with respect to time taken for prosthesis insertion velocity	99
5 2 2 3 Maximum pressure developed in the bone cement	102
5 2 3 Effect of bone cement thickness	105
5 2 3 1 Penetration of bone cement through porous cancellous bone	106
5 2 3 2 Trends of penetration with respect to bone cement thickness	107
5 3 Comparison of the numerical results	108
5 3 1 Comparison experiments	109
5 3 2 Comparison using published data by previous researchers	111

5 4	Remarks on result	113
Chapter six	Conclusions and recommendations	
6 1	Findings of the study	114
6 2	Recommendations for further work	115
6 3	Contributions of the work	116
Reference		117
Appendix A	Simulation softwares	129
Appendix B	Time step and mesh density convergence	131
Appendix C	Pressure distribution figures	134
Appendix D	Example of input (log) files for the simulation	151
Appendix E	List of data tables	162
Appendix F	List of publications	169
Appendix G	CAD Drawing	170

List of figures

<u>Figure</u>	<u>Page no</u>
Figure 1-1 Schematic diagram showing the three important areas of THR	3
Figure 1-2 Schematic representation of the upper third of the tibia, an example of long bone, i c s =inner circumferential system, o c s =outer circumferential system	9
Figure 1-3 Illustration of the reinforcement of the bone cement around the prosthesis to resist radial and hoop stress on the cement mental by incorporating a wire coil	16
Figure 1-4 Syringe application of plane CMW3 and CMW3 with Gentamicin - Clinical timing and usage chart	30
Figure 1-5 Shear rate dependence of shear stress τ (left) and shear viscosity η (right) of Newtonian, shear thickening or dilatant, and shear thinning or pseudoplastic fluids and Bingham plastic time independent fluids	33
Figure 3-1 Section of the assembled PTFE mould	54
Figure 3-2 Cure temperature vs elapsed time from continuous temperature record of curing PMMA bone cement as acquired using Pico Log	55
Figure 3-3 Cadaveric femur bone	56
Figure 3-4 Exeter taper pin reamer	56
Figure 3-5 Exeter rasp	57
Figure 3-6 Exeter rasp handle	57
Figure 3-7 Femoral cement restrictor (a) one side, (b) other side	57
Figure 3-8 CMW3 bone cement	58
Figure 3-9 CEMVAC vacuum mixing system	58
Figure 3-10 CEMVAC gun system	58
Figure 3-11 CMW vacuum pump system	59
Figure 3-12 Ultraseal standard femoral pressuriser	59
Figure 3-13 Exeter V40 stem	59
Figure 3-14 Exeter stem introducer	60
Figure 3-15 Prepared femur bone to start bone cement injection	60

Figure 3-16 Treated femur bone after polymerization of bone cement for total hip replacement	61
Figure 3-17 Vertical section of treated femur bone in which prosthesis inserted after 4 minute	62
Figure 3-18 Femur bone cut at a distance of 17 cm below the femur head	62
Figure 3-19 Sectioned bone from second experiment	62
Figure 3-20 Vernier calipers used to measure the penetration of bone cement	63
Figure 3-21 Sectioned bone from second experiment with location of measurement	63
Figure 4-1 (a) Femur bone and (b) Simplified axi-symmetric model	65
Figure 4-2 Viscosity of bone cement (Pa s) as a function of Shear rate	67
Figure 4-3 Viscosity of bone cement (Pa s) as a function of elapsed time	67
Figure 4-4 The plot shows the FE model with the initial boundary conditions	69
Figure 5-1 Temperature vs elapsed time from continuous temperature record of curing CMW3 mixed at different vacuum levels	74
Figure 5-2 Temperature vs elapsed time from continuous temperature record of curing Simplex P® mixed at different vacuum levels	75
Figure 5-3 Temperature vs elapsed time from continuous temperature record of curing Palacos R® mixed at different vacuum levels	75
Figure 5-4 Maximum temperature with vacuum level for mixing pressures from atmospheric pressure to -0.7 bar	77
Figure 5-5 Cure temperature with vacuum level of mixing pressure from atmospheric pressure to -0.7 bar	78
Figure 5-6 Setting time change with vacuum level of mixing pressure from atmospheric pressure to -0.7 bar	79
Figure 5-7 The pressure (Pa) distribution with bone cement interface in pseudoplastic CMW3 bone cement at the start of simulation. A pressure (76000 Pa) applied on proximal end of femur from 3 to 5 minute and prosthesis insertion velocity 20 mm/s from 5 to 6 minute	81
Figure 5-8 The pressure (Pa) distribution with bone cement interface in pseudoplastic CMW3 bone cement at the end of simulation (720 seconds). A pressure (76000 Pa) applied on proximal end of femur from 3 to 5 minute and prosthesis insertion velocity 20 mm/s from 5 to 6 minute	81
Figure 5-9 Penetration of pseudoplastic Simplex p® bone cement through	

cancellous bone.	83
Figure 5-10: Penetration of pseudoplastic Zimmer bone cement through cancellous bone.	84
Figure 5-11: Penetration of rheopectic CMW3 bone cement through cancellous bone.	85
Figure 5-12: Penetration of rheopectic Zimmer bone cement through cancellous bone.	85
Figure 5-13: Penetration of rheopectic CMW3 bone cement through cancellous bone.	86
Figure 5-14: Penetration of rheopectic Zimmer bone cement through cancellous bone.	86
Figure 5-15: Penetration of bone cement through cancellous bone as a function of the prosthesis insertion velocity.	87
Figure 5-16: Maximum pressure as a function of prosthesis insertion velocity.	88
Figure 5-17: Penetration of pseudoplastic Simplex p® bone cement through cancellous bone at a prosthesis insertion velocity of 5 mm/s.	90
Figure 5-18: Penetration of pseudoplastic Simplex p® bone cement through cancellous bone at a prosthesis insertion velocity of 10 mm/s.	91
Figure 5-19: Penetration of pseudoplastic Simplex p® bone cement through cancellous bone at a prosthesis insertion velocity of 15 mm/s.	91
Figure 5-20: Penetration of pseudoplastic Simplex p® bone cement through cancellous bone at a prosthesis insertion velocity of 20 mm/s.	92
Figure 5-21: Penetration of pseudoplastic Zimmer bone cement through cancellous bone at a prosthesis insertion velocity of 5 mm/s.	93
Figure 5-22: Penetration of pseudoplastic Zimmer bone cement through cancellous bone at a prosthesis insertion velocity of 10 mm/s.	93
Figure 5-23: Penetration of pseudoplastic Zimmer bone cement through cancellous bone at a prosthesis insertion velocity of 15 mm/s.	94
Figure 5-24: Penetration of pseudoplastic Zimmer bone cement through cancellous bone at a prosthesis insertion velocity of 20 mm/s.	94
Figure 5-25: Penetration of rheopectic CMW3 bone cement through cancellous bone at a prosthesis insertion velocity of 5 mm/s.	95
Figure 5-26: Penetration of rheopectic CMW3 bone cement through	

cancellous bone at a prosthesis insertion velocity of 10 mm/s.	95
Figure 5-27: Penetration of rheopectic CMW3 bone cement through cancellous bone at a prosthesis insertion velocity of 15 mm/s.	96
Figure 5-28: Penetration of rheopectic CMW3 bone cement through cancellous bone at a prosthesis insertion velocity of 20 mm/s.	96
Figure 5-29: Penetration of rheopectic Zimmer bone cement through cancellous bone at a prosthesis insertion velocity of 5 mm/s.	97
Figure 5-30: Penetration of rheopectic Zimmer bone cement through cancellous bone at a prosthesis insertion velocity of 10 mm/s.	97
Figure 5-31: Penetration of rheopectic Zimmer bone cement through cancellous bone at a prosthesis insertion velocity of 15 mm/s.	98
Figure 5-32: Penetration of rheopectic Zimmer bone cement through cancellous bone at a prosthesis insertion velocity of 20 mm/s.	98
Figure 5-33: Penetration of pseudoplastic Simplex p® bone cement through cancellous bone as a function of time duration of prosthesis insertion.	99
Figure 5-34: Penetration of pseudoplastic Zimmer bone cement through cancellous bone as a function of the time taken for prosthesis insertion.	100
Figure 5-35: The penetration of rheopectic CMW3 bone cement through cancellous bone as a function of the time taken for prosthesis insertion.	101
Figure 5-36: Penetration of rheopectic Zimmer bone cement through the cancellous bone as a function of the time taken for prosthesis insertion.	101
Figure 5-37: Maximum pressure as a function of prosthesis insertion duration time for pseudoplastic Simplex p® bone cement.	102
Figure 5-38: Maximum pressure as a function of prosthesis insertion time for pseudoplastic Zimmer bone cement.	103
Figure 5-39: The maximum pressure as a function of the prosthesis insertion time for rheopectic CMW3 bone cement.	104
Figure 5-40: The maximum pressure as a function of prosthesis insertion time for rheopectic Zimmer bone cement.	105
Figure 5-41: Penetration of pseudoplastic Simplex p® bone cement through two different cancellous bone thickness at different prosthesis insertion velocity.	106
Figure 5-42: Penetration of pseudoplastic Zimmer bone cement through two different cancellous bone thickness at different prosthesis insertion velocity.	107

Figure 5-43 Penetration of bone cement through cancellous bone as a function of bone cement thickness at a prosthesis insertion velocity of 5 mm/s, 10 mm/s, 15 mm/s and 20 mm/s	108
Figure 5-44 First section from the proximal end	109
Figure 5-45 Second section from the proximal end	109
Figure 5-46 Third section from the proximal end	110
Figure 5-47 Fourth section from the proximal end	110
Figure 5-48 Fifth section from the proximal end	110

List of tables

<u>Tables</u>	<u>Page no</u>
Table 1-1 Composition of stainless steel 316L	5
Table 1-2 Physical properties of stainless steel	5
Table 1-3 Composition of cobalt-chromium alloys (ASTM F75, ASTM F90)	6
Table 1-4 Composition of titanium alloy (ASTM F136)	7
Table 1-5 Mechanical properties of Titanium alloy (Ti6Al4V)	7
Table 1-6 Mechanical properties of cortical bone	10
Table 1-7 Direction independent mechanical properties of cancellous bone	10
Table 1-8 Comparison of permeability values for cancellous bone Values are shown as mean \pm standard deviation (when applicable)	12
Table 1-9 Possible Combination of materials in total hip replacement	14
Table 1-10 Composition of Simplex® P bone cement	19
Table 1-11 Composition of Zimmer bone cement	20
Table 1-12 Composition of CMW3 bone cement	20
Table 1-13 Density of cured Bone Cements	22
Table 1-14 Depth of penetration of bone cement with shear strength from different works	37
Table 4-1 Power index and K of bone cement as a function of time	66
Table 4-2 Viscosity of rheopectic bone cement	67
Table 4-3 Physical and mechanical properties of cancellous bone	68
Table 5-1 Temperature parameters of bone cements determined using the Summit Mix in syringe® system	76
Table 5-2 Best fitting equation and R^2 values for pseudoplastic and rheopectic behaviour of bone cement	88
Table 5-3 Numerical and experimental result with percentage of error for CMW3	111
Table 5-4 Comparison of average depth of penetration with percentage error	112

Chapter one

Background and Introductory Materials

1.1 Total hip joint replacement (THR)

The age profile of the recipients of joint replacements continues to decrease, with the result that replacements are required to last for longer, and very often under higher service loads. To engineer improved implants which will increase the longevity of the arthroplasty, an understanding of the factors governing the durability of the replacement is required.

Three categories of femoral hip replacements can be described:

- (a) Cemented type I implants which rely on bone cement to maintain good fixation with both the prosthesis and the bone into which it intrudes
- (b) Cemented type II implants which rely on bone cement to maintain a good bond with the cancellous bone, but allow slip to occur along the prosthesis/cement interface
- (c) Non-cemented replacements which are dependent on the osteointegration of bone around the prosthesis for support

Both cemented type replacements fail through a combination of biological and mechanical factors which can comprise of damage accumulation in the cement mantle, dissolution or degeneration of bone tissue resulting from disease-osteolysis, failure of interfaces and sometimes through fracture of the prosthesis or supporting bone. The strength of the interlock is largely determined by the nature of the interdigitation of cement through bone. Interdigitation characteristics vary with the cancellous bone morphology, the quality and strength of bone, canal preparation techniques, the flow properties of the cement, cement mixing and insertion techniques, and the distribution of pressure during prosthesis insertion.

The prosthesis for total hip replacement consists of a femoral component and an acetabular component. The femoral stem is divided into head, neck and shaft. The femoral shaft is made of Ti alloy or CoCr alloy, (316L stainless steel can also be used

although it is used less often today), and is fixed into a reamed medullary canal by cementation or press fitting. The femoral head is made of CoCr alloy, alumina or zirconia. The acetabular component is generally made of ultra-high molecular weight polyethylene (UHMWPE).

The femoral head and acetabulum are covered by a specialized surface, articular cartilage, which allows smooth and painless motion of the joint. With hip injury or disease, articular cartilage undergoes degeneration and wears away. The joint surfaces become rough and irregular, resulting in pain and stiffness [1].

Osteoporosis is becoming one of the largest medical problems for an aged population, which leads to an enormous increase of the incidence of bone fracture. Arthroplasty is a surgical procedure widely performed throughout the world, for patients suffering from rheumatoid arthritis, arthrosis, osteoarthritis, traumatic arthritis and avascular necrosis of the hip [2, 3]. Over 800,000 hip replacements are performed annually worldwide [4]. Pioneering Orthopaedic Surgeon, Professor Sir John Charnley, revolutionised joint replacement surgery in the late 1950s and early 1960s on the advice of Dr Dennis Smith (1958) [5]. His major achievements were the development of the Charnley® Hip Replacement and the use of acrylic bone cement for prosthesis fixation.

Failure of hip prosthesis is generally due to fixation problems. Most frequent fixation problems are related to [6, 7]

- 1 Infection,
- 2 Wear and wear particulate,
- 3 Migration and failure of implants, and
- 4 Loosening especially “long-term loosening” of the implant

These problems manifest into osteolysis in the bone bed which is the major cause of long-term loosening, mostly for the femoral stem. Some major factors related to loosening are

- 1 Mismatch of the physical properties between tissues and implant
- 2 Biocompatibility of the implant
- 3 Deterioration of physical properties of implant materials
- 4 Surgical technique

- 5 Design of the implant
- 6 Selection of patients
- 7 Post surgical care

There are a large number of different types of hip joint prosthesis available. They vary depending on the materials used, the implant design and the fixation method used. Each particular type of prosthesis is designed to have a particular fixation method.

There are also numerous types of bone cement available. The outcome of the THR may depend on the type of bone cement used,

- 1 Low- vs high-viscosity,
- 2 Plain vs antibiotic impregnated, and
- 3 Low vs high heat of polymerisation cement, etc

Basically, the hip joint can be considered as three parts,

- 1 acetabular cup,
- 2 cup-femoral head-articulating surface, and
- 3 femoral stem

Figure 1-1 shows different areas of a typical total hip replacement

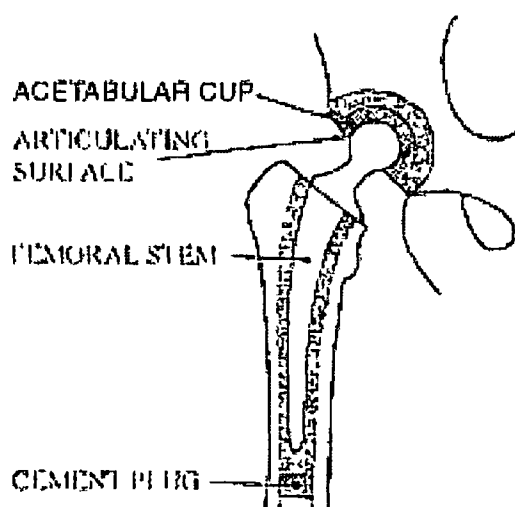


Figure 1-1 Schematic diagram showing the three important areas of THR [8]

1.2 Commonly used implant biomaterials

Metals, ceramics and polymers are used to replace bone in the human body. Metals have strength and stiffness that make them suitable for many load-bearing applications. Ceramics, compounds of metallic and non-metallic elements, have a wide range of properties that make them suitable for implantation; in particular, oxide ceramics are highly wear resistant and calcium phosphate and bioactive glass ceramics have excellent osteoconductive properties. Polymers are most often used in joint replacement prostheses. In all cases, prosthesis materials must have the required biocompatibility. In general, an implant alters the mechanical and chemical environment in its immediate neighborhood (locally) and throughout the body (systemically).

1.2.1 Metals

Metals have strength and stiffness that make them suitable for many load-bearing applications, but the problem when using metals in the body is corrosion since very few metals are in a passivated state while in vivo. Metallic implant materials are subject to several types of corrosion: galvanic, crevice, pitting, intergranular, and stress/fatigue. Only three metals are recommended for use in the body, these are, in order of increasing corrosion resistance, stainless steel, cobalt-chromium alloys, titanium and its alloys.

1. Stainless steel (usually 316L): Surgical stainless steel of specification ASTM F138 and F139 (grades 316 and 316L) achieves corrosion resistance by forming a chromium oxide (Cr_2O_3) layer on the implant surface. Nickel further improves the corrosion resistance and improves the formability of the metal for manufacturing by stabilizing a face-centered cubic crystal structure. Molybdenum is added as it increases resistance to pitting corrosion. The other elements are added to overcome manufacturing problems [9].

Low carbon content prevents chromium-carbides from depleting chromium content near the grain boundaries, which would lead to intergranular corrosion [9]. Table 1-1 shows the composition of 316L steel. A problem with stainless steel is its slow but finite corrosion rate. Crevice corrosion can also occur if two stainless steel components are in contact.

Table 1-1 Composition of stainless steel 316L [9]

Element	%
Chromium	16 00-18 00
Nickel	10 00-14 00
Molybdenum	2 00-3 00
Manganese	2 00 Max
Iron	Balance
Carbon	0 03 Max *
Silicon	1 00 Max
Phosphorus	0 045 Max
Sulfur	0 03 Max

* In 316 Carbon content is 0 08 % Max Other composition is same as 316L

The possibility of corrosion means that stainless steel is used mainly for temporary implants Table 1-2 shows physical properties of stainless steel

Table 1-2 Physical properties of stainless steel [9]

Properties	316	316L
Density (g/cm ³)	8 0	8 0
Elastic modulus (GPa)	193	193

2 Cobalt-chromium (Vitalium) alloys Cobalt-chromium displays better corrosion resistance than stainless steel It can be either cast or forged, the latter having much greater fatigue resistance [10] ASTM F-75 is the casting alloy and ASTM F-90 is the forging alloy, the latter containing tungsten and nickel for forgability The compositions of each are shown in table 1-3

3 Titanium alloys The value of titanium in biomedical application lies in its inertness in the human body, that is, resistance to corrosion by body fluids Titanium and its alloys have better corrosion resistance than stainless steel or cobalt-chromium alloy This is conferred by a TiO₂ layer on the surface There is no evidence of pitting or intergranular corrosion with titanium in the biological environment Titanium alloys are

used in biomedical applications ranging from implantable pumps and components for artificial hearts, to hip and knee implants. This alloy is becoming increasingly popular because its tensile and yield strength are as good as stainless steel 316L and cobalt-chromium alloy, but it is only half as stiff. This is potentially important because a large elastic modulus mismatch between implant and bone causes stress concentrations in some places and tends to unload the bone in others. However, the elastic modulus of titanium and its alloy is still several times greater than bone. Unalloyed commercially pure titanium is sometimes used for sintering surface layers. The alloy used is commonly called Ti-6Al-4V alpha-beta alloy. Table 1-4 shows composition and table 1-5 shows mechanical properties of Ti-6Al-4V alloy. Long and Rack [12] evaluated the physical and mechanical properties of Ti-6Al-4V alloys with respect to the long-term requirements of prosthesis, e.g., fatigue and wear.

Table 1-3 Composition of cobalt-chromium alloys (ASTM F75, ASTM F90)

Element	% (F75-92) Cast	% (F90-92) Wrought (Forged)
Chromium	27.00-30.00	19.00-21.00
Nickel	1.00 max	9.00-11.00
Molybdenum	5.00-7.00	-
Tungsten	-	14.00-16.00
Manganese	1.00 max	1.00-2.00
Silicon	1.00 max	0.40 max
Iron	0.75 max	3.00 max
Carbon	0.35 max	0.05-0.15
Phosphorus	-	0.040 max
Sulfur	-	0.030 max
Cobalt	Balance	Balance

Elastic Modulus 200-230 GPa, Density 7.8 g/cm³ in cast /annealed condition [11]

Table 1-4 Composition of titanium alloy (ASTM F136)

Element	%
Aluminum	5.5-6.5
Vanadium	3.5-4.5
Iron	0.25 max
Titanium	Balance
H, C, O, N	Trace amounts

Table 1-5 Mechanical properties of Titanium alloy (Ti6Al4V) [13]

Density (g/cm ³)	4.43
Average Modulus of elasticity (GPa)	113.8
Poisson's ratio	0.342

1.2.2 Ceramics

There are three categories of ceramics used to replace bone

- 1 The first is structural ceramics (alumina, Al_2O_3 , and zirconia, ZrO_2). These have higher stiffness and hardness than metals and much better wear resistance. Both alumina and zirconia are used for heads of hip prostheses [83].
- 2 The second category of ceramic used to replace bone is calcium phosphate. Hydroxyapatite (HA), $[\text{Ca}_{10}(\text{PO}_4)_6(\text{OH})_2]$, is a calcium phosphate that is found naturally in bone. Another calcium phosphate is tricalcium phosphate (TCP), $[\text{Ca}_{10}(\text{PO}_4)_6]$. TCP biodegrades more quickly than HA. Calcium phosphates have useful osteoconductive properties and are used to coat metallic implants that aim to bond to the bone by osseointegration [83].
- 3 The third category of ceramic is bioactive glass [83].

1.2.3 Polymers

A wide range of polymers are used for implantable devices. The first category is polymers with no cross-linking of polymer chains- called thermoplastics. Well-known examples of thermoplastics are polyethylene (PE) and polymethylmethacrylate (PMMA). Ultrahigh-molecular-weight polyethylene (UHMWPE), polyacetal,

polyetheretherketone (PEEK) and polytetrafluoroethylene (PTFF) have been used as components in hip replacement prostheses [83] The second category is polymers with heavy cross-linking of polymer chains (called thermoset), e g , polyester (PET) is used in the augmentation of the soft tissues in the musculoskeletal system [83]

Polymethylmethacrylate (PMMA) is used in orthopedic bone cement The Young's modulus of PMMA is 0.018-0.033 Pa [14] and the Poisson's ratio is 0.4-0.43 [14] Bone cement serves to interlock the prosthetic component to the bone Polymerisation takes place during the mixing of the powder and liquid components, which is carried out in the operation theatre The mixing process is critical as it determines the porosity of the cement and thus its strength

1.3 Human bone

Bone is a composite of the calcium phosphate hydroxyapatite ($\text{Ca}_{10}(\text{PO}_4)_6(\text{OH})_2$) [67], (about 43 percent by weight), and type I collagen (about 36 percent by weight) It also contains about 14 percent water and a small amount of mucopolysaccharides, or ground substance [15] The primary determinant of its mechanical properties is its porosity Cortical or compact bone is about 90 percent solid bone tissue, spongy or trabecular bone is 80-90 percent cavities filled with marrow [15] Bone is demonstrably viscoelastic, but it can usually be modelled as a brittle solid Bone usually has a lamellar structure Like most biological materials, bone behaves as an anisotropic, nonhomogeneous, viscoelastic material [11] Figure 1-2 shows structure of a long bone

1.3.1 Bone properties

Bone is a highly heterogeneous tissue, its composition and structure both vary in a way that depends on the skeletal site, physiological function, the age and sex of subjects, and the type of vertebrate species

There are many reasons of the variations of the bone properties [16, 17]

1. Different treatment of specimens: dry bone is stiffer, stronger, and considerably more brittle than wet bone. Very small samples produce values for stiffness and strength less than those from larger samples.
2. Differences between bones by location in the body.
3. Different age and health of donors.

There are three ways of testing bone. [16]

1. Mechanically by relating stresses to strains.
2. The ultrasonic technique used to measure elastic properties by subjecting the bone to ultrasound and measuring the velocity of shear and longitudinal wave propagation in particular directions in the bone specimens.
3. An alternative to mechanical tests, micro-finite-element (μ FE) analyses to calculate the elastic constants of bone specimens directly from computer models [22, 31].

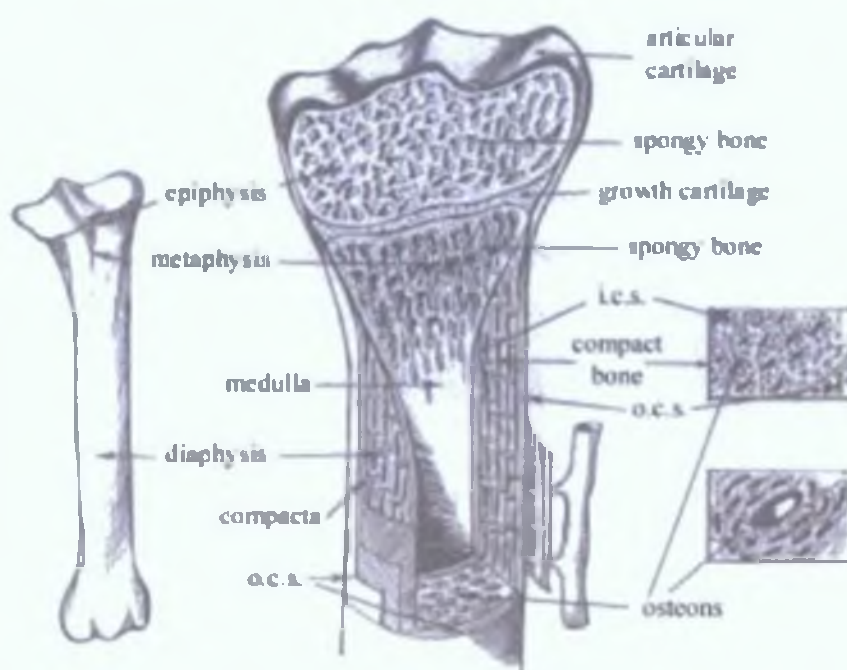


Figure 1-2: Schematic representation of the upper third of the tibia, an example of long bone; i.c.s.=inner circumferential system; o.c.s.=outer circumferential system. [18]

Cortical bone is a solid, compact tissue constituting the diaphyses of long bones and outer shell of the metaphyses. At a tissue level, human cortical bone consists of secondary osteons (100 to 300 μ m in diameter) surrounding Haversian canals and

embedded in interstitial tissue [19, 20] Each osteon is made of concentric lamellae (1 to 5 μm thick) [21, 22] Table 1-6 shows mechanical properties of cortical bone Y H An [23] has collected the mechanical properties of cortical bone Bone tissue modulus is related to density/porosity, mineral content and microstructural features such as lamellar orientation, lacunae and cement lines

Table 1-6 Mechanical properties of cortical bone

Wet density (kg/m^3)	Elastic modulus (GPa)	Poisson's ratio	Tensile strength (MPa)
1990	20 [15], 14.7-34.3 (Average 23 \pm 4.8) [24-26]	0.22-0.42 [24, 25]	200 [15]

Cancellous bone is a porous type of tissue mainly found near the ends of long bones and in vertebral bodies In long bones, it distributes the mechanical loads from the articular surfaces to the cortical shaft, whereas in vertebral bodies it is the main load-carrying constituent Cancellous bone is a biphasic structure consisting of a continuous three-dimensional network of interconnected rods and plates (trabecular solid) and a pore space filled by a viscous fluid phase The hydraulic nature of this fluid-solid interaction enhances the tissue's load bearing capacity [27, 28] Bone marrow viscosity falls in the range of 0.04-0.4 Pa s at 37°C [29] Bone fractures due to conditions such as osteoporosis usually occur in cancellous bone regions

Mechanical behavior of cancellous bone is best described as viscoelastic [30] For strain rates as they occur during normal activities having frequencies ~ 1 Hz, cancellous bone can be well described as an elastic material [31] The elastic modulus of cancellous bone is anisotropic The mechanical properties of cancellous bone are quite structure dependent [32-34] Table 1-7 shows direction independent mechanical properties of cancellous bone

Table 1-7 Direction independent mechanical properties of cancellous bone [35]

Apparent density (kg/m^3)	Average elastic modulus (MPa)	Poisson's ratio
140-1110 (Average 620)	10 – 1570	0.4

Little is known about the time dependent viscoelastic properties of bone, including creep and fatigue. As a result, most finite element analyses are based on the assumption that the mechanical behavior of cancellous bone has no time dependency [35]

1.3.2 Cancellous bone. anisotropic permeability

Several researchers have quantified the intrinsic permeabilities of cancellous bone based upon Darcy's Law describing flow through porous media. Porosity, the ratio of void volume to total volume, and architecture are the two most important variables for determining the intrinsic permeability of cancellous bone. There are few problems associated with the measurement of cancellous bone permeability [36]

1. **Range of porosity** One problem associated with the measurement of permeability of cancellous bone is that the tissue displays a wide range of porosity. Darcy's law is applicable only to a range of seepage velocity. This range is characterized by the Reynolds number of fluid for the porous medium.
2. **Specimen Size** The size of the specimen must be large enough to allow the microscopic heterogeneity of the trabeculae to be ignored, but small enough to avoid including macroscopic variation of the cancellous bone density. These measurements suggest that a cancellous bone specimen approximately 5 to 8 mm is required for testing [36].
3. **Shape of Fluid Channel** There should be a correlation between the porosity of a material and its permeability. However, previous attempts to correlate these two material properties have failed to produce any convincing results [36]. It has been suggested that this failure is due to the inability of the porosity measurement to describe the shape of the voids or channels through which the fluid must filter. Histological investigations indicate that cancellous bone displays no such void shape consistency when samples are taken from different species or anatomical sites. Thus, to get porosity/permeability correlation for cancellous bone samples should be taken from the same anatomical site of the same species.

Table 1-8 shows the permeability values for cancellous bone at different orientation found by different researchers.

Table 1-8: Comparison of permeability values for cancellous bone. Values are shown as mean \pm standard deviation (when applicable)

Study	Species, Anatomic site	Orientation	Permeability ($\times 10^{-10} \text{ m}^2$)
Kohles et al. (2001) [38]	Bovine, Distal femur	Superior-inferior	4.65 \pm 3.50
		Anterior-posterior	4.52 \pm 2.74
		Medial-lateral	2.33 \pm 1.55
Lim and Hong (2000) [39]	Bovine, Vertebral body	Cephalad-caudal	1.63 \pm 0.80
Nauman et al. (1999) [40]	Human, Vertebral body	Longitudinal	80.5 \pm 47.5
		Transverse	35.9 \pm 19.0
	Human, Proximal femur	Longitudinal	27.6 \pm 19.1
		Transverse	1.2 \pm 1.1
	Bovine, Proximal tibia	Longitudinal	31.7 \pm 10.2
		Transverse	7.4 \pm 8.3
Grimm and Williams (1997) [29]	Human, Calcaneus	Medial-lateral	35.4 \pm 25.7 (22 Samples)
Hui et al. (1996) [41]	Rabbit, Proximal tibia	Medial-lateral	0.49 \pm 0.30
		Anterior-posterior	0.59 \pm 0.10
Beaudoin et al. (1991) [42]	Human, Proximal tibia	Superior-inferior	78.4 \pm 36.2

The hydraulic permeability of the bone, while injecting the cement, depends on bone porosity and changing cement viscosity, which is time and shear-rate dependent.

1.4 Fixation of the stem

The development of a permanent fixation mechanism of implants to bone has been one of the most formidable challenges in the evolution of joint replacement. The fixation methods are largely divided into four categories [43]

1. Mechanical Fixation

a. Active-use of Screws, bolts, nuts, wires, etc.

- b Passive-interference fit and non-interference fit
- 2 Bone Cement Fixation
 - a Pure cement
 - b Modified cement-composite cement
- 3 Biological Fixation
 - a Porous ingrowth
 - b Modified porous ingrowth-electrical and pulsed electromagnetic field (PEMF) stimulation
- 4 Direct (Chemical) Bonding Fixation
 - a Osteogenic/inductive-glass-ceramics
 - b Osteoconductive hydroxyapatite

A previous study revealed that a better surgical outcome could be achieved where cements were used regardless of the various factors involved, such as types of implants, materials, patients, etc [8]

Any stiff material contacting the surface of the bone will cause bone density change due to the altered stress pattern and bone lysis due largely to the particulate generated at the articulating surface between the acetabular cup and femoral head [151] The initial mode of failure of the femoral prosthesis is the debonding of the stem/bone cement interface followed by osteolysis at the distal end of the stem where the particulate may accumulate by gravity [44] Most of the osteolysis is located in the distal and proximal end of the prosthesis [5] The aseptic loosening of the implants, which in turn causes the accelerated wear of the UHMWPE acetabular cup, can accelerate the osteolysis [5]

1 4 1 Cemented fixation

Cemented prostheses are by far the most common Bone cement is used to fill cavities and distribute the forces exerted on the bone and the prosthesis Although the introduction of advanced surface treatments for metal implants has established a place for cementless fixation, the use of acrylic cement remains the most widely used method of implant fixation

The cement is forced down the track of the medulary canal as a stiff dough and the insertion of the point of the tapered stem of the prosthesis expands the stiff dough and injects it into the cancellous lining of the marrow space. Because the cement is stiff it does not escape proximally round the prosthesis. Though there is no adhesion between the polished surface of the prosthesis and the cement, the tapered shape of the prosthesis is very suitable for weight transmission since it will get tighter under load [45].

Some believe [45] that the strengthening of the bone cement may not be beneficial to the enhancement of the fixation due to the unfavourable stress distribution. On the other hand, the bone cement is the weakest link between bone and prosthesis. Failure of the bone cement itself and interface loosening between cement and stem may be large contributing factors toward the failure of the fixation of the prosthesis. Possible combination of materials in total hip replacement is shown in table 1-9. [46]

Table 1-9: Possible combination of materials in total hip replacement.

FEMORAL COMPONENT			ACETABULAR COMPONENT		
FIXATION	STEM	BALL	CUP	BACKING	FIXATION
PMMA	CoCr alloy	CoCr alloy	CoCr alloy	PMMA	
Bone		Alumina	UHMWPE	Metal	Screw, or
Ingrowth		Zirconia	Alumina	None	press fitting
Press fitting	Ti alloy				Bone
					Ingrowth

In spite of many drawbacks of bone cement, the survival probabilities of implanted cemented arthroplasties, especially those of the hip and knee in patients aged over 50 years, are very high, averaging at least 90% after 15 years [47]. Improvements in the surgical and cementing techniques and in prosthesis design will result in better success rates and fewer re-operations.

1 5 Cement/Prosthesis interface

The primary function of the bone-implant interface is to provide a safe and effective load transfer from the prosthesis to the bone. Bone cement fixation creates two interfaces

- 1 Cement-bone
- 2 Cement-implant

According to Amstutz et al [48], the incidence of loosening for the femoral prosthesis were evenly divided at about 10% and 11% for cement-bone and cement-implant interfaces respectively. It has been reported that the initiation of loosening of the cemented femoral components originates from the prosthesis-cement interface, especially the pores trapped between them [44]. Pre-coating with bone cement or polymethylmethacrylate polymer can minimize the cement implant interface loosening [49-53]. Pre-coating can achieve good bonding between the “cement” and prosthesis during the manufacturing process. During surgery, the fresh cement adheres well to the pre-coated cement [52, 54].

The high strains or stresses on the cement at the tip of the prosthesis are strong indications that this location is a likely site for the initial event of failure [55].

Placement of reinforcing material around the stem enhances the cement/prosthesis interface strength to resist the radial and hoop-stress caused by body loading. A coil or mesh of wire conforming to the contours of the prosthesis could be placed prior to bone cement injection during surgery as can be seen in figure 1-3.

Orthopedic surgeons often suggest that the fixation of implants should not be too strong since it would be difficult to remove, should it become necessary to have a revision arthroplasty to restore its function. The two requirements could be mutually exclusive since the interface must be strong enough to hold the prosthesis in vivo but not so strong that it may impair any remedial measures.

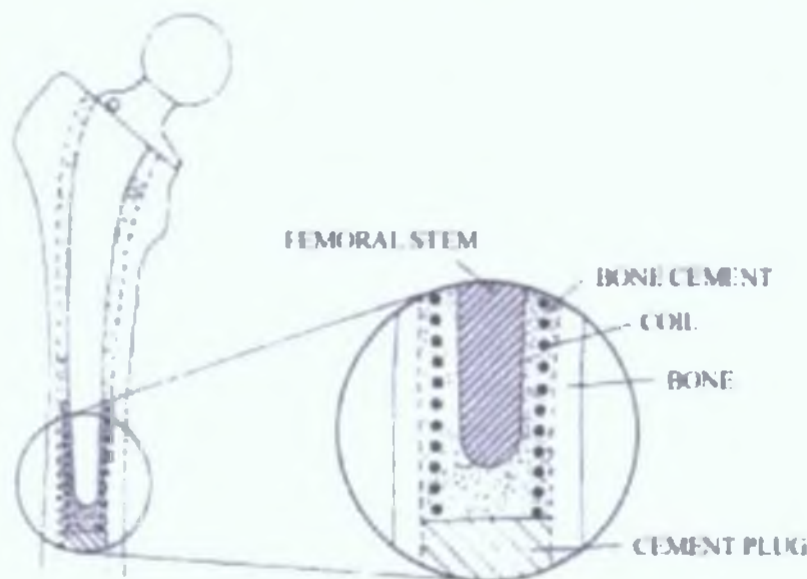


Figure 1-3: Illustration of the reinforcement of the bone cement around the prosthesis to resist radial and hoop stress on the cement mental by incorporating a wire coil [56].

1.6 Strength of interface among bone, cement and prosthesis

Implant surface configuration, implant surface coatings for cementless prosthesis, implant geometry, material properties of the implant, quality of cement and cementing techniques, which have gone through several generations of improvement, are the most important factors that affect the strength of the bone-implant interface.

Due to the interdigitation of cement through the bone, there is not a single bone-cement interface. Instead, there is a composite region of cancellous bone and cement which interfaces with cancellous bone on one side and with cement on the other. The size of the composite region has a direct effect on the strength of the bone-cement interface [57-59]. Increasing the amount of PMMA penetration into the cancellous bone improves the mechanical interlock between bone and cement, this leads to an increase in the interface shear strength. In addition, the fracture toughness of the interface is improved with increased interdigitation [60]. A positive relationship between the bone strength and interface shear strength has been shown [57].

It has been demonstrated that bone density is the most significant factor affecting the interface shear strength. A specimen with low bone density and good cement

penetration may have a lower interface shear strength than a sample with higher bone density and less cement penetration [59] However, for a given bone density, increasing the cement penetration increases the interface shear strength

An increase in cement depth does not directly mean an increase in interface strength The ultimate interface strength is always limited by the intrinsic strength of the bone [49] Weak bone with large porosity will allow deep penetration, but the cement/bone composite will fail easily at the composite/bone interface due to low bone strength Dense bone will not easily be penetrated and with decreased penetration a large fraction of a fracture interface will show non-penetration [62]

Cement pressure is accepted as a significant parameter in determining the strength of cement/bone interfaces and hence preventing loosening of the prosthesis Heyse-Moore and Ling [61] found that the level of effective penetration and ultimately the success of the hip replacement is a function of the intramedullary pressure (IMP) generated in the femoral cavity, which is determined by the method of mixing the bone cement, time and technique of introducing the acrylic cement during the polymerisation and the design of the implant

The implant should fill at least 80% of the cross section of the medullary canal with an optimal cement mantle of 4 mm proximally and 2 mm distally [62]

1 7 Bone implant interface mechanics

In a cemented joint arthroplasty, the main function of the bone cement is to transfer joint loads from the prosthesis to the bone The bone-cement interface plays a primary role in this process [63] Normal and shear loads are transferred to the bone by developing and maintaining a mechanical interlock between the cancellous bone and bone cement [64] Locally, the strength of the interface materials and the bond between them must be able to withstand the stresses that occur during the load transmission [65] The pattern of local stresses depends on the magnitude and direction of the load and the geometry of the involved site as well as the interface materials

It has been shown [66] that for a given load and geometry, and assuming that the two contacting materials have the same Poisson's ratio, the maximum principal and shear stresses follow the proportionality

$$\sigma_{\max}, \tau_{\max} \propto \left(\frac{1}{E_1} + \frac{1}{E_2} \right)^{-2/3} \quad (1-1)$$

As is apparent, reducing the elastic modulus of either material produces a reduction in the contact stresses between the two materials. Physically, with contact deformation, as the elastic modulus decrease, the contact area will increase for a given load [68]. This distributes the load over a larger area, lessening the contact stresses.

Yetkinler [69] in 1994 then Yetkinler and Litsky [70] in 1998 investigated the viscoelastic properties of a reduced-modulus bone cement, poly(butyl methyl methacrylate) (PBMMMA) and standard polymethylmethacrylate, PMMA, bone cement using unconstrained stress relaxation experiments. Their results illustrate the elastic nature of PMMA specimens and the viscoelastic nature of PBMMMA specimens. PMMA becomes brittle after curing and PBMMMA showed more viscoelastic behaviour and greater ability to recover from strains when the load is released. Considering the reduced-modulus of the PBMMMA it can be used as an alternate to PMMA bone cement. Rheological and penetration properties of PBMMMA bone cement can be studied along with penetration property of PMMA bone cement.

1.8 Commercially available bone cements

Bone cements have no adhesive properties but rely on close mechanical interlock between the irregular bone surface and prosthesis, allowing even distribution of weight and stress between prosthesis and bone. Bone cement has been used for clinical applications to secure a firm fixation of joint prosthesis for hip and knee joints, and to infiltrate and reinforce osteoporotic vertebrae (**Vertebroplasty**). It is primarily made of PMMA powder and liquid monomer methyl methacrylate. There are different types of bone cement commercially available.

They can be classified as being either:

- 1. Non-bioactive bone cement-Bone cement manufactured without any bioactive agent.
- 2. Bioactive bone cement- Bioactivation of PMMA bone cement by using bioactive fillers may also strengthen bone-cement interface. Antibiotic bone cement decreases the infection after arthroplasty, particularly revision arthroplasty.

The compositions of three different bone cements are as follows:

- 1. **Surgical Simplex P®** radiopaque bone cement is manufactured by Howmedica Int. Ltd. It contains 40g of pre-polymerised powder and 20 ml of monomer liquid in each packet. The liquid component is sterilised by membrane filtration and the powder component is sterilised by gamma irradiation [71]. Table 1-10 shows the composition of surgical simplex P® bone cement. At the time of use the powder and liquid are mixed, resulting in the exothermic formation of a soft, pliable, dough-like mass. As the reaction progresses, within a few minutes a hard, cement-like complex is formed.

Table 1-10: Composition of Simplex P® bone cement [71-73]

Liquid component (20 ml)	Volume (ml)	Volume or weight (%)
Methyl methacrylate (monomer)	19.5	97.5
N,N-dimethyl para toluidine (accelerator)	0.5	2.5
Hydroquinone (inhibitor)	1.5 mg	75±15 ppm
Solid powder component (40g)	Weight (g)	
Methyl methacrylate-styrene copolymer (for strength)	30.0	75
Poly methyl methacrylate	6.0	15
Barium Sulphate (BaSO ₄ contrast medium or radiopacifier)	4.0	10
Benzoyl peroxide (initiator/activator)	0.6	-

- 2. **Zimmer** radio-opaque bone cement is produced by Osteobone. Each packet contains 40.0g of polymer powder and 18.8 g of monomer liquid. The liquid

monomer is sterile filtered and the powder polymer is sterilised by ethylene oxide [74] Table 1-11 shows the composition of Zimmer bone cement

Table 1-11 Composition of Zimmer bone cement [73, 74]

Liquid component (18.8 g)	Weight (g)
Methyl methacrylate (monomer)	18.28
<i>N,N</i> -dimethyl para toluidine (accelerator)	0.52
Hydroquinone (inhibitor)	80 ppm
Solid powder component (40.8 g)	Weight (g)
Poly (methyl methacrylate)	35.70
Barium sulphate (BaSO ₄ , contrast medium or radiopacifier)	4.00
Benzoyl peroxide (initiator/activator)	0.32

3 **CMW3** Bone cement is manufactured by DePuy International Ltd. Each packet contains 40 g of sterile powder and 17.90 g of sterile liquid. It is a medium viscosity cement designed with easy syringing in mind for total knee replacement, THR and all other joints. It is available with and without antibiotics (Gentamicin). Table 1-12 shows the composition of CMW3 bone cement.

Table 1-12 Composition of CMW3 bone cement [73, 75]

Liquid component (17.9 g) (19.04 ml)	Weight (g)
Methyl methacrylate (monomer)	17.45
<i>N,N</i> -dimethyl para toluidine (accelerator)	0.45
Hydroquinone (inhibitor)	25 ppm
Solid powder component (40 g)	Weight (g)
Polymethyl Methacrylate/Methyl methacrylate	35.2
Barium Sulphate (BaSO ₄ , contrast medium or radiopacifier)	4
Benzoyl peroxide (initiator/activator)	0.8

Monomer/powder ratio of these commercial bone cements is about 0.5. This provides an optimum balance between viscosity and monomer release [77]. Hydroquinone is

added to prevent premature polymerisation, which may occur under certain conditions, e.g. exposure to light or elevated temperatures. *N,N*-dimethyl para toluidine is added to promote or accelerate cold curing of the finished cement. The term cold curing is used here to distinguish it from high temperature and pressure curing used to make articles in dental laboratories. The liquid component is sterilised by membrane filtration. The solid component is a finely ground powder (mixture of PMMA, activator, radiopaque agent and sometimes colouring agents). Bone cements containing barium sulphate (BaSO_4) are less abrasive against stainless steel surfaces than bone cements containing zirconium oxide (ZrO_2). [76].

There are other commercial bone cements such as Palacos R®, Zimmer LVC and Sulfix. Commercially available bone cements with their composition, physical and chemical properties were listed by Kuhn [73].

1.8.1 Properties of bone cement

There are a number of major drawbacks related to the use of PMMA bone cement. These include [78, 72]:

1. **Thermal necrosis:** Thermal necrosis of the bone occurs due to the high exothermic temperature of the cement, which is between 67 and 124 °C at the centre of the cement mantle in vivo (depending on the cement formulation). It is postulated that this thermal necrosis of the bone impairs local blood circulation and causes membrane formation at the cement-bone interface.
2. **Chemical necrosis:** Chemical necrosis of the bone by cement is postulated to be due to the release or leakage of unreacted monomer (MMA) liquid before polymerisation of the cement in the bone bed.
3. **Shrinkage** of the cement occurs during polymerisation.
4. Poor cement distribution around the implant.
5. The large **stiffness mismatch** between the cement and the bone.
6. The identification of the cement mantle, the implant-cement interface, and the cement-bone interface to be the three "**weak-link zones**".
7. The **cement particles** can interact with the surrounding tissues, evoking inflammatory periprosthetic tissue responses and increasing bone destruction.

Despite these drawbacks Poly methyl methacrylate (PMMA) is currently used in commercial bone cement. It is a self-polymerizing amorphous polymer. Approximately 70% by weight, of the polymer consists of pre-formed polymeric beads, with the remainder of the polymer being formed by chemical and physical reactions upon mixing. The glass-transition temperature of PMMA is 114°C. As an amorphous polymer it is glassy below its glass-transition temperature. Thus at body temperature (37°C), PMMA fractures in a brittle manner [102]. Table 1-13 shows the density of three commercial bone cements.

Table 1-13 Density of cured Bone Cements [79]

Properties	Simplex P®	Palacos R	CMW3
Density (g/cm ³)	1.23	1.23	1.24

The physical properties of uncured bone cement are important in determining handling and mixing characteristics, penetration of the cement into bone, cement porosity, and thus, strength of the bone-cement-prosthesis interface. The physical property of most importance is the rheology of the cement.

Cement is a grout not a glue [80]. It is very important to understand that bone cement is not an adhesive, nor is it a bone filler. It is a grout and to be effective, it must penetrate the uneven surface and porous spaces in the prepared bone. As the cement hardens this interdigitation of cement into bone results in a load bearing micro interlock that is capable of stabilising the implant over a prolonged period.

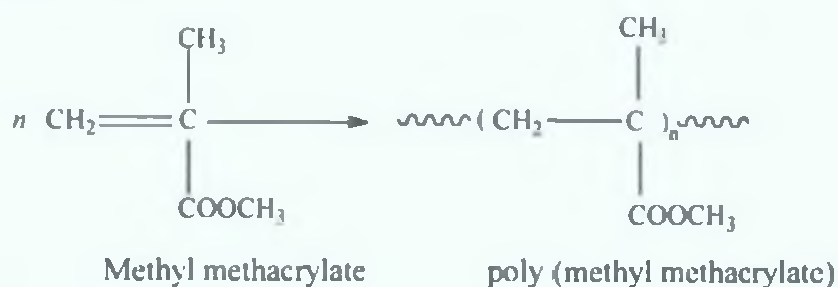
1.8.2 Polymerisation of bone cement

The process of joining the monomer together is called polymerisation and number of these units in the long molecules is known as the degree of polymerisation. There are different kinds of polymerisation.

- 1 **Addition polymerisation** Bone cement polymerisation is completed by this mechanism. It is also known as free radical polymerisation [81].
- 2 **Condensation polymerisation** In this process each group reacts with other groups and eliminates water or some other compounds.

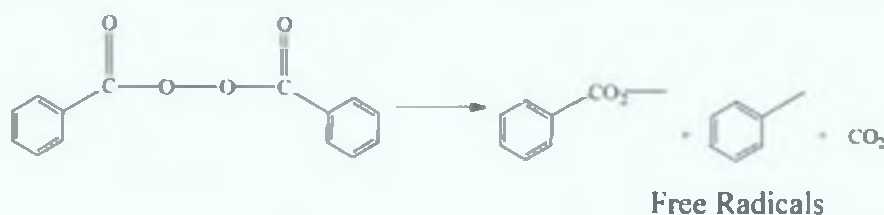
3. **Rearrangement polymerisation:** In many respects it is intermediate between addition and condensation polymerisations.

In **addition polymerisation** low molecular weight molecule, referred as a monomer, which possesses a double bond, is induced to break the double bond and the resulting free valences are able to join up to other similar molecules. In these cases the monomer is converted into polymer, and no side products are formed. This approach is used with the majority of thermoplastics materials, such as poly methyl methacrylate (a polymer of methyl methacrylate).



Addition polymerisation is effected by the activation of the double bond of a monomer thus enabling it to link up to other molecules. It has been shown that this reaction occurs in the form of a chain addition process with initiation, propagation and termination steps.

The **initiation stage** may be activated by free radical or ionic systems. In this stage, a material can be made to decompose into free radicals on warming, by irradiation with ultra violet light or in the presence of a promoter that is added to the monomer and radicals are formed. In the above mentioned commercial bone cements such material is benzoyl peroxide which decompose as indicated in the following reaction [82]



Such free radical formation may be generally indicated as



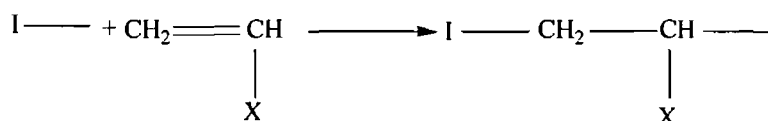
The rate of formation of radicals will depend on a number of features [82]

1. The concentration of initiator

2 Temperature

3 The presence of other agents

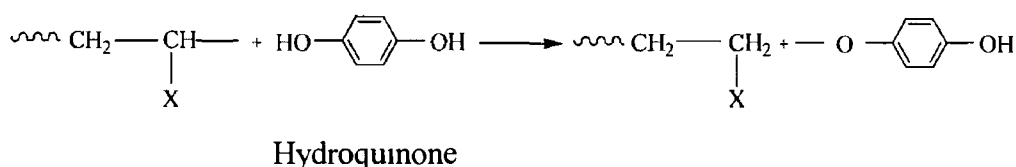
The radicals formed may then react with a monomer molecule by addition, producing another radical



This radical then reacts with a further molecule of monomer, generating yet another free radical of the same order of reactivity

This reaction may then repeat itself many times so that several thousand monomer units are joined together in a time of the order of 1 second, leading to a long chain free radical. This is the **propagation or growth stage**

There are materials available that completely prevent chain growth by reacting preferentially with free radicals formed to produce a stable product. These materials are known as inhibitors, an example is hydroquinone. This is the **Termination stage**



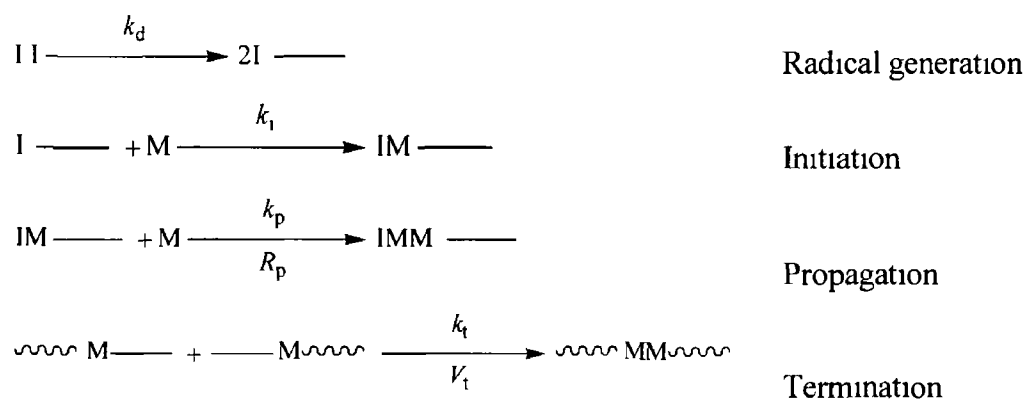
These materials are of particular value in preventing the premature polymerisation of monomer whilst in storage, even during manufacturing

It is frequently possible to polymerise two monomers together so that residues from both monomers occur together in the same polymer chain. In addition polymerisation normally occurs in a somewhat random fashion and the product is known as a binary copolymer or simply **copolymer**. It is possible to copolymerise more than two monomers together and in the case of three monomers the product is referred to as a ternary copolymer or terpolymer. The term homopolymer is sometimes used to refer to a polymer made from a single monomer.

Mixing of prepolymerised powder and monomer liquid forms acrylic bone cements. In the initiation stage of the polymerisation, the liquid component containing the accelerator (*N,N*-dimethyl-*p*-toluidine) is mixed with solid component containing the activator benzoyl peroxide, which decomposes to produce the free radicals under 25°C, which, in turn, react with monomer molecules to form active centres [114]. The active centres will then attack another monomer to form a dimer radical. The process will continue until long chain molecules are produced in the propagation stage of the polymerisation. When the concentration of the liquid is depleted, the viscosity of the system increases. Termination becomes more difficult as the growing chains are unable to diffuse and this makes it difficult for two chain ends to meet [114].

1.8.2.1 Elementary kinetics of free radical addition polymerisation

In a simple free radical initiated addition polymerisation, the principal reactions involved are [72, 82]



where M, I, M \cdot and I \cdot indicate monomers, initiators and their radicals respectively, each initiator yielding two radicals. All k are rate constants. The suffixes denote different steps of the polymerisation reaction.

The kinetics of the polymerisation reaction can be represented as a first order reaction [72]

$$R_p = k[M] \quad (1-2)$$

$$\text{where, } k = k_p \left(2f \frac{k_d}{k_t} [I] \right)^{1/2} \quad (1-3)$$

The equation indicates that the reaction rate is proportional to the square root of the initiator concentration and to the monomer concentration

1 8 3 Setting time of self-curing cement

The polymerisation reaction speed, after the mixing of the liquid and powder, is controlled by methods of manufacture and depends on a number of factors such as, molecular weight of the polymer, texture of the powder, proportion of activator and initiator, proportions of liquid and powder, ambient temperature and humidity [45]

1 8 4 Desired characteristics of bone cement

The ultimate goal in joint fixation is the achievement of a homogenous, pore-free grout, which hardens to form a strong anchoring material capable of holding the implant in place and evenly transferring forces to the surrounding bone [78]

1 9 Hip replacement prostheses

Hundreds of different designs of hip joint prostheses are currently on the market. They may be broadly classified into cemented or cementless devices, with fixation in the former achieved by cementing with PMMA bone cement and in the latter by osseointegration. If cement is used for the femoral side and cementless fixation for the acetabular side, the implant is a "hybrid" design [83]

Variations in prosthesis design include the size of the prosthesis head. Charnley [45] described the effect of head size; he proposed a small head because it would create a lower frictional torque than a larger head and thus reduce the potential for loosening. However, smaller heads apply greater contact stresses on the polyethylene cup. The size of the head and geometry of the neck determine the range of motion of the reconstruction. For a given neck geometry, a large head size will permit a greater range of motion of the artificial joint. As wear progresses, the head penetrates the acetabular cup, decreasing the range of motion. For these reasons, head diameter is a crucial design variable for which a compromise is required.

For cemented femoral stems, the stem cross-sectional shape determines the stress concentrations in cement, circular cross sections minimize stress concentrations but have the lowest resistance to slip within the cement mantle. Stem shape also affects the pressure generated within the bone cement and, therefore, the interdigitation of the bone cement with the cancellous bone. Another geometric difference between femoral components is the presence of a collar. The collar can either overhang the bone or just overhang the cement mantle.

The taper of the stem is also very different between prosthetic designs. A steeper taper means that the proximal stem is more rigid than the distal stem. A steeper taper generates a greater wedging action of the stem within the medullary cavity.

1.10 Cementing technique

Bone cements may be applied in two ways. Most simply, the cement can be mixed and allowed to reach a doughy state when its viscosity is high enough that it can be manually manipulated and inserted into the bone. Alternatively, cements can be applied using a syringe or cement gun to inject the cement. This method of application has the advantage that it can be easier to reach into a femoral canal and the application of pressure aid penetration into the bone. The above two methods require different flow characteristics of the cements prior to setting. Manual manipulation requires a cement which rapidly reaches a doughy state. Conversely, injection requires a cement which maintains a low viscosity.

1st Generation cementing Technique Initiated by Sir John Charnley [45]. The method involves mixing in an open bowl and working the cement digitally (prior to the introduction of high viscosity).

2nd Generation cementing Technique Developed from the first generation cementing technique, restrictors are used to close off the distal femur, before syringing lower viscosity cement into the femur.

Modern cementing Technique Involves preparation and cleaning of bone cavity using modern instruments, such as a high-pressure pulse lavage to remove blood and debris from the cancellous bone interface. Bone cement mixing under a partial vacuum is then

carried out in order to reduce the porosity of cement. This is followed by introduction into the joint using syringing and pressurisation to drive the cement into the bone.

1.11 Bone cement mixing

PMMA bone cement has not substantially changed since it was first introduced more than 35 years ago, however, its physical properties are influenced by the cement mixing method used. These mixing methods have evolved greatly since they were introduced. In first generation systems, bone cements were mixed using a bowl and a spatula, this can introduce a high degree of porosity into the cement structure due to atmospheric pressure. Also, it would have a negative effect on the person mixing the cement by exposing him to a high level of noxious methyl methacrylate vapours [79]. Due to these reasons, a modified mixing bowl was designed (second-generation). The new model allowed the cement to be mixed under a low vacuum (-39 kPa) to reduce the level of monomer fumes exhausted into the theatre environment and also as an attempt to reduce the quantity of air bubbles dispersed through the acrylic cement structure. However, it was felt throughout the orthopaedic industry that such a mixing system still produced highly porous bone cement [79]. In contemporary third-generation mixing systems, the bone cement is mixed under an increased vacuum (<-86 kPa) to improve the cement quality and also reduce the level of fumes circulating within the theatre atmosphere. The cement is mixed and transferred within the mixing barrel, thus there is no human contact with the bone cement. This generation of cement mixing system is classified as a sealed, combined cement mixing and delivery system [79].

The main mixing systems can be summarized as the following:

- 1 Manual or hand mixing system
- 2 A number of proprietary Vacuum mixing systems
 - a Howmedica Mixkit I (1st Generation)
 - b Zimmer Osteobone vacuum system (2nd Generation)
 - c Zimmer Quick-Vac System (3rd Generation)
 - d Cemvac, Cemvac System Corp, Sweden (3rd Generation)
 - e Stryker High Vacuum Cement Injection System (3rd Generation)
 - f Summit LoVac® Bowl
 - g Summit Hi Vac Syringe

- h. Optivac, Biomet Merck Cement and cementing systems division
- i. Ultramix, DePuy

1.12 Femoral pressuriser

The use of a femoral pressuriser allows maximum pressurisation during cement insertion and achieves better interdigitation of cement into cancellous bone [84]. This device is produced by silicon according to FDA approval. The main purpose of the pressuriser is to apply pressure to the curing acrylic cement in the proximal portion of the femur prior to stem insertion into the intermedullary cavity.

1.13 Surgical technique

As designers and surgeons look for ways to limit failure, attention has been focused upon the following factors:

1. Careful cement preparation
2. The viscosity and porosity of cement
3. Careful and thorough bone preparation
4. Appropriate timing and effective insertion and pressurisation of the cement

These are all now seen to be important in the long-term. It is helpful to understand the nature of cement and the way it works, in order to get the best results.

The time available for each stage of cementing technique is dictated by the speed of cement viscosity increase. It is important to select either high or lower viscosity cement, depending upon the type of cementation planned and technique to be used. As polymerisation progresses, cement becomes more viscous and therefore does not flow as easily. With this increase of viscosity the potential for cement to penetrate through bone, even under pressure, is reduced. Therefore, accurately timing all stages of bone cement use is very important. When the cement is first mixed it is pliant and for 1 to 2 minutes it can be handled or syringed into the prepared bone. If the cement is too fluid, it may be easily injected into the bone, but blood pressure will force its retreat. This will prevent cement interdigitation into the cancellous bone and possibly weaken the cement itself by creating blood laminations. The correct time to introduce bone cement is after it has developed an initial viscosity, so that the mix is no longer fluid and can resist

pouring The surface of the cement should cease to appear wet or shiny To achieve this, the cement should be left to rest after mixing for 20 to 30 seconds with high viscosity cements, and up to 1 minute for low/medium viscosity cements

After cement insertion at the correct time, the bleeding pressure must still be resisted by rapid and sustained pressurisation. This ensures that the interstices of the bone are extensively penetrated with cement. Thus, the full interlock of cement with cancellous bone required for long-term fixation of the prosthesis will be achieved. The general consensus is that a consistent cement mantle of between 2 to 4 mm is the optimum thickness to avoid weakness or fracture under load [85].

At 4 to 6 minutes after mixing the cement becomes stiff enough to support the prosthesis. At this point the prosthesis must be inserted straight away. This avoids the risk of laminations caused by prosthesis insertion. After 7 to 9 minutes polymerisation accelerates. Exothermic heat is given off, and the cement finally hardens. It is fully interlocked with the surrounding bone and no longer requires pressurisation.

A typical clinical timing and usage chart for CMW3 is shown in figure 1-4

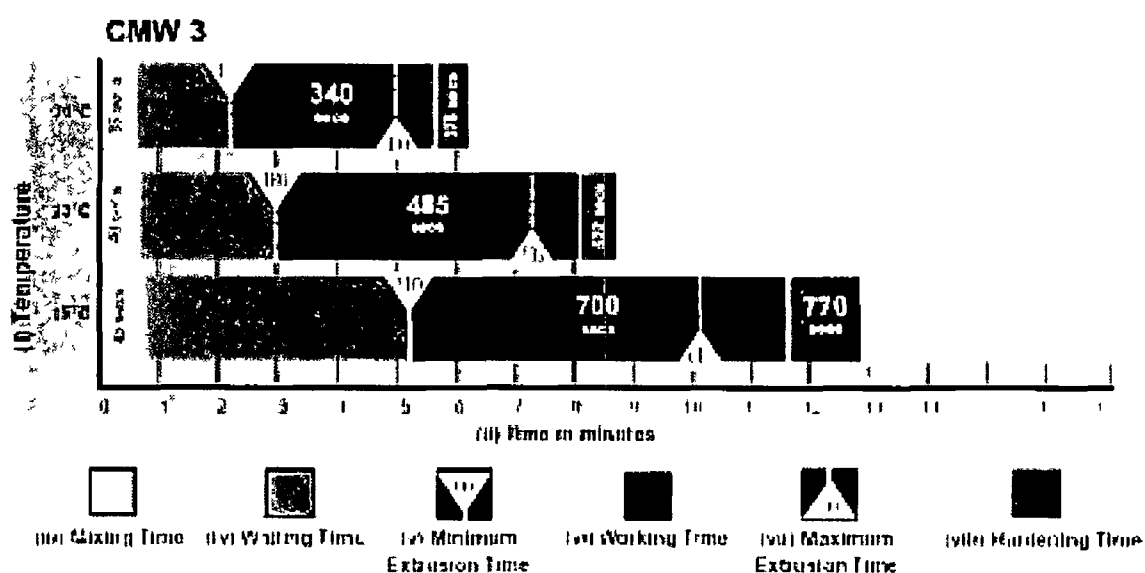


Figure 1-4 Syringe application of plane CMW3 and CMW3 with Gentamicin - Clinical timing and usage chart [86, 87]

The steps followed in a typical total hip replacement operation can be summarized as follows [6]

1 Planning

2. Exposure to the joint
3. Hand reaming
4. Broaching
5. Acetabular preparation
6. Lavage
7. Cement mixing
8. Cement introduction by retrograde fashion
9. Acetabular digital introduction
10. Cement pressurisation to improve the mechanical interlock at the femoral bone/cement interface
11. Cup introduction
12. Femoral cement introduction
13. Cement pressurisation
14. Stem introduction

Optimum cement viscosity will resist blood pressure and avoid blood lamination within the cement mantle. Lamination can halve the strength of the cement mantle [88]. Increasing the stem insertion rate has been found by Baleani et al. [89] not to have a significant effect on the porosity distribution within the bulk cement mantle. However, for all stem insertion rates investigated in this study, the porosity concentration increased significantly moving from the cement/pseudofemur interface through to the stem/cement interface [89].

1.14 Bleeding pressure

Bleeding pressures occurring at intermedullary bone interface were measured in vivo during a total hip replacement by Benjamin et al. [90]. Maximum bleeding pressures of 3.6 kPa were recorded. Majkowski et al. [91] developed a model to simulate bleeding from the cancellous bone at physiological pressures and flow rates that occur during a total hip replacement. It was found that blood flowing at 2.7 kPa and at a flow rate of 70 ml/min creates voids and laminations within bone cement. The conclusion reached was that the optimum cement technique in bleeding bone involves extreme cleaning of cancellous bone with pulse pressurised lavage, rapid application of normal viscosity

bone cement that has reached the dough stage, and immediate pressurisation for at least 30 seconds.

1.15 Rheology of bone cement

Rheology is a science of the deformation and flow of materials. Viscosity is a rheological property that provides a measure of the relative ease or difficulty of creating a state of flow of material. Viscosity is defined by a rheological equation of state which is the ratio of the shear stress to the shear rate of a material when the material is undergoing steady state flow [92].

Considering a simple shear flow, Newton's law of viscosity relates shear stress, τ , to the velocity gradient or shear rate, $\dot{\gamma}$, through the equation [93, 95]:

$$\tau = \eta \dot{\gamma} \quad (1-4)$$

where η is the coefficient of viscosity, or simply the viscosity.

A material can be classified as either Newtonian or non-Newtonian depending on the relationship between shear stress and shear rate. The fluid is classified as Newtonian when the shear stress is a linear function of shear rate and the shear stress is zero at zero shear rate [95]. Viscosity of Newtonian fluid is constant and independent of shear rate for Newtonian fluids. The fluid is classified as non-Newtonian when the shear stress does not have a linear relationship with shear rate. The viscosity of non-Newtonian fluid is not a coefficient but a function of the shear rate and/or the time of shearing [95]. Figure 1-5 shows the different types of Newtonian and non-Newtonian fluids. For example, it is common for viscosity to decrease with increase in shear rate-behaviour, known as "shear thinning" or pseudoplastic fluids [98]. A pseudoplastic fluid shows a negative second derivative of the relationship between shear stress and shear rate, that is a downward concave curve, as shown in figure 1-5. Conversely, it is possible for viscosity to increase with increasing shear rate, referred to as "shear thickening" or dilatant [98]. This type of fluid shows a positive second derivative of the relationship between shear stress and shear rate, that is a upward concave curve, as shown in figure 1-5.

To describe the shear stress versus shear rate relationship for various types of fluid behaviour, a mathematical relationship known as the power law [95, 97-101, 122] is used such that the shear stress is proportional to the shear rate raised to the power n

$$\tau = K\dot{\gamma}^n \quad (1-5)$$

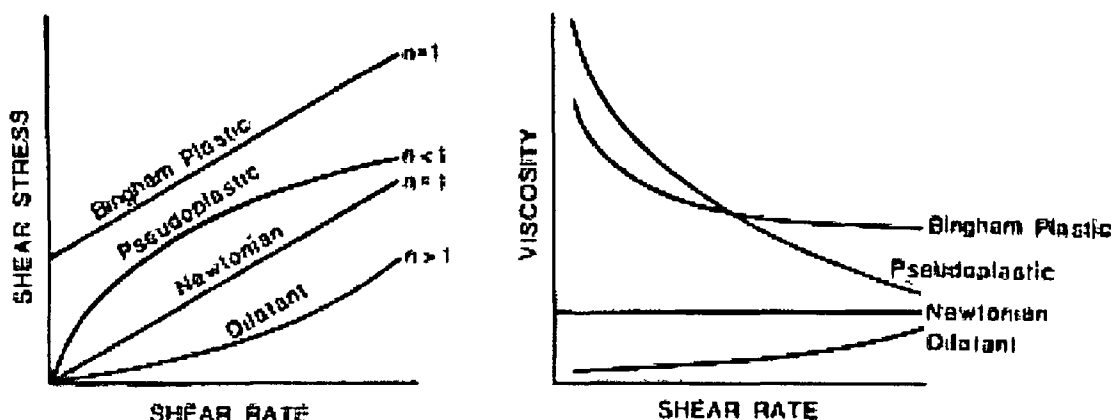


Figure 1-5 Shear rate dependence of shear stress τ (left) and shear viscosity η (right) of Newtonian, shear thickening or dilatant, and shear thinning or pseudoplastic fluids and Bingham plastic time independent fluids [95]

where n is the power law index or flow behaviour index, and K is the consistency coefficient. Both K and n are constants describing the flow behaviour. Taking the logarithm of both sides of the equality gives

$$\log \tau = \log K + n \log \dot{\gamma} \quad (1-6)$$

This relationship plots as a straight line on the log log graph, n is equal to the slope of the line and K is equal to the intercept with the ordinate axis (shear stress) when the log of the shear rate equals zero.

The power law relationship can be used to describe the type of fluid behaviour of a material

- $n=1$ Newtonian
- $n<1$ Pseudoplastic, common range is 0.2 to 0.5
- $n>1$ Dilatant, usually extend to 1.2 or 1.3

The character n is referred to as the power index value and is a measure of the non-Newtonian character of the material. Since viscosity relates shear stress to shear rate, viscosity can also be expressed as a power relationship by substituting $\tau = K\dot{\gamma}^n$ in the expression for viscosity in terms of shear stress and shear rate [95, 97, 122]:

$$\eta = \frac{\tau}{\dot{\gamma}} = \frac{K(\dot{\gamma})^n}{\dot{\gamma}} = K(\dot{\gamma})^{n-1} \quad (1-7)$$

Some non-Newtonian fluids show a time-dependent change in viscosity. Fluids that exhibit a decrease in viscosity with time at constant shear rate are known as thixotropic fluid. On the other hand, those that exhibit an increase in viscosity with time at constant shear rate are known as rheopectic or antithixotropic fluids [93].

Accordingly, the viscosity of the monomer-powder mixers prior to completion of the setting reaction is clinically an important physical property of methylmethacrylate bone cements. The viscosity of bone cement is of fundamental importance with regard to the achievement of the fixation between the cement and bone and ultimately between a prosthesis and bone.

A viscoelastic material, as the name implies, exhibits both viscous and elastic properties. Most real materials are viscoelastic, and this is clearly going to be the case for curing bone cements, where the cement changes from having predominantly liquid-like properties immediately after mixing, to having predominantly solid-like properties once set. It is, therefore, useful to characterise curing bone cements as viscoelastic materials, which can be conveniently done by application of an oscillatory shear in a rheometer.

Viscosity is a function of temperature, time and shear rate for viscoelastic materials. Viscoelastic materials can be characterised by storage modulus (G'), which is elastic behaviour, or loss modulus (G''), which is viscous behaviour and phase angle (δ).

It has been shown that PMMA bone cement is a non-Newtonian pseudoplastic material. It follows the 'Power Law'. The viscosity of Bone cement decreases with respect to increases in shear rate [77, 78, 95, 97, 122]. Clinically, this can be achieved by rapid motion or perhaps multiple short thrusts to insert prosthesis. During placement of the cement, the surgeon can influence the shear rate by the velocity at which the cement is

delivered through the injection gun nozzle and hence the viscosity. Rapid insertion of the acrylic bone cement creates a high shear rate at the pore opening, thus decreasing the viscosity of the cement and allowing better penetration. This mode of insertion was advocated by Charnley [94] by means of finger packing the intermedullary canal and prosthesis insertion. The stem insertion rate and consequent cement displacement will also influence the viscosity of the cement layer between the prosthesis and bone. Bone cement should be applied in femoral cavity within 3 minutes of mixing as viscosity increases with time.

The rheological and curing or handling properties of bone cement are the main factors that determine the efficiency of acrylic bone cement to anchor the implant to the contiguous bone in cemented arthroplasties [130]. These properties affect how the cement dough flows into the micro interstices and other irregularities on the surface of the intramedullary bone canal. The rheological properties may also play a role in the formation of pores in the cement during polymerisation. It has been postulated that these pores can act as sites for the initiation of cracks that can cause or contribute to aseptic loosening of the prosthesis [5]. Thus, cement's rheological properties affect the degree to which the patient is satisfied with the cemented arthroplasty.

1.16 Flow through porous media

One-dimensional flow of an incompressible substance through a porous media is governed by Darcy's Law [29, 36, 38]

$$Q = A \frac{k}{\mu} \frac{dP}{dx} \quad (1-8)$$

where, Q = volumetric flow rate (dimension L^3T^{-1})
 A = cross-sectional area (dimension L^2)
 k = specific or intrinsic permeability (dimension L^2)
 μ = dynamic viscosity (dimension $ML^{-1}T^{-1}$)
 $\frac{dP}{dx}$ = pressure gradient

Darcy's law is a statement that an area-averaged fluid velocity Q/A is related to an applied pressure gradient through a constant of proportionality k . Further, the flow is inversely proportional to the fluid viscosity μ . Permeability (ability of a material to transmit fluids) provides a measure of the fluid conductivity of the porous medium. The usual unit for permeability is the *darcy*, or more commonly the *milli-darcy* or *md* ($1 \text{ darcy} = 1 \times 10^{-12} \text{ m}^2$) [105]

In general, Darcy's law for a three-dimensional anisotropic medium can be written as [36]

$$Q = A \frac{k}{\mu} \nabla p \text{ or } Q = A \frac{k_{ij}}{\mu} \frac{\partial p}{\partial x_j} \quad (i, j = 1, 2, 3) \quad (1-9)$$

∇p = Vector pressure gradient

k = second-rank tensor of permeability

This relationship between the flow rate of a fluid within a medium and the pressure gradient necessary to induce such a flow includes the properties of both the medium and the fluid. Darcy's law [36] is valid when investigating the flow rate with no more than 100 to 110 mm/s through tubes of small diameter. Although Darcy's law has been shown to be invalid for high flow rates, there is no universal critical Reynolds number for porous media. Indeed, investigators have suggested critical Re as low as 0.1 and as high as 75 [36]. Part of the uncertainty is due to the lack of definition for the characteristic length, diameter, for a porous material.

The flow characteristics of curing acrylic bone cements represent important material properties which need to be understood in order to realize the full benefits of a total hip replacement, total knee replacement and vertebroplasty operation. The ease of flow of cement into the pore openings of cancellous bone, under pressure, determines interface properties and fixation.

The flow of bone cement in cancellous bone is complicated by the non-Newtonian nature of the cement. For the cement infiltration procedure, k is generally a function [134] of the intertrabecular bone porosity, α , and cement viscosity, η .

$$k = k(\alpha, \eta) \quad (1-10)$$

The penetration and flow of acrylic bone cement is a mechanical phenomenon and as such is directly influenced by insertion techniques used at surgery. Within the span of a relatively short working time bone cement is transformed from a liquid slurry exhibiting predominantly fluid properties into a rubbery viscoelastic solid which will neither sustain hydrostatic pressure nor will flow. Therefore, the time at which the material is pressurized within the prepared cancellous cavity is of critical importance in achieving the desired mechanical interdigitation. Table 1-14 summarizes the work of different researchers on the penetration depth of bone cement and shear strength.

Table 1-14 Depth of penetration of bone cement with shear strength from different works

Researchers	Parameters varied	Shear strength (MPa)	Depth of penetration (mm)
Majowski et al [107]	Surface preparation techniques	1.5-36.1	0.2-7.9
Askew et al [108]	Cementing pressurization and storage of bone		3.58±3.30
Rey et al [109]	Cement type, pressurization, bone porosities, environmental conditions		Up to 17.4
Kusleika and Stupp [110]	Cementing pressurization and storage of bone	3.6-7.5	0-10
Krause et al [58]	Preparation techniques	9.55-41.99	Up to 12
Majowski et al [111]	Cementing techniques, simulated back bleeding	20.4-35.4	2.9-9.2
Markolf and Amstutz [112]	Cemented into aluminium plugs under different pressures		Up to 10
S. A. Maher and B. A. O. McCormack [113]	Semi automated procedure to measure the depth of penetration		Penetration depth 1.3-4.3 Penetration width 3.4-5.9

Pressure magnitude is the most influential of the factors considered in the cement penetration behaviour and in the development of failure load capacity. The duration of the pressure does not appear to be significant factor [106]. The cement penetration is a decreasing function of the bone strength, reflecting a decrease in the porosity and an increase in the area fraction. The effect of increasing bone strength on the failure load is nonlinear. The development of adequate failure load capacity is the result of a balance between the cement penetration allowed by the porosity of the bone and the inherent strength of the cancellous bone itself.

Weak bone, although adequately penetrated by cement, cannot provide strong fixation. Stronger, denser bone limits cement penetration, but pressurization enhances development of failure load capacity through more complete infusion and interlocking of the cement in the available pore space. The strength of the fixation achievable for any bone is limited by the intrinsic strength of the bone.

1.17 Brief objective of the project

Rheological property is an important factor for the optimal penetration of bone cement through cancellous bone in THR, TKR and vertebroplasty. In this project, flow patterns and degree of penetration of bone cement were determined using finite element software (FIDAP). Rheological properties at different times were used as the inputs to the finite element software. Three different parameters were studied in this project. (a) Effect of prosthesis insertion velocity, (b) Effect of variation of prosthesis insertion time duration (c) Effect of bone cement amount variation. The simulation results were compared in two ways.

1. By performing experiments with similar boundary condition of simulation using CMW3 bone cement and
2. By using published data of previous researchers.

1.18 Structure of thesis

This thesis is divided into seven chapters. A description of each chapter is as follows:

Chapter 1 “Background and Introductory Materials” This chapter describes the introductory materials and related technology that have been used for this project

- The types of THR, main problems related to THR, main parts related to THR, cemented fixation with cement/prosthesis interface mechanics and strength, cementing technique, bone cement mixing methods and surgical technique were described briefly
- The properties of bone, cortical bone and cancellous bone were described, concentrating on the description of cancellous bone permeability
- A brief description of bone cement was given for three bone cements (Simplex P®, Zimmer and CMW3) with properties, polymerisation mechanism and setting time
- The rheology of bone cement with measuring techniques were described The principle of fluid flow through a porous media such as cancellous bone was also described

Subsequently the objectives of the research have been defined briefly

Chapter 2 “Literature Review and Objective” This chapter describes the work of previous researches The related works are divided into three groups

- The influence of mixing methods on the mechanical and thermal properties of curing acrylic bone cement, and the polymerisation characteristics of bone cement
- The rheological properties of bone cements The dependency of viscosity on shear rate and elapsed time Viscosity measurement of curing bone cement using capillary, rotational and dynamic compressive viscometers
- Bone cement flow through cancellous bone in vitro using a standard biological model and proximal femur of adult mongrel dogs in vivo The use of numerical models to investigate the non-Newtonian flow of acrylic bone cement in a porous medium

Chapter 3 “Experimental method and procedure” This chapter is divided into two parts The first part presents the measurement of the thermal properties (maximum temperature, setting temperature and setting time) of bone cements using the standard

method The second part presents the materials, accessories and surgical procedures used for comparison experiments

Chapter 4 “Finite Element Analysis of bone cement penetration in total hip replacement” This chapter briefly describes Finite Element Analysis (FEA) The steps used for creating the Model, the materials properties used and the boundary conditions applied in the finite element model are described here

Chapter 5 “Results, comparison and discussion” This chapter describes the results found in this research work All results can be divided into three groups

- The thermal properties of bone cement
- 2D simulation of bone cement flow through cancellous bone to get the flow patterns and degree of penetration Three different parameters were studied in this research work
- Comparison of the numerical results with the results obtained from the experimental work and also the results of other researchers

Chapter 6 “Conclusions and recommendations” This chapter presents the main results achieved during this research It also outlines the contributions of this work and recommends future work based on the findings from the study

Chapter two

Literature Review and Objective

2 1 Literature review

Lewis [78] in 1997 reviewed the physical and mechanical properties of six commercial acrylic bone cements (Simplex P®, Zimmer Regular, Zimmer Low Viscosity Cement, Palacos R, CMW 1 and CMW 3). Lewis reviewed the dynamic viscosity, porosity, quasistatic tensile properties, quasistatic compressive properties, flexural strength and modulus, shear strength and modulus, work of fracture (WOF), fracture toughness, fatigue properties and creep of bone cements. The effect of mixing methods (manual or hand mixing, centrifugation, vacuum mixing and combined mechanical mixing) was discussed. Antibiotic-impregnated variations of some of these formulations and some efforts to improve the properties of bone cements were also reviewed.

DiMaio [114] in 2002 reviewed the science of bone cement. The composition of bone cement, thermal and chemical effects of PMMA bone cement, mechanical properties of PMMA bone cement (static and dynamic, failure of PMMA cement), effects of variations in the preparation of bone cement and also effect of antibiotic agents on bone cement were included in this review.

2 1 1 Mixing of bone cement

Kurdy et al [115] in 1996 demonstrated that there is a significant increase in unmixed powder content in cement prepared using a vacuum mixing system with a fixed central axis compared with both the rotating axis system and hand mixing. It was concluded that the use of different rotating systems in mechanical mixers could influence void and unmixed powder content. It was also demonstrated that unmixed powder has an effect on the mechanical properties of acrylic cement, causing a reduction in the bending strength of the cement.

Smeds et al [116] in 1997 studied the influence of temperature and vacuum mixing on bone cement properties. They concluded that vacuum mixing improves cement quality.

Dunne and Orr [79] in 2001 studied the influence of mixing techniques on the physical properties of acrylic bone cement. They found that the best results were obtained from cement that had been mixed using the Mitab Optivac® or Summit HiVac® Syringe systems at a reduced pressure level of between -72 and -86 kPa below atmospheric pressure. The result showed that cement porosity varies from 1.44 to 3.17%, compressive strength varies from 74 to 81 MPa, flexural modulus varies from 2.54 to 2.60 GPa and flexural strength from 65 to 73 MPa. It was concluded that the lower the porosity in the cement the better the compressive and flexural properties. Mixing the cement in a sealed, combined cement mixing and delivery system (third-generation mixing device) under the application of reduced pressure, can lower the porosity.

2.1.2 Thermal characteristics of curing acrylic bone cement

Dunne and Orr [120] in 2001 studied the thermal properties of various curing acrylic bone cements (Palacos R and CMW3) as a function of preparing bone cement by different techniques, such as hand mixing and vacuum mixing (first, second and third-generation). A number of parameters were calculated, maximum temperature, cure temperature, cure time and cumulative thermal necrosis index. It was found that particular formulations of bone cements are suited for certain mixing systems due to the design of the mixing system. They found that peak temperature was the lowest for first generation mixing system, Howmedica Mix-Kit I.

He et al. [117] in 2003 studied the effect of different mixing methods on the setting properties of bone cement. It was found that vacuum mixing decreases the setting time of the bone cement by nearly 2 min (10%), compared to mixing in air. Also the setting time increases significantly as the oxygen concentration increases. He suggested that the decrease in the setting time by vacuum mixing might be attributed to the lower oxygen levels present in the mixer. Varying the oxygen concentrations in the bone cement mixer was found to have no significant effect on dough time or maximum exothermic temperature.

Vacuum mixing has been reported by some researchers to affect the setting properties of bone cement, however the published results are not consistent. Lidgren et al. [118] reported that vacuum mixing delays the setting time but also decreases the maximum

temperature, while a study by Hansen and Jensen [119] showed a decrease in setting time by vacuum mixing, compared to hand mixing. A compelling argument has not yet been made to address this influence since other variables, such as mixing speeds, mixing time and vacuum, are also involved.

2.1 3 Polymerisation of bone cement

Yang [72] in 1997 found that the polymerisation of acrylic bone cement is approximately a first order reaction. Two types of reaction rate constants for the polymerisation reaction were reported. The existence of the two rate constants means that the polymerisation reaction takes place at a slower reaction rate at the beginning due to the presence of more monomers of low viscosity. After the peak time (time at which the maximum heat is generated by polymerisation reaction), the polymerisation reaction occurred at a faster

Oldfield and Yasuda [121] in 1999 found by using electron spin resonance (ESR) spectroscopy that in the MMA polymerization process, oxygen would lower the free radical concentration, and thus the early phase of radical polymerization of MMA during bone cement curing was retarded.

2 1 4 Rheological properties of bone cements

Schoenfield [77] in 1974 studied dental acrylic and measured the viscosity as a function of

- (1) Shear rate
- (2) Lapsed time after mixing of the liquid monomer and polymer powder
- (3) Proportion of monomer liquid and polymer powder using capillary viscometer

It was assumed that bone cement is a Pascallian steady state laminar fluid and incompressible material. Also it was assumed that there was no slippage at the wall during viscosity measurement. It was found that this dental acrylic could be characterized as a pseudoplastic material, indicating that the viscosity decreases as the shear rate increases. With respect to time from mixing, the viscosity increased rapidly due to the polymerisation reaction. The results also showed that the viscosity decreased with respect to increases in the monomer/powder ratio.

Ferracane and Greener [122] in 1981 studied the rheological properties of setting acrylic bone cements (Simplex P®, Zimmer and Zimmer LVC) with a rotational cone and plate viscometer. The cements were tested over two orders of magnitude of shear rate to determine the nature of any non-Newtonian flow behaviour. Cements behaved as a pseudoplastic (shear thinning) fluid during setting. A series of sieving experiments were performed to determine the particle size distributions of the powder components. The results showed that low viscosity cements (i.e. Zimmer LVC) contain a larger proportion of smaller polymer particles.

In 1982, Krause et al. [95] studied the rheological properties of Surgical Simplex P®-RO (radiopaque), Zimmer (normal) and Zimmer LVC (low viscosity cement) bone cements over a three decade range of shear rates (0.04 to 94.4 s^{-1}) using rotational and capillary extrusion rheometer. In addition, CMW BaSO₄, sulfix 6 and AKZ Howmedica bone cements were studied at a single shear rate. The results indicate that all the acrylic bone cements are non-Newtonian pseudoplastic materials with significant differences between them. It was shown that the viscosity increases at different rates with respect to increases in time (during the working time of three to seven minutes after mixing) for different bone cements. For the majority of cements there are a steady or increasing rate of viscosity change with time.

Weber and Barger [96], in 1983, compared the mechanical properties and viscosity of three bone cements (Simplex P®, Zimmer and Zimmer LVC). All cements were equal in compressive, tensile and fracture toughness testing. Zimmer regular cement was significantly weaker in flexural testing and had significantly decreased modulus of elasticity when compared to Zimmer LVC and Simplex P® cements. The viscosity varied between these bone cements. Viscosity versus time of bone cement mixture was determined in a temperature and humidity controlled room (22°C and 66% humidity) using a capillary rheometer. The dough and set times in minutes were 4.0 and 8.25 for Zimmer regular, 4.5 and 10.0 for Simplex P®, and 6.5 and 8.0 for Zimmer LVC. The temperature of polymerisation was 68°C for Zimmer, 78°C for Zimmer LVC and 87°C for Simplex P®.

In 1998, Dunne and Orr [97] characterised the flow property of curing PMMA bone cement using a capillary extrusion rheometer that was been manufactured in-house.

They assume a steady state flow, isothermal conditions and acrylic bone cement to be an incompressible material. Flow rate of the curing bone cement using nozzles of different lengths (10 and 51 mm) and two different loads (44 and 74 Newton) were measured. It was concluded that acrylic bone cements are non-Newtonian, pseudoplastic materials, i.e. the apparent viscosity decreases as the shear rate increases, since the power index (n) values of power law were less than 1.0 during curing stage. It was found that the apparent viscosities of the cements increase with respect to time increment, but at different rates for different bone cement. Dunne and Orr determined the true apparent viscosity with higher accuracy compared to Krause et al [95].

Nzihou et al [123], in 1998, studied the effect of concentration (volume fraction) of solids, temperature and nature of inorganic compounds used as filler, and opaque substances to X-ray radiations, on the viscosity of the suspension of PMMA powder and methyl methacrylate. It was found that rheological behaviour of bone cement (suspensions of PMMA particles and inorganic powder in methylmethacrylate and butylmethacrylate) corresponds to a shear-thickening model and data fits to a modified Chong equation.

Farrar and Rose [124], in 2001, characterised the rheological behaviour of poly(methyl methacrylate) bone cements during the curing phase using an oscillating parallel plate rheometer. Viscosity has been measured as a function of time for a range of commercial cements, Palacos R, Simplex P®, Zimmer low viscosity cement, Zimmer regular, Osteobond and CMW 3. The results show different viscosity time profiles. It is clear that the cements not only have different initial viscosities, but also show marked differences in the shapes of the viscosity-time curves. It was also determined that a number of factors affect the initial viscosity and rate of swelling of the polymer beads, and hence the rate of viscosity rises. These include polymer particle size and shape distribution, composition of the polymer particles (e.g. whether a co-polymer), and molecular weight distribution of the polymer component. Measurements have been made over a range of temperatures (19-25°C). The results have demonstrated that the viscosity increases at higher temperatures. Viscoelastic parameters, such as storage modulus, loss modulus and phase angle have been obtained and showed that the cements change from primarily viscous to elastic behaviour as it set.

Lewis and Carroll [125], in 2002, studied the rheological properties of curing acrylic bone cement and role of the size of the powder particles. They used a dynamic compressive rheometric technique to determine the true or complex viscosity of three PMMA-based bone cement formulations, (Orthoset ® 3 and two experimental cements), as a function of time from the start of hand mixing the cement constituents. Cure onset time and critical cure rate (CCR) were determined for each cement. Particle analysis was carried out to obtain the powder particle size distribution, from which the overall mean particle diameter and the relative amounts of small-sized (mean diameter between 0 and 40 μm) PMMA beads (α) and large-sized ($d > 75 \mu\text{m}$) PMMA beads (β) were determined. It was found that the key particle parameter is not mean diameter but the relative amount of smaller and larger sized PMMA beads. The highest values of cure onset time and CCR were obtained from a cement with the highest values of α and β . It can be demonstrated that the cement's rheological properties during curing should be based on α and β rather than on the mean particle diameter.

2.1.5 Cement pressurisation and flow through cancellous bone

Markolf and Amstutz [112], in 1976, studied the effect of insertion time (the time after initial mixing of the powder and liquid) and insertion pressure on the depth of acrylic penetration into specially prepared cancellous cavities. They machined a series of aluminium plugs of 13 mm diameter and 9.6 mm thick, 9 identical holes ranging from 1 to 3 mm were created on flat surface of plugs that was anticipated as normal cancellous bone porosity. It was clear that acrylic penetration increased uniformly with increasing pressure, and better acrylic penetration was found in larger hole and thus better penetration is expected in bone having large cancellous interstices. The depth of filling for early pressurization was greater in all cases than that for late pressurisation. More than 64% of penetration occurred within the first second of pressure applied. The depth of acrylic penetration was not linear with time and the rate of filling decreased with increasing pressurization time. They demonstrated quantitatively the advantages of early cement placement and high, the short duration pressure pulses obtained by vigorous acrylic packing to achieve maximum mechanical penetration.

Noble & Swarts [127], in 1983, studied the depth of penetration of five commercial bone cements, Simplex P®, Palacos R, CMW, Zimmer and Sulfix 6, into cancellous

bone (from femoral condyles of cadaveric femora) in vitro using a standard biological model under controlled conditions. Penetration was critically influenced by the coarseness of the cancellous bone and increased directly with the effective volume of the cells within the osseous matrix. To describe this in a simple quantitative way, the cancellous structure was visualized as an array of packed interconnected cylinders of a constant mean diameter. Any one cylinder was assumed to contain internal constrictions at a range of intervals along its length. Final penetration depths of 5.4 mm, 5.01 mm, 3.01 mm, 3.00 mm and 2.72 mm were reported (22°C, 90 s following dough stage, 82% mean porosity, 0.035 MPa pressure) for Simplex P®, Zimmer, Palacos R, Sulfix 6 and C M W respectively. The depth of penetration was influenced by the cement viscosity. An inverse correlation was determined between the mean cement viscosity during flow into the bone and final penetration depth. The dough time, set time and working time of each acrylic formulation was found to have no significant effect upon the depth of cement penetration.

Inadequate insertion pressure generation is one of the main causes of failure at the acrylic bone cement/cancellous bone layer interface. It has been quoted by Askew et al [108], in 1984, that an intermedullary pressure of at least 76 kPa is required to obtain sufficient bone cement infiltration into spongy cancellous bone. They also stated that a 2-4 mm penetration depth is necessary to achieve a mechanical interlock between the cement and one layer of transverse trabeculae, depending on the density of bone stock. Penetration depths greater than 4 mm will result in excessive heat necrosis and tissue cell loss.

In 1987, Rey et al [109] subjected bovine cancellous bone, with an average porosity of 61%, to different pressures and cement viscosities. Cement penetration was proportional to the injection pressure. At 140 kPa the penetration depths for high, medium and low viscosity cement were 1.4, 2.2 and 8.00 mm respectively.

Beaudoin et al [42], in 1991, developed a numerical model to investigate the non-Newtonian flow of acrylic bone cement in porous cancellous bone. Cement penetration into the bone bed was measured by a quasi-steady model applying a constant pressure (0.14 MPa). For the reported range of cancellous bone porosity between 81 and 88% [109, 127] the model suggests a corresponding range of permeability of between

5.6×10^{-9} and $8.6 \times 10^{-9} \text{ m}^2$ for linear (Newtonian) flow. The average permeability determined in the experimental study was $7.84 \times 10^{-9} \text{ m}^2$. They used cancellous bone specimens from the proximal tibia of fresh-frozen human autopsy. A finite element model with a porosity of 85% was required to develop permeability equal to the experimental permeability. The velocity for Simplex® at an elapsed time of 180 s was reported to be $0.197 \times 10^{-3} \text{ ms}^{-1}$. The model predicts a final penetration depth of 5.6 mm for surgical Simplex® at an applied pressure of 35 kPa. The depth of penetration is strongly dependent on the surface to volume ratio. It was found that the reduction in surface to volume ratio for osteoarthritic bone is associated with a greater depth as predicted by the model.

Macdonald et al [59], in 1993, showed that the shear strength at the interface is increased by 82% and penetration by 74% when distal bone plugging, pressure lavage and pressurized insertion of cement were employed. Use of a lower-viscosity cement gave a further 18% increase in penetration and shear strength. The proximal femur of adult mongrel dog was used in vivo. It was found that penetration increases with distance from proximal end to distal end due to the decreased bone density along this path. It was concluded that the penetration achieved is dependent on the technique used and the viscosity of the cement. Also, the shear strength of the interface is linearly dependent on that penetration. The calculated interfacial mean shear strength was 6.2, 7.3 and 3.4 MPa for Palacos, Simplex® and CMW respectively.

A 3D computational fluid dynamics (CFD) analysis was conducted in order to characterize the cement flow pattern during insertion of the femoral stem into a cement-filled bone cavity by Canabal and Katz [128] in 1994. The CFD analysis consists of the simulation of an incompressible flow of a Newtonian fluid flowing within the space bounded by the surfaces of the stem and the reamed, as well as the air-cement surface. The insertion rate of the stem into the cavity was estimated to be 0.396-1.219 cm/s. In the simulation the only independent variable was Reynolds number ranged from 25 to 80, using a kinematic viscosity of $0.186 \text{ cm}^2/\text{s}$. At the distal end of the cavity, the cement remains stagnant, with the highest static pressure. The induced pressure gradient drives the cement outward along the space between the stem and the bone surface. Conversely, the stem drags the cement inward, creating a three-dimensional swirl (vortex).

McCaskie et al. [126], in 1997, measured the pressure generated at the cement-bone interface during total hip replacement. During cement insertion, the gun technique produced consistently greater maximum pressure than finger packing. The mean peak pressure by finger packing was 81.1 kPa and by gun technique was 156.9 kPa. Average mean pressure by finger packing was 16.91 kPa while by gun technique was 42.88 kPa. It was also noted that finger packing generated more pressure at proximal than at distal levels, while the pattern was reversed when using the gun technique. Similar trends were shown for mean pressures. During insertion of the stem, both techniques recorded much greater pressure distally than proximally.

Dunne et al. [129], in 1998, developed a pressure measuring device that is suitable for recording the cement pressures when a metal stem is inserted into the femoral cavity. By using this system they validated the intermedullary pressure results that were collected from other researchers in vitro. The device was tested using a cadaveric femur. Pressure data was collected under two conditions, early femoral prosthesis insertion at 185 seconds (condition 1) and also late introduction at 300 second (condition 2). It was observed that the femoral prosthesis inserted at condition 2 generated a higher level of intermedullary pressures (350 kPa) when compared to the introduction at condition 1 (201 kPa), but only for a short duration. The high intermedullary pressure in condition 2 was due to more viscosity with a higher degree of polymerisation.

Maher and McCormack [113], in 1999, quantified the interdigitation at bone cement/cancellous bone interfaces in cemented femoral reconstructions. In particular, the depth of penetration cannot fully describe the morphological interlock between cement and bone. To fully characterize the morphological state of the interface it was necessary to have data on the depth and width of the penetrated bone cement and the variation of these quantities all along the interface. They prepared four femora in vitro (group A) and two femora in vivo (group B). Each bone was sliced into nine sections after the bone was moulded in a plaster block. The penetration depth was found to be between 1.3-2.6 mm for group A and between 2.1-4.3 mm for group B, and the penetration width was 3.4-5.9 mm for group A and 3.4-5.7 mm for group B. Also, it was found that the penetration depth increased from distal end to proximal end.

Dunne and Orr [130], in 2000, worked to develop a numerical model that describes the cement flow in (a) a simple parallel cylinder, (b) a tapered conical mandrel and (c) an actual femoral prosthesis. The study aimed to predict the cement pressures generated during the course of a typical hip replacement operation. The predicted pressures generated around a femoral prosthesis as it is being introduced into the femoral cavity were close to those measured experimentally, maximum pressures being in the range of 10 to 160 kPa. This may be compared with a threshold of 76 kPa proposed for effective interdigitation with cancellous bone. To validate the model they performed an experiment. A 316 Stainless steel mandrel was introduced under a constant load of 100N. They used a total of three femoral prosthesis (Charnley 40 flange stem, DePuy International custom prosthesis and Exeter No. 3 femoral component) [131]. Regardless of cement mantle thickness, the generated pressure increased down the length of the model.

Breusch et al. [132], in 2002, studied the interrelationship of cement viscosity and cement interdigitation using thirteen sheep. The low viscosity cement yielded lower rates of cement penetration despite adequate and sustained pressurization. The use of high viscosity cement ran a higher risk of fat embolism, but improved cement interdigitation. 3.8 bar pressure was applied using two simultaneous syringes, which corresponds to an intermedullary pressure of about 390 kPa. The mean rates of cement penetration were 21% in the Osteopal group ($n = 12$) and 35% in the Palacos group ($n = 12$).

Bohner et al. [133], in 2003, worked to predict theoretically the behaviour of the cement paste during its injection into a porous matrix. The law of Hagen-Poiseuille and the law of Darcy were combined to simulate the behaviour of a cement paste injected through a needle into a porous matrix, e.g. an osteoporotic cancellous bone. Particular attention was paid to the effects of injection parameters (flow rate, cement viscosity, matrix geometry) on the injection force and the occurrence of cement extravasation.

Baroud et al. [134], in 2003, analysed the cement flow through osteoporotic bone. It was considered that the cement permeability was dependent on time, bone porosity, and cement viscosity. It was investigated, theoretically and experimentally, the permeability of cancellous bone with respect to time and porosity. It was found that the

intertrabecular bone permeability decreases with time. For instance, the initial permeability ($60.89 \text{ mm}^4/\text{N.s}$) reduced to approximately 63% of its original value within 18 seconds.

Baroud and Yahia [135], in 2004, modelled rheopectic and pseudoplastic rheological behaviour of PMMA bone cement using finite element (FE) method (ANSYS software) to examine the extra-vertebral flow conditions of vertebroplasty. The FE analysis showed a logarithmic increase of the injection pressure, where it almost doubled from 1.2 to 2.3 MPa over two minutes. This unanticipated non-linear increase is due to the highly nonuniform viscosity profile in the cannula.

2.2 Objective and outline of the project work

Poly methyl methacrylate (PMMA) bone cement has been in use from the early 1960s as a grout for prostheses. Bone cement is mainly used in THR and TKR to support the prosthesis within the intermedullary cavity of bone. During polymerisation PMMA bone cements demonstrate complex viscoelastic characteristics. Within a short period of time they transform from dough-like consistencies to solid cements. Mechanical interlocking among the bone, bone cement and prosthesis by interdigitation of bone cement through porous cancellous bone depends on cancellous bone porosity, prosthesis design and the flow property of bone cement. Obtaining adequate interlock increases the area for load transfer and reduces localised bone/cement interface stresses. The longevity of the total hip replacement surgery depends also on the interdigitation of bone cement in the porous bone. Optimum penetration of the bone cement ensures adequate load transfer during stamping or jumping of a human being.

The rheological characteristics of the bone cement are an important factor that effect the optimum penetration of bone cement through cancellous bone. There is a lack of information in the flow characteristics of PMMA bone cement. Considering this point, the present project concentrates on modelling the rheological characteristics of bone cement during the total cycle of PMMA bone cement polymerisation. The aim of this project was to define the flow characteristics of bone cement and the degree of bone cement penetration into the cancellous bone. To achieve this aim, the rheological properties of curing PMMA bone cement were used as the input to the finite element

analysis software Rheological properties include pseudoplastic and rheopectic viscosity of bone cement Three factors were studied in this finite element simulation, (a) the effect of prosthesis insertion velocity, (b) the effect of prosthesis insertion time duration and (c) the effect of bone cement quantity used The numerical analysis results were compared with experiment results and results of other researchers work

Chapter three

Experimental method and procedure

3 1 Experimental determination of thermal property

3 1 1 Materials

CMW3 (DePuy International Ltd England), Palacos R® and Surgical Simplex P® (Howmedica Int Ltd Limerick, Ireland) bone cements, and the Summit Mix in syringe® system were used in this study. The Stryker Instruments, Automatic High Vacuum pump 206-500 (Air input pressure 70-100 PSIG) was applied for vacuum mixing.

3 1 2 Methods

3 1 2 1 Mixing at different vacuum level

Cements were mixed using Summit Medical Mix in syringe® system, a Third-generation mixing device, as per the manufacturers instruction. Three different pressure level, 0 bar, 0.4 bar and 0.7 bar vacuum were used in this study. A single unit of cement was used for each test. It should be noted that all tests were conducted at room temperature (20 to 22°C) and relative humidity was 37%±5%.

3 1 2 2 Measurement of setting properties

The temperature of the curing acrylic bone cement was measured using a k-type (chromel-alumel) thermocouple. The temperature measurements were recorded using a data acquisition software called Pico Log, developed by Pico Technology Ltd [136]. The software was able to display real-time results, which can be imported into a spreadsheet software package, such as Microsoft Excel, for data analysis.

The temperature information was sent to Pico Log through a hardware interface called TC-08, which was an eight-channel thermocouple data logger manufactured by Pico technology Limited [136]. This interface was connected with a microcomputer via a 25-

pin male (DTE- Data terminal equipment) and 9-pin female (DCE- Data circuit termination equipment) cable of RS232 standard for serial port.

Once the cement was mixed, it was poured using Summit Medical H716 (Stryker 206-600) dual speed cement injector/gun into the sample holder mould made of PTFE (polytetrafluoroethylene) according to ASTM Specification [137]. It was equipped with a No. 24 gage wire K-type thermocouple (chromel-alumel), positioned with its junction in the center of the mould. Figure 3-1 shows section of the assembled mould. CAD drawings are shown in the appendix G.



Figure 3-1: Section of the assembled PTFE mould.

In the mean time, the plunger was set to produce the specimen of 6.00 mm height. Data acquisition package was enabled at the beginning of cement mixing. Temperature data was recorded at regular intervals of 1 second for a time span of 30 minutes. From the results it was feasible to determine maximum temperature, cure temperature and cure time [120, 137, 138]. A typical plot of temperature vs time for the polymerisation reaction can be seen in figure 3-2.

The maximum temperature, setting temperature and setting time were measured following the method described in ASTM F 451-95 [137] and ISO 5833:1992 (E) [138].

The maximum exothermic temperature was reported at the highest temperature of the temperature/time curve

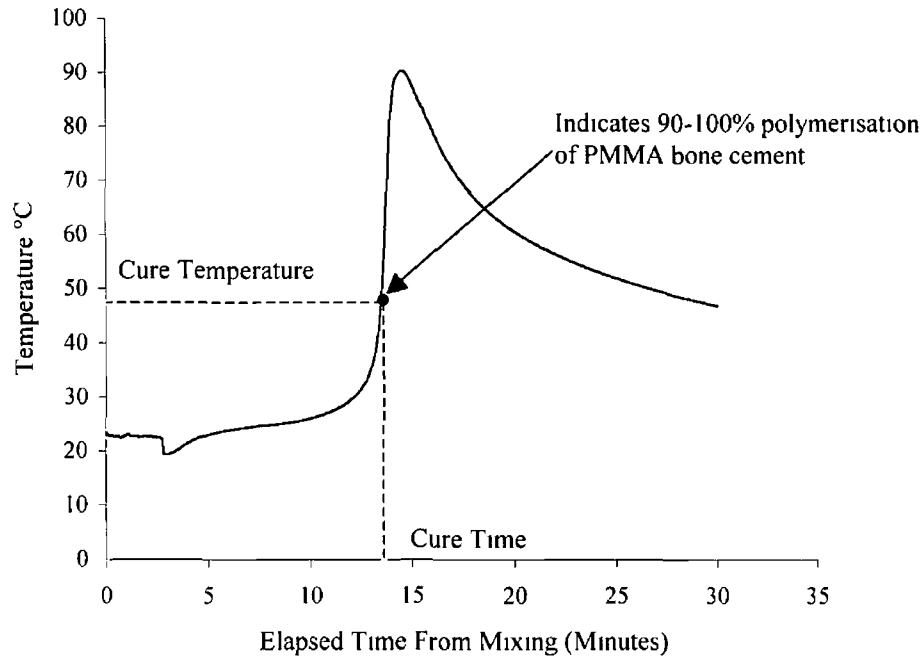


Figure 3-2 Cure temperature vs elapsed time from continuous temperature record of curing PMMA bone cement as acquired using Pico Log [120]

The curing or setting temperature can be determined by using equation (3-1) [137]

$$\text{Cure Temperature}(T_{\text{set}}) = \frac{T_{\text{Maximum cure temperature}} + T_{\text{Ambient temperature}}}{2} \quad (3-1)$$

The setting or curing time was considered as the time when the exothermic temperature rose to the midpoint between the ambient and maximum temperatures. From the continuous time versus temperature recording the setting time (T_{set}) is the time at cure temperature.

3.2 Experimental procedure for comparison to simulation work

3.2.1 Materials and accessories

The following materials and accessories were used to perform the comparison experiments.

1. Two cadaveric femur bone (Sawbones REF: 5507) as shown in figure 3-3.



Figure 3-3: Cadaveric femur bone.

2. Exeter taper pin reamer large (Stryker Howmedica Osteonics, REF: 09322000) as shown in figure 3-4.



Figure 3-4: Exeter taper pin reamer.

3. Exeter rasp 44 mm offset No 2 (Stryker Howmedica Osteonics, REF: 05809442) as it can be shown in figure 3-5.



Figure 3-5: Exeter rasp.

4. Exeter rasp handle (Stryker Howmedica Osteonics, REF: 0930-9-003) as shown in figure 3-6.



Figure 3-6: Exeter rasp handle.

5. Two-piece of femoral cement restrictor (DePuy orthopaedics, REF: 9632-03-000, LOT: 1173949) as shown in figure 3-7.

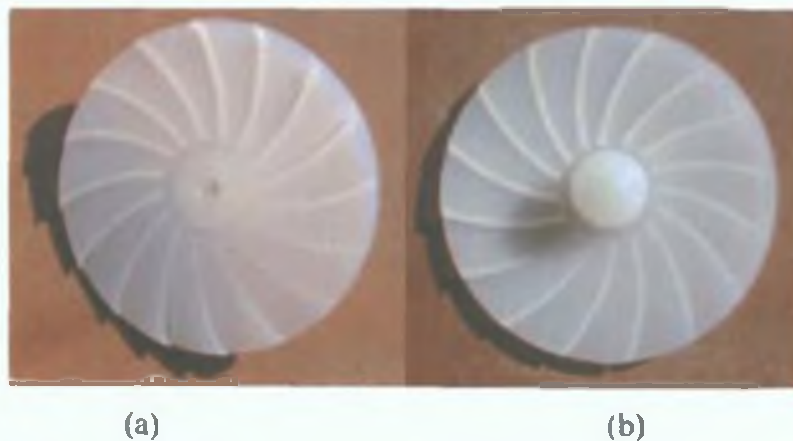


Figure 3-7: Femoral cement restrictor (a) one side, (b) other side.

6. Four pack of CMW3 40 gm bag of powder and 20 ml liquid monomer ampoule (DePuy International, REF: 3032-040, LOT: E357L40) bone cement as shown in figure 3-8.



Figure 3-8: CMW3 bone cement.

- 7 Two pieces of disposable CEMVAC® vacuum mixing system (DePuy international, REF 831215, LOT 04031638) as shown in figure 3-9

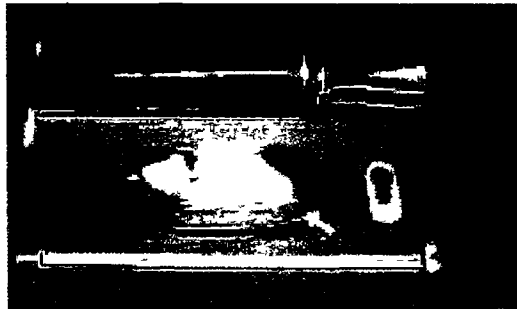


Figure 3-9 CEMVAC vacuum mixing system

- 8 CEMVAC gun system (DePuy international, REF 1203-00-10) to deliver bone cement using mixing system through femur bone as shown in figure 3-10

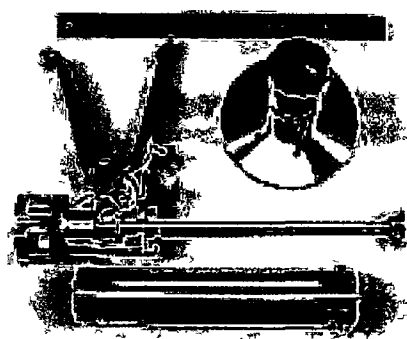


Figure 3-10 CEMVAC gun system

- 9 CMW vacu-mix plus (DePuy international) was applied for vacuum mixing as shown in figure 3-11

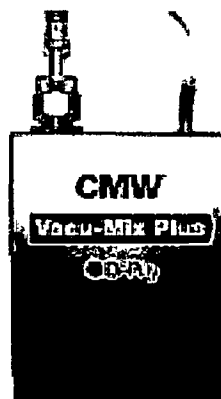


Figure 3-11 CMW vacuum pump system

- 10 One piece ultraseal standard femoral pressuriser (DePuy international, REF 3206-005) as shown in figure 3-12

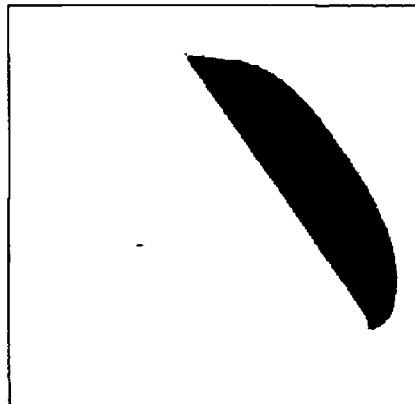


Figure 3-12 Ultraseal standard femoral pressuriser

- 11 One piece Exeter V40 stem 44 mm offset (Stryker Howmedica Osteonics, REF 058-00-443) cemented hip prosthesis as shown in figure 3-13

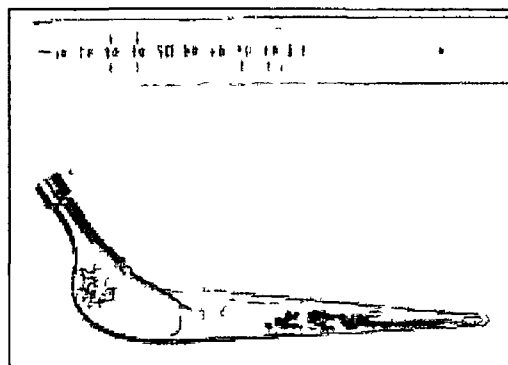


Figure 3-13 Exeter V40 stem

- 12 Stem introducer Exeter (V40) (Stryker Howmedica Osteonics, REF 0930-3-002, LOT GV278451) as shown in figure 3-14

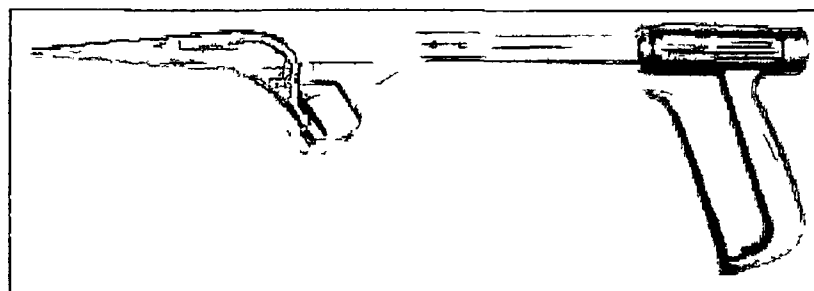


Figure 3-14 Exeter stem introducer

3.2.2 Experimental works

3.2.2.1 Procedure of hip replacement surgery

In this project, hip replacement surgery using cadaveric femur bones was performed. The steps followed here were established after consulting with the supplier [145] and manufacturer [146-148] of Stryker Howmedica Osteonics. The procedure involved in hip replacement surgery can be summarized in the following steps:

1. The femoral canal was initiated in piriformis fossa and canal reaming was started.
2. In this work, neck osteotomy (43-45 degree) was performed by sectioning the neck. Here 45-degree angle was used.
3. The femoral canal was prepared using a rasp. During an in vivo operation it is required to clean the canal by pulsed irrigation followed by vacuum suctioning, etc. Figure 3-15 shows the femur bone after preparation.



Figure 3-15: Prepared femur bone to start bone cement injection.

4. Femoral cement restrictor was introduced (10-20 mm below the tip of stem).
5. Bone cement was mixed in a vacuum mixing system (CEMVAC) according to the instruction given by the manufacturer under air vacuum pressure of 85 kPa at room temperature, 20°C.
6. Following the clinical time that is supplied by the bone cement manufacturer to use bone cement properly, CMW3 bone cement was introduced in the retrograde fashion in to the prepared canal. To ensure enough bone cement in the cavity, two packs of 40 g bone cement were mixed at a time using the CEMVAC

vacuum mixing system. The pressure was maintained using the ultraseal standard femoral pressuriser until the prosthesis inserted.

7. The prosthesis was introduced in to femoral canal after 4 and 6 minutes from the start of mixing the bone cement. After insertion of prosthesis, 5 minutes were allowed to complete bone cement polymerization. Figure 3-16 shows the treated femur bone.



Figure 3-16: Treated femur bone after polymerization of bone cement for total hip replacement.

8. The first femur bone from experiment was cut vertically from the cortical bone to the bone cement. The bone was cut into two parts, the prosthesis was relieved from the treated bone without any harm. This prosthesis was used in second experiment. Figure 3-17 shows the bone found from first experiment.



Figure 3-17: Vertical section of treated femur bone in which prosthesis inserted after 4 minute.

3.2.2.2 Measurement of the depth of penetration

The bone was cut down from the head of the femur down to a length of 17 cm as shown in figure 3-18.



Figure 3-18: Femur bone cut at a distance of 17 cm below the femur head.

Then the bone was sectioned perpendicular to the axis of femur shaft. The treated bone was sectioned from the neck of prosthesis in 10 mm interval using a handsaw. Figure 3-19 shows a section of the bone.



Figure 3-19: Sectioned bone from second experiment.

Penetration of bone cement through cancellous bone was clearly visible with the naked eye. The cancellous bone, cement-bone interface and bone cement were very clearly distinguishable with the naked eye. Using the vernier calipers the penetration depth was calculate precisely up to one tenth of a millimeter. Figure 3-20 shows the vernier calipers used to measure the penetration.



Figure 3-20: Vernier calipers used to measure the penetration of bone cement.

Penetration was calculated from each section of the femur bone at six different locations as indicated in figure 3-21. The location of measurement is indicated in this figure. Three lines (blue color line in figure 3-21) were used to locate the six positions of measurement.



Figure 3-21: Sectioned bone from second experiment with location of measurement.

The long blue color line divides the prosthesis into two equal parts. Two other blue parallel lines perpendicular to the long line were used. These two lines were positioned away from the short edges of the prosthesis but they remain inside the area of the prosthesis. The distance from short edges was equal to the radius of the corresponding fillet. Six points on the periphery of the prosthesis indicate the points for the measurement. The direction of measurement was such that it was perpendicular to the tangent of the circumference of bone cement-cancellous bone interface. The average penetration was calculated from the six readings for each section of femur bone.

Chapter four

Finite Element Analysis of bone cement penetration in total hip replacement

4 1 Brief introduction of Finite Element Analysis

Finite element analysis (FEA) is the simulation of a physical system (geometry and loading environment) by a mathematical approximation of the real system. Using simple, interrelated building blocks called elements, a real system with infinite unknowns is approximated with a finite number of unknowns [139, 140]. The basic steps in any FEA consists of the following [141]

Preprocessing Phase

- Create and discretize the solution domain into finite elements, that is, subdivide the problem into nodes and elements
- Assume a shape function to represent the physical behavior of an element, that is, an approximate continuous function is assumed to represent the solution of an element
- Develop equations for element
- Arrange and assemble the elements to present the entire problem
Construct the global stiffness matrix
- Apply boundary conditions, initial conditions, and loading

Solution Phase

- Solve a set of linear or nonlinear algebraic equations simultaneously to obtain nodal results, such as displacement values at different nodes in a structural problem, temperature values at different nodes in a heat transfer problem, or flow rate values at different nodes in a CFD problem

Postprocessing Phase

- Using the nodal values and interpolation functions, other important information, such as strain, stress etc, inside each element may be determined

4.2 Model for simulation

The porosity of cancellous bone is an essential feature that should be included in the simulation. Porous cancellous bone is obtained using the porous entity from the finite element software. Though femur bone is not symmetric, for simplicity it is assumed symmetric, an axi-symmetric model was used in this project. In reality the femur bone is a tapered cylindrical shape. But it can be assumed to be a parallel cylinder [130]. Figure 4-1 shows axi-symmetric model.

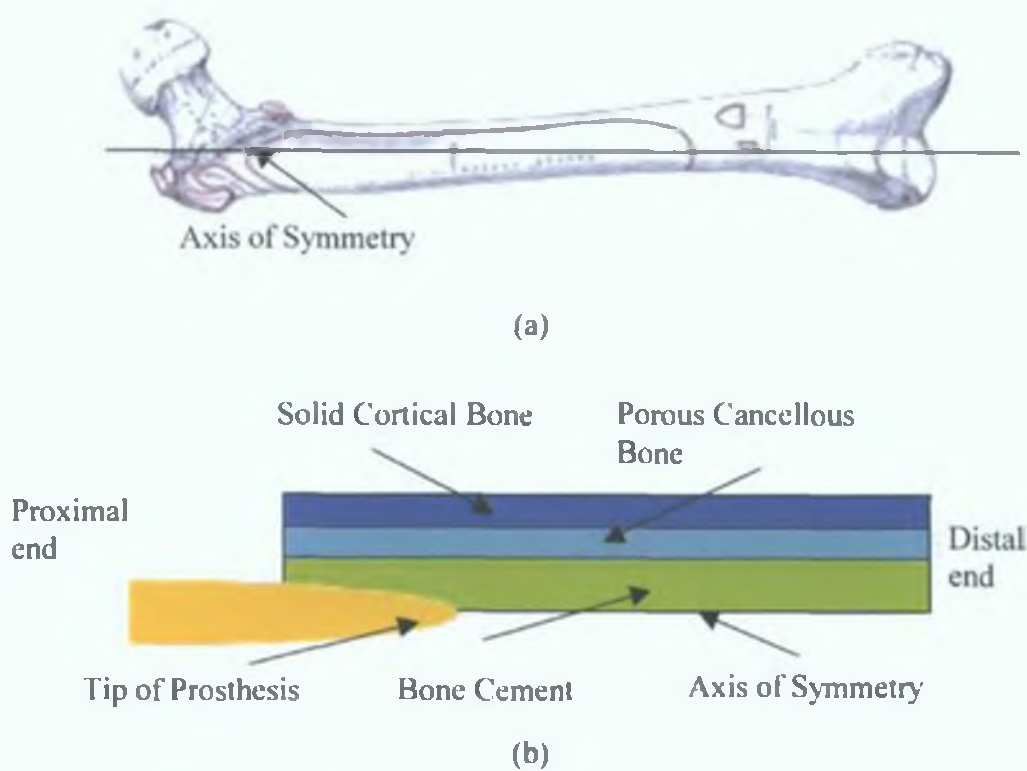


Figure 4-1: (a) Femur bone [37] and (b) Simplified axi-symmetric model.

This model shows all entities present during total hip replacement surgery. Penetration of bone cement through cancellous bone is the main objective of this simulation. So only the bone cement and the porous cancellous bone are key entity for this model. Figure 4-4 shows only these two entities after meshing with initial boundary conditions. Considering the length of the prosthesis, the length of the femur bone was selected as 15 cm for the simulation model. The amount of bone cement in the prepared cavity of femoral bone depends on the length of the femur bone and thus length of the prosthesis. The thickness of porous cancellous bone was selected as 0.7 cm. The amount of bone

cement, that is the thickness of bone cement inside the femoral canal was selected as a parameter for this study Two values were used for the axi-symmetric model, 0.8 cm and 1 cm

4.3 Defining material properties

4.3.1 Material properties of bone cement

Density and viscosity were used as the material properties of curing PMMA bone cement

The **density** of Simplex P®, Zimmer and CMW3 bone cement are 1290 kg/m³, 1230 kg/m³ and 1240 kg/ m³ respectively [73, 79]

The **viscosity** of bone cement was introduced as pseudoplastic and rheopectic independently in this simulation The effect of **pseudoplastic** behaviour using Simplex P® and Zimmer bone cements as well as **rheopectic** behaviour using Zimmer and CMW3 bone cements were studied separately

Table 4-1 shows the viscosity of two commercial bone cements (Zimmer and Simplex P®) as power law of the form of equation 1-7 Figure 4-2 shows the viscosity change with shear rate for Zimmer and Simplex P® bone cement **Pseudoplastic behaviour of Zimmer and Simplex P® bone cement** was introduced using the power law equations in the simulation

Table 4-1 Power index and Consistency coefficient of bone cement [95]

Cements formulation	Flow or power index (n)	Consistency coefficient (K)	Viscosity (η)
Zimmer	$n = 0.57$	$K = 158.49e^{0.37}$	$\eta = 158.49e^{0.17} \gamma^{-0.43}$
Surgical Simplex P®	$n = 0.65$	$K = 265.15e^{0.39}$	$\eta = 265.15e^{0.39} \gamma^{-0.35}$

The equations of viscosity verses time represent the rheopectic behaviour of bone cement as given in table 4-2 Figure 4-3 shows the trend lines of viscosity change with time for Zimmer and CMW3 bone cements [124]

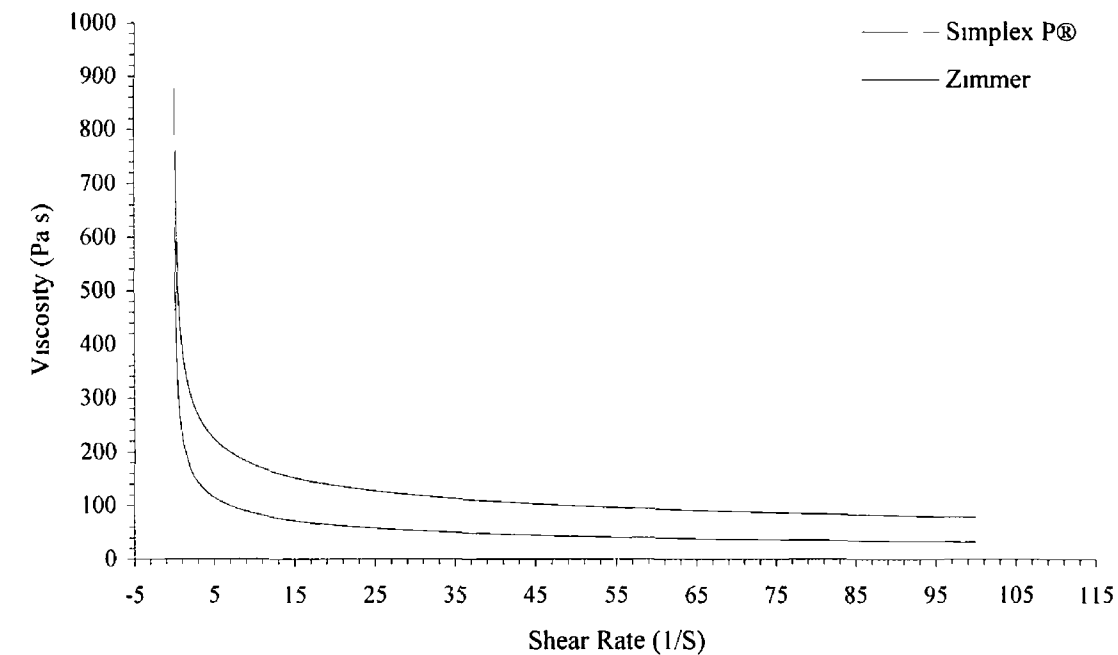


Figure 4-2 Viscosity of bone cement (Pa s) as a function of Shear rate [95]

Table 4-2 Viscosity of rheopectic bone cement [95]

Cements formulation	Equation
CMW3	$\eta = 0.0092t^2 - 3.1643t + 291.71$
Zimmer	$\eta = 0.0131t^2 - 4.0855t + 329$

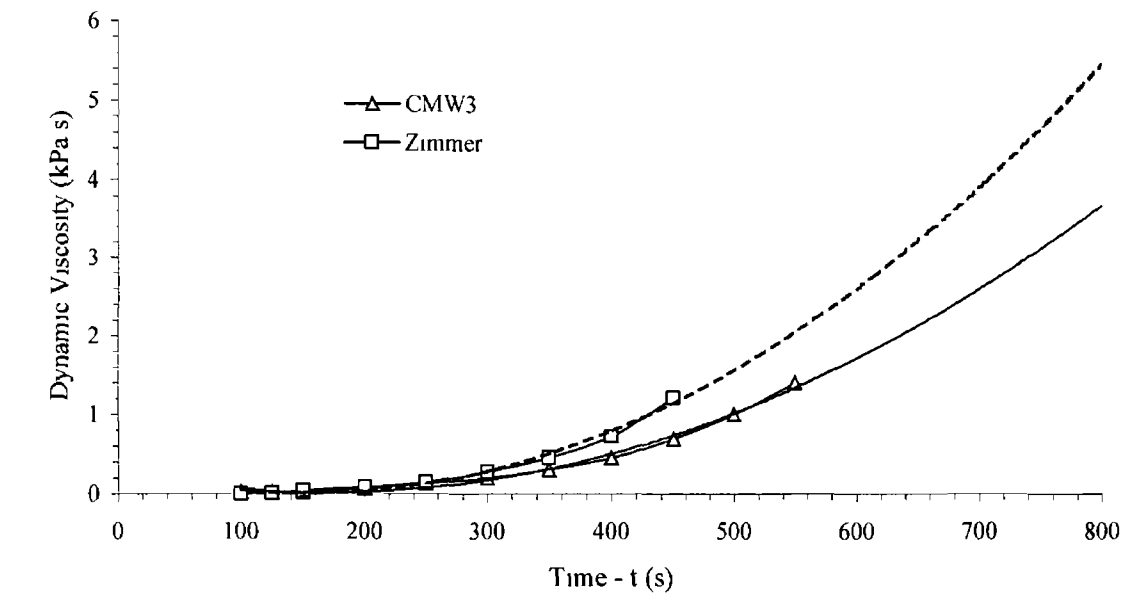


Figure 4-3 Viscosity of bone cement (Pa s) as a function of elapsed time [124]

The **rheoplectic behaviour of Zimmer and CMW3** bone cement was introduced in this simulation using the “USRVSC” subroutine This subroutine is inside a fortran source code (fisolv_user f) file Digital visual Fortran 6 5 was used to compile this source code

4 3 2 Material properties of cancellous bone

Table 4-3 lists physical and mechanical properties of cancellous bone that have been used in this simulation

Table 4-3 Physical and mechanical properties of cancellous bone

Density (kg/m ³)	Elastic Modulus (MPa)	Poisson ratio v	Porosity %	Intrinsic permeability k (m ²)	Viscosity of bone marrow (Pa s)
300 [36]	389 [35]	0 4 [35]	85 [129]	1x10 ⁻⁹ for 85% porosity [36, 42]	0 067 in vivo at 37°C [142]

4 4 Boundary condition

The boundary conditions (BCs) used in the simulations carried out were chosen to be close to the surgical procedures used in THR The load was applied in two different steps Figure 4-4 shows the BCs applied in meshed geometry

- 1 Bone cement was applied in the prepared bone cavity using a cement delivery gun in a retrograde fashion after 2 min of mixing the bone cement [108, 129] Then after waiting for 1 minute, 76 kPa pressure [108, 130] was applied using a femoral pressuriser on the femoral cavity
- 2 After 1-3 minutes [95] of applied pressure, the prosthesis was inserted into the cavity at a rate of 5-20 mm/s, that is close to the range of 3 96-12 19 mm/s [128]

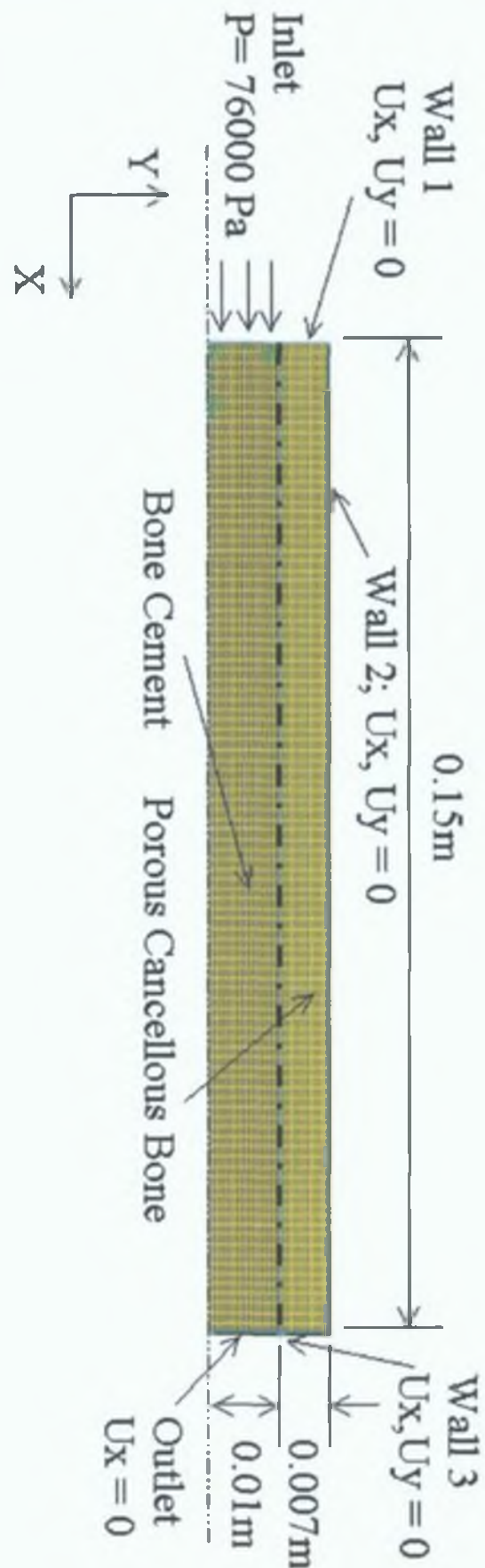


Figure 4-4: The plot shows the FE model with the initial boundary conditions.

4.5 Study parameter of this project

Three different parameters have been studied in this simulation. All of them were based on the variation of amount and duration of applied load for pseudoplastic and rheopectic bone cement. All of them are mentioned as follows:

- 1 **Effect of prosthesis insertion velocity** Two bone cements with different pseudoplastic behaviour (Simplex P® and Zimmer) and two bone cements with different rheopectic behaviour (CMW3 and Zimmer) were used to study the effect of different prosthesis insertion velocity. Pressure of 76 kPa was applied from the 4th minute to the 5th minute (2 minutes duration) of the twelve minutes simulation time for all cases. Then prosthesis insertion velocities for the four different values (5 mm/s, 10 mm/s, 15 mm/s and 20 mm/s) were applied at the 6th minute (1 minute duration) for each type of bone cement. Sixteen different simulations were carried out for this parameter. Effect of applied pressure duration: Two bone cements with different rheopectic behaviour (CMW3 and Zimmer) were used to study the effect of varying the duration of applied pressure. Pressure of 76 kPa was applied for three different time durations (1 minute, 2 minutes and 3 minutes) started from the 4th minute of the twelve minutes simulation for all cases. Six different simulations were carried out for this parameter.
- 2 **Effect of prosthesis insertion time duration** Two different bone cements with different pseudoplastic behaviour (Simplex P® and Zimmer) and two bone cements with different rheopectic behaviour (CMW3 and Zimmer) were used to study the effect of prosthesis insertion time duration. A pressure of 76 kPa was applied from the 4th minute to the 5th minute (2 minutes duration) of the twelve minutes simulation for all cases. Then the different prosthesis insertion velocities (5 mm/s, 10 mm/s, 15 mm/s and 20 mm/s) were applied at the 6th minute for three different time durations (0.5 minute, 1 minute and 1.5 minute) for each type of bone cement. Forty-eight different simulations were carried out for this parameter.
- 3 **Effect of bone cement thickness** Two bone cements with different pseudoplastic behaviour (Simplex P® and Zimmer) were used to study the effect of bone cement thickness. A model was created with two different thicknesses (8 mm and 10 mm) of bone cement as mentioned in section 4.2. A pressure of 76

kPa was applied from the 4th minute to 5th minute (2 minutes duration) of the twelve minutes simulation for all cases. Then four different prosthesis insertion velocities (5 mm/s, 10 mm/s, 15 mm/s and 20 mm/s) were applied at the 6th minute (1 minute duration) for each type of bone cement. Sixteen different simulations were carried out for this parameter.

4.6 Finite element analysis software

In this project, five different simulation software packages were studied to find the most suitable software for this type of modelling. After studying the features of these software packages, Fidap from Fluent Inc. was selected as a more appropriate software for this project. Appendix A shows a list of other softwares that have been studied. The features of the Fidap FEA software that has been used in this simulation are as follows:

- a. Fidap version 8.6.2 from Fluent Inc. has the capacity to include porous media implicitly by entering the desired parameters.
- b. There is no restriction on the number of nodes that can be used during meshing.
- c. Fidap supports multiphase simulations. Porous media and fluid can be treated as separate phases [149]. The elastic properties of porous cancellous bone were included in this analysis.
- d. The volume of Fluid (VOF) feature is available for both 2D and 3D.

The following conditions were assumed throughout the finite element analysis:

1. Bone cement was assumed to be a Pascalian fluid.
(A Pascalian fluid is a fluid where the pressure applied to a confined fluid at any point is transmitted undiminished throughout the fluid in all directions and acts upon every part of the confining vessel at right angles to its interior surfaces.)
2. The pressure was applied on the cavity. The mass flow during injection of the bone cement using the bone cement delivery system was neglected.

4.7 Solution parameters of the simulation

In this work, the 4-node quadratic element was used for each simulation. The finite element model consisted of 3030 elements. The mesh density convergence was checked.

using four different amounts of elements in the model for the penetration of pseudoplastic Simplex P® and rheopectic CMW3 bone cement (Appendix B) The aspect ratio was in the range of 1 to 1.2

Time step increments of 0.001 second and 0.0008 second were used in this transient analysis for rheopectic and pseudoplastic bone cements respectively. This time step was determined by checking the time step convergence for the penetration of pseudoplastic Simplex P® and rheopectic CMW3 bone cement (Appendix B)

High-order of upwinding schemes was used as the **convergence criteria**. It uses second-order accuracy [150]. The velocity convergence tolerance was set to 0.001.

The fluid problem is nonlinear in nature. A steady state algorithm may not yield satisfactory results. Instabilities can result from a number of factors [143]

1. The matrices may have poor condition numbers because of the finite element mesh or very large gradients in the actual solution.
2. The fluid phenomena being observed could be unstable in nature.

The segregated **algorithm** was used to solve the model. The segregated approach substantially reduces disk storage requirements compared to the fully coupled solver. Due to its sequential and uncoupled nature, the segregated solver requires more iterations than the coupled solvers. On the other hand, as the size of the problem grows (that is, the number of mesh points) the time required for each full iteration of the segregated approach will be increasingly less than that of the coupled approach [151].

Overall convergence of the segregated solver is measured through the convergence monitoring parameters. A convergence monitor is calculated for each degree of freedom at each global iteration. It is loosely normalized rate of change of the solution from one global iteration to the next and is calculated for each degree of freedom (DOF) as follows

$$M_f = \frac{\sum_{i=1}^N |f^k - f^{k-1}|}{\sum_{i=1}^N |f^k|}$$

where M_f = Convergence monitor for degree of freedom f

N = Total number of finite element nodes

f = Degree of freedom

k = Current global iteration number

Chapter five

Results, comparison and discussion

5 1 Polymerisation study

The temperature variation with polymerisation time was experimentally determined, detailed in chapter 3 Two sets of data were used as the inputs for the simulation, as mentioned in chapter 4 In this section, the maximum temperature, the setting temperature and the setting time of the bone cement mixed under different vacuum level were investigated Figures 5-1 to 5-3 show temperature variation with polymerisation time for three bone cements mixed at three different vacuum pressures Maximum temperature, setting temperature and setting time were calculated from these figures according to the definition given by the ASTM [137] as mentioned in section 3 1 2 2 of chapter 3 Table 5-1 presents the values of these parameters

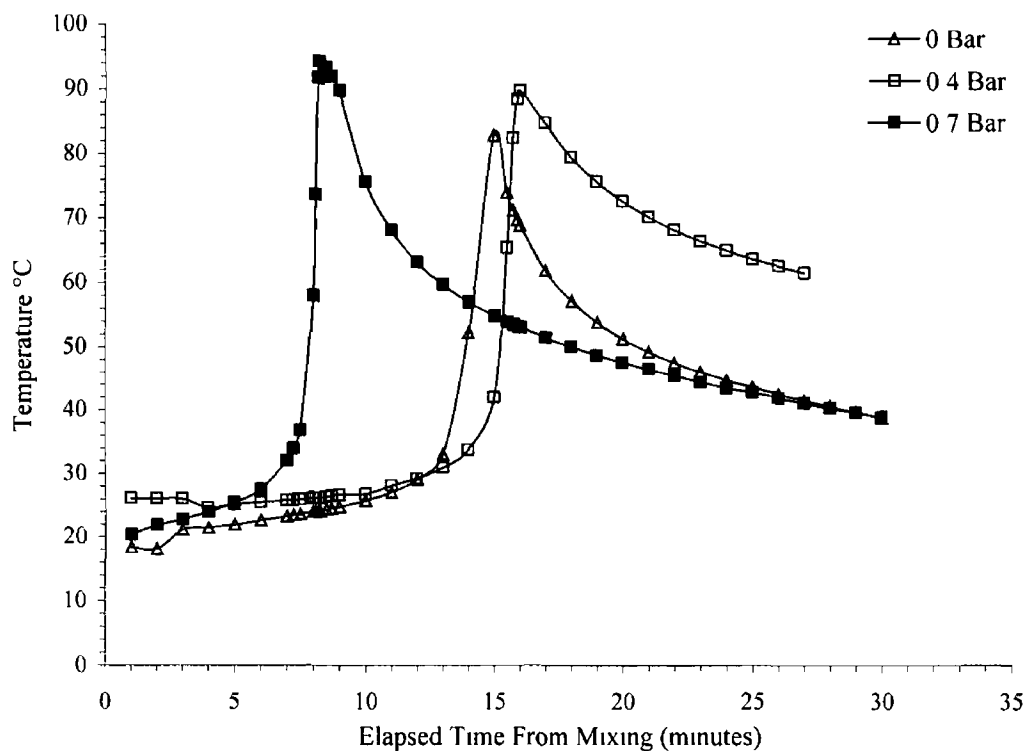


Figure 5-1 Temperature vs elapsed time from continuous temperature record of curing CMW3 mixed at different vacuum levels

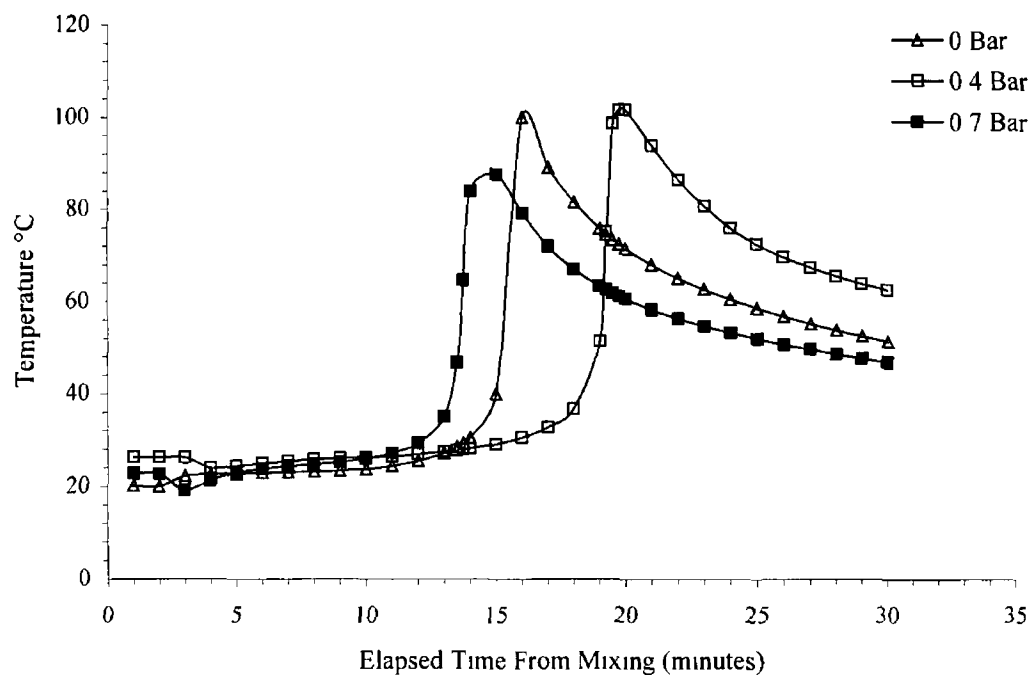


Figure 5-2 Temperature vs elapsed time from continuous temperature record of curing Simplex P® mixed at different vacuum levels

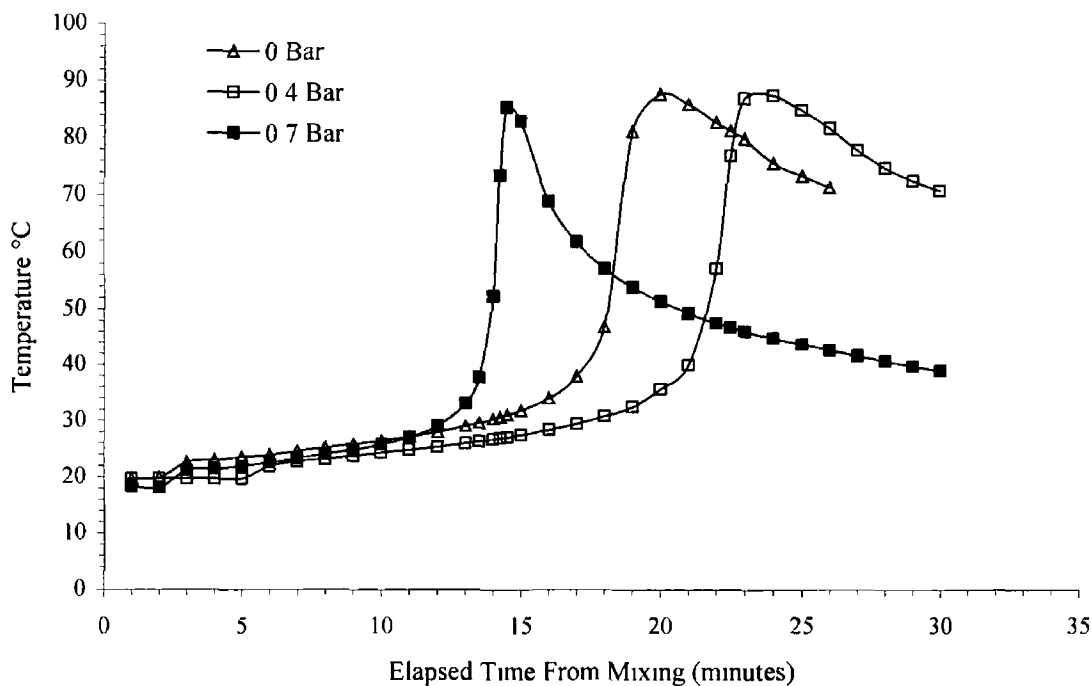


Figure 5-3 Temperature vs elapsed time from continuous temperature record of curing Palacos R® mixed at different vacuum levels

Table 5-1 Temperature parameters of bone cements determined using the Summit Mix in syringe® system

Pressure Level	Bone Cement	Maximum temperature (°C)	Cure Temperature (°C)	Setting time (minutes)
0 Bar (Atmospheric pressure)	Palacos R®	88 62	53 08	18 20
	CMW 3	86 38	51 53	13 97
	Simplex P®	104 25	60 83	15 34
-0 4 bar (-39 kPa)	Palacos R®	87 78	52 19	21 87
	CMW 3	90 19	53 45	15 29
	Simplex P®	101 84	59 52	19 12
-0 7 bar (-70 kPa)	Palacos R®	86 38	51 53	13 97
	CMW 3	94 16	55 63	7 98
	Simplex P®	90 17	53 69	13 61

5 1.1 Maximum temperature

It can be observed by examining the maximum temperature data of all bone cements that Simplex P® bone cement generates the highest maximum temperature, 104 °C and 101 84 °C, mixed at atmospheric pressure and 0 4 bar vacuum respectively It can be observed from table 1-10 that powder to liquid ratio is 1 0 5 for Simplex P® [71, 73] The powder to liquid ratios are 1 0 46 and 1 0 45 for Palacos R® and CMW3 respectively [73, 74] It is likely that the lower powder to monomer liquid ratio in Simplex P® causes an increase in the specific mass of polymerising monomer materials and thus the increase in the maximum temperature

Figure 5-4 shows maximum temperature change with the change of vacuum level for different mixing pressures The maximum temperature decreases with increasing vacuum level during mixing for Simplex P® and Palacos R® bone cement The decrease is greater for Simplex P® than Palacos R® bone cement Bettencourt et al [144] found that for vacuum pressures close to 0 150 bar the monomer release was reduced compared to the hand stirring in air or vacuum mixing at pressure less than 0 154 bar This was due to increased volatilisation and a decrease in the boiling point temperature of the monomer at low pressure At a higher vacuum pressure than 0.154 bar vacuum pressure, the amount of monomer decreases from the mixing system As a result, powder to liquid ratio increases and maximum temperature decreases Opposite

trends are observed for CMW3 bone cement. Unmixed powder was observed in the Summit mixing syringe® system during mixing of CMW3 bone cement at increased vacuum pressure. It has been reported that there are significant amounts of unmixed powder during mixing in a vacuum mixing system with a fixed central axis [115]. As a result, it is likely that the powder to liquid ratio decreases in the mixture for CMW3 bone cement that is mixed at a lower vacuum pressure. This results in a higher maximum temperature at a decreased mixing pressure for CMW3 bone cement.

The maximum temperatures of CMW3 and Palacos R® that were mixed at the same vacuum level are almost equal.

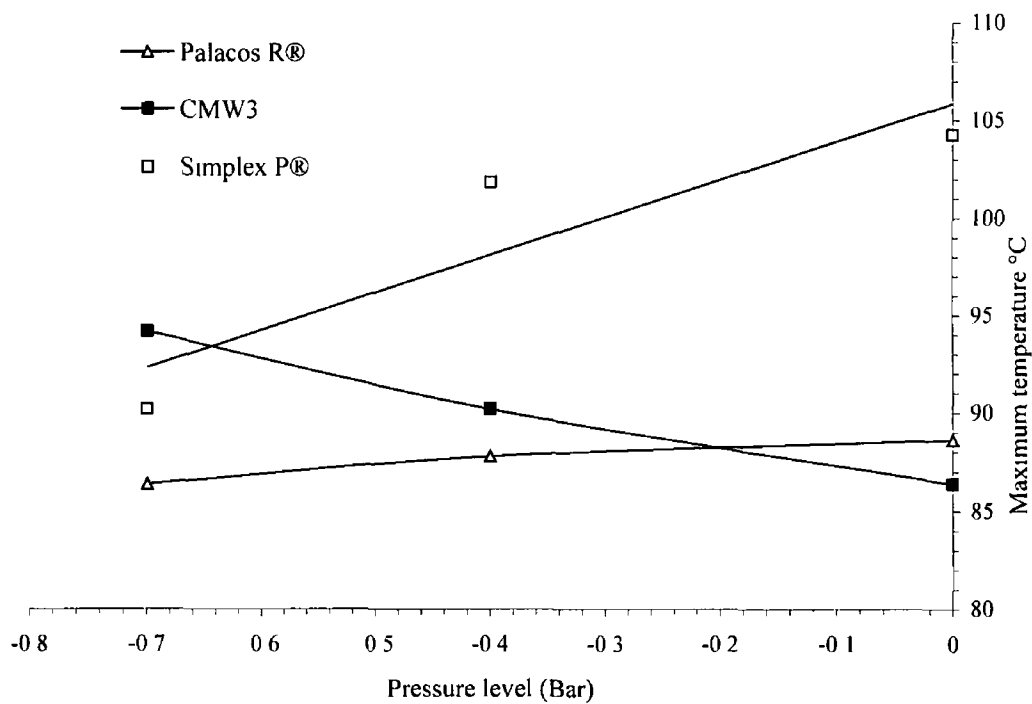


Figure 5-4 Maximum temperature with vacuum level for mixing pressures from atmospheric pressure to -0.7 bar

5.1.2 Setting temperature

Figure 5-5 shows that the cure or setting temperature data have similar trends for the maximum/peak temperature results. Due to that the cure temperature of the bone cement is proportional to the peak temperature according to equation (3-1), CMW3 mixed at atmospheric pressure and Palacos R® mixed at 0.7 bar vacuum results in a minimum

setting/curing temperature of 51.53 °C Simplex P® mixed at atmospheric pressure results in a maximum setting temperature of 60.83 °C

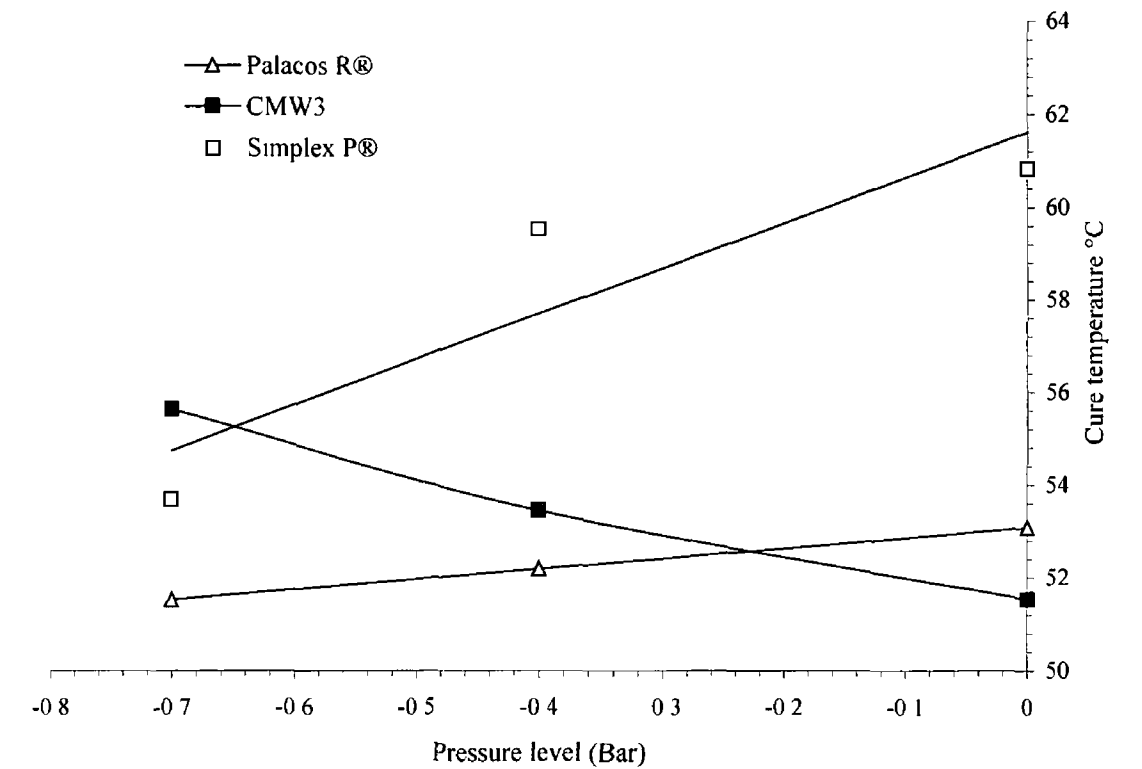


Figure 5-5 Cure temperature with vacuum level of mixing pressure from atmospheric pressure to -0.7 bar

5.1.3 Setting time

The setting/curing time is the time at which the acrylic bone cement reaches between 90-100% cure. It can be noted from figure 5-6 that the setting time of bone cements mixed at atmospheric pressure to 0.4 bar vacuum pressure increases. The increasing rate is insignificant for CMW3. Then setting time of bone cements decreases for all cements that are mixed at further lower vacuum pressure like 0.7 bar.

The results show that as the cure temperature decreases the cure time increases up to 0.4 bar vacuum pressure with minor increase of CMW3, due to the reduced rate of polymerisation for all three types of bone cements (due to increased powder to monomer ratio). At the higher-level vacuum (-0.7 bar) mixing bone cement polymerisation reaction rate increases and thus setting time decreases for the same type of bone cement. For CMW3 bone cement reaction rate is also faster for the cement that is mixed at lower vacuum level. Setting time is 7.98 minutes for CMW3 mixed at -0.7

bar, whereas it is 15.29 minutes and 13.97 minutes for those that are mixed at -0.4 bar and atmospheric pressure respectively. It can be observed that for each bone cement minimum setting time is found by maximum vacuum pressure during mixing.

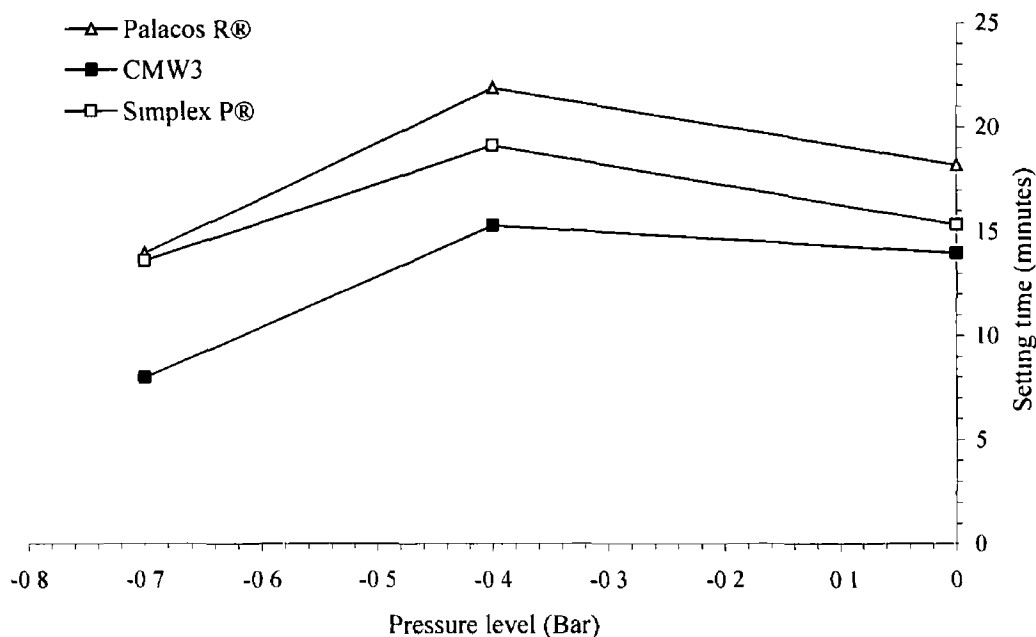


Figure 5-6 Setting time change with vacuum level of mixing pressure from atmospheric pressure to -0.7 bar

The decrease in setting time by vacuum mixing can be attributed to the reduced oxygen concentration in the mixer [117]. It was found using Electron Spin Resonance (ESR) spectroscopy [121] that in the MMA polymerization process, oxygen lowered the free radical concentration from the mixture of powder and monomer. Thus the early phase of radical polymerization of MMA during bone cement curing is retarded. It can be noted that mixing at reduced oxygen content polymerisation occurs at a higher rate. This results in the completion of the polymerisation reaction in a shorter time period and thus the setting time also decreases.

In the clinical point of view, understanding the difference in setting temperature and setting time of different bone cements may improve the surgeon's ability to handle bone cement better. Surgeon uses bone cement at an operation condition that results in the lowest cure temperature so that less thermal necrosis occurs in living bone tissue. Along with this property setting time is also considered to choose a bone cement for a particular operation such as THR, TKR or vertebroplasty. The proper time for different

steps in the operation, such as application of bone cement in cavity or insertion of prosthesis, determines the suitable setting time for a bone cement.

5.2 2D Simulation of bone cement flow in total hip replacement

The main objective of the study was to incorporate the flow properties of pseudoplastic and rheopectic behaviour of PMMA bone cements using finite element software. In this research FIDAP version 8.6.2 module of fluent simulation software was used. FIDAP gives better results for the penetration of bone cement through cancellous bone compared to other simulation software (See Appendix A for the list of simulation software that were studied for this work).

Fluent software has more than six modules. One of those is FIDAP, which is used for analysis of dynamic fluids. It has the capacity to use Volume of Fluid (VOF) in both 2D and 3D analysis. In a Volume of Fluid (VOF) analysis, simulation software uses an algorithm to track the evolution of the free surface [149].

The pseudoplastic behaviour of Simplex P® and Zimmer bone cements along with the rheopectic behaviour of Zimmer and CMW3 bone cements were used to analyse the flow of bone cement through porous cancellous bone during a total hip replacement surgery. The simulation was performed for a period of twelve minutes using a transient analysis. This time was enough to complete 99% polymerisation of the bone cement. The values of bone marrow viscosity and porosity of cancellous bone were taken as 0.067 Pa.s and 85% respectively as mentioned in table 4-2. The rest of the material properties used in this simulation are given in section 4.3 of chapter 4.

Three different parameters were studied in this project.

- a. Effect of prosthesis insertion velocity.
- b. Effect of prosthesis insertion time duration.
- c. Effect of bone cement thickness.

Figures of pressure distribution with free surface of bone cement were obtained for different simulations. Appendix C shows figures of the pressure distribution with the free surface of the bone cement at the end of simulation for all parameters. As an

example figure 5-7 and 5-8 shows the pressure distribution with the free surface of the bone cement at the start and end of the simulation.

Figure 5-7 shows the pressure distribution in the bone cement and the free surface of the bone cement at the start of simulation. The proximal and distal end are also indicated. A pressure of 76 kPa was applied on the proximal end for 2 minutes duration 3 minutes after the start of the bone cement mixing. Later on, velocity was applied on the axis of symmetry for 1 minute duration 5 minutes after the start of the bone cement mixing. (Figure 4-4 shows the FE model with the initial boundary conditions).

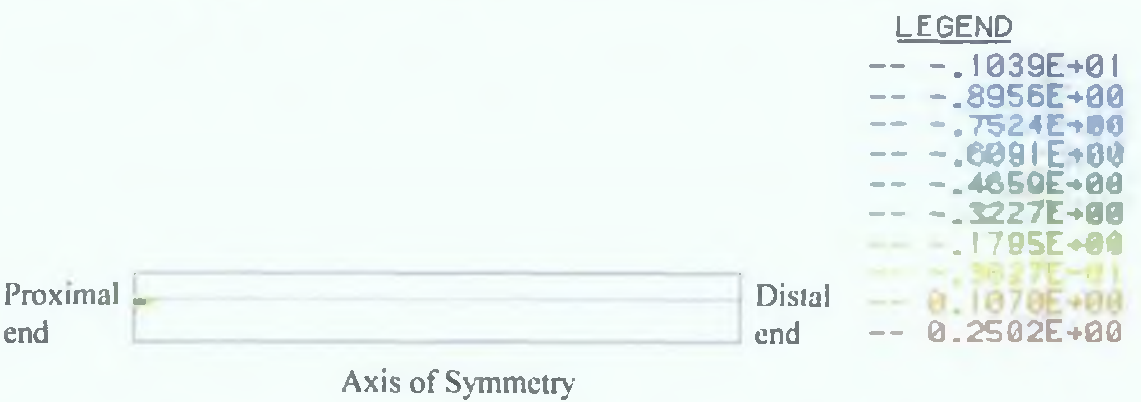


Figure 5-7: The Pressure (Pa) distribution with the free surface of the bone cement for pseudoplastic CMW3 bone cement at the start of the simulation. A pressure of 76 kPa was applied on the proximal end of the femur from 3 to 5 minutes and the prosthesis insertion velocity of 20 mm/s was applied from 5 to 6 minutes.

Figure 5-8 shows the pressure distribution in the bone cement and the free surface of the bone cement at the end of the simulation (12 minutes).



Figure 5-8: The pressure (Pa) distribution at the free surface of the bone cement for pseudoplastic CMW3 bone cement at the end of the simulation (720 seconds). A pressure of 76 kPa was applied on the proximal end of the femur from 3 to 5 minute and the prosthesis insertion velocity of 20 mm/s was applied from 5 to 6 minute.

Each simulation gives two figures for the free surface of the bone cement. One figure shows the free surface at the beginning of the simulation and other figure shows the free surface at the end of the simulation. The distance between the free surfaces of these two figures denotes the depth of penetration of the bone cement through the cancellous bone. The present version of FIDAP does not provide any feature to measure the position of the free surface. To calculate the depth of penetration, figure 5-8 was printed to get a hard copy (1:1 scale ratio). Vertical lines were drawn at intervals of 1 cm from the proximal end to the distal end. Then penetration was calculated using a vernier calliper. Bone cement penetration was greater in the proximal end than the distal end of the axisymmetric femoral bone.

Appendix D shows an example of the input or log files (Journal file for pre-processor, Gambit, and FIPREP file for FIDAP) for this study. The pseudoplastic behaviour of the bone cement was introduced in the model using the power law. On the other hand, rheopectic behaviour was introduced in the model using a user-defined subroutine. In Appendix D, one example of the user-defined subroutine that was used to introduce rheopectic behaviour into the bone cement is also included.

5.2.1 Effect of prosthesis insertion velocity

Prosthesis insertion rate is an important parameter in total hip replacement surgery. It was reported in literature that this rate is in the range of 3.96-12.19 mm/s [128]. Considering this range, four prosthesis insertion rates (5 mm/s, 10 mm/s, 15 mm/s and 20 mm/s) were selected to study the effect of prosthesis insertion velocity. Bone cement was injected into the prepared femoral cavity using a bone cement delivery system. Then, a pressure of 76 kPa was applied on the bone cement at the proximal end for a duration of minutes 2, 3 minutes after the start of bone cement mixing. Later a 5-20 mm/s prosthesis insertion velocity was applied for a duration of 1 minute 5 minutes after the start of bone cement mixing. The penetration of the bone cement was calculated for each boundary condition according to the steps that have been mentioned in the previous section (section 5.2). Appendix E shows all tables for the bone cement penetration under different simulation conditions. The penetration of bone cement was

plotted for different prosthesis insertion velocities as a function of distance from the proximal end of the femur bone for each bone cement

5 2 1.1 Penetration of bone cement through porous cancellous bone

Figure 5-9 shows that increased prosthesis insertion velocity increases the penetration of bone cement through cancellous bone for **pseudoplastic behaviour** of Simplex P® bone cement It can be observed from figure 5-8 that more pressure is developed on bone cement up to 25 mm distance from proximal end In that particular boundary condition it can also be noted that up to 25 mm distance 11 to 72 kPa pressure is sustained Similar pressure distribution pattern can also be observed for other boundary conditions (Appendix C) Due to this, penetration up to 30 mm from proximal end is greater than in other location A greater insertion rate generates more shear rate on the porous bone This is the reason for grater penetration when a higher prosthesis insertion rate is used The average penetration of Simplex P® bone cement for pseudoplastic behaviour is 2 3 mm

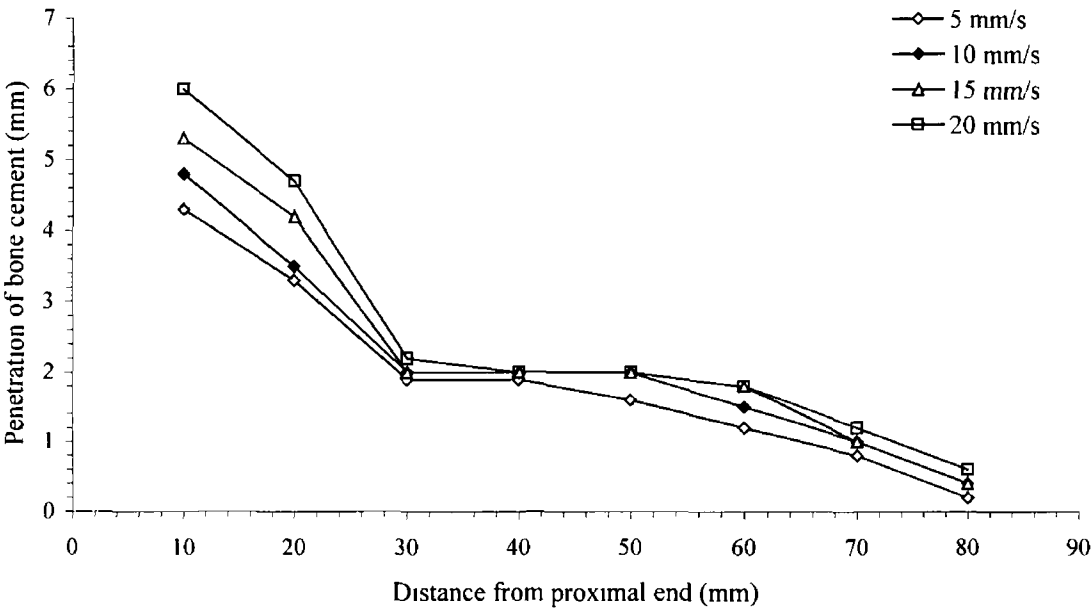


Figure 5-9 Penetration of pseudoplastic Simplex p® bone cement through cancellous bone

Increasing the insertion velocity of prosthesis results in greater penetration for pseudoplastic behaviour of Zimmer bone cement, as shown in figure 5-10 Increased

penetration was found due to the greater shear rate at higher prosthesis insertion rate
The average penetration of Zimmer bone cement for pseudoplastic behaviour is 3.1 mm

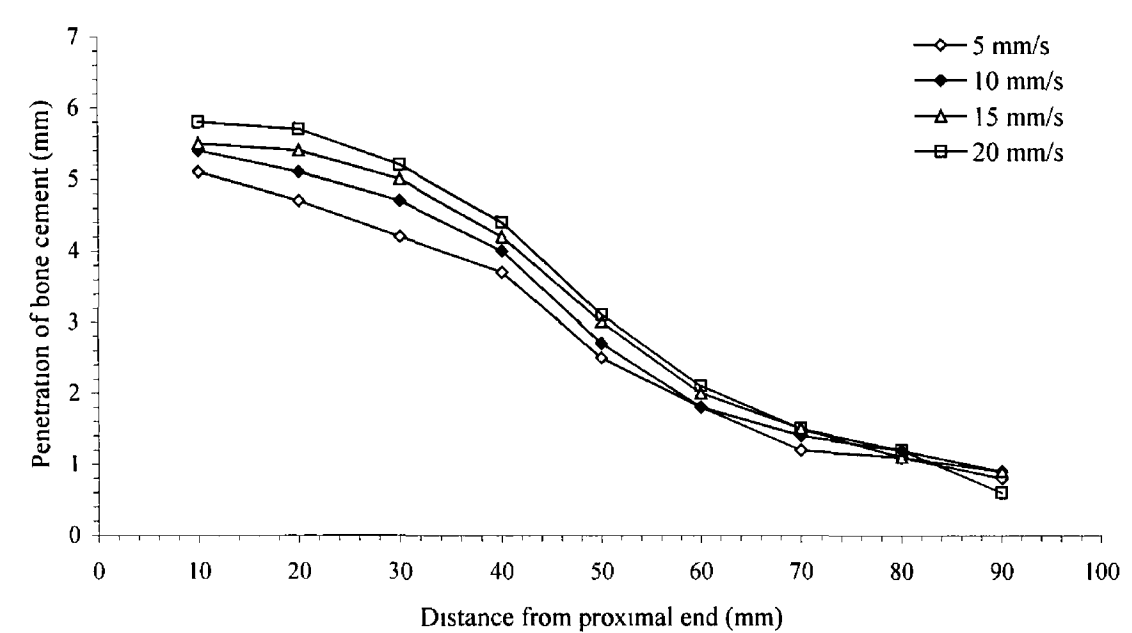


Figure 5-10 Penetration of pseudoplastic Zimmer bone cement through cancellous bone

Figure 5-11 and 5-12 shows the penetration for **rheoplectic behaviour** of CMW3 and Zimmer bone cement. Here the boundary condition was similar to the pseudoplastic behaviour of Simplex P® and Zimmer bone cement.

Figure 5-11 shows that increases in the prosthesis insertion velocity has no significant influence in CMW3 bone cement penetration through cancellous bone in a particular location. Influence of prosthesis insertion rate was observed at a location of 30 mm from proximal end due to the sustained pressure up to this depth. The average penetration of rheoplectic CMW3 bone cement is 2 mm. Figure 5-12 shows similar trends of no significance for rheoplectic Zimmer bone cement. The prosthesis insertion rate was seen to have little influence at 30 to 70 mm from proximal end. The average penetration of rheoplectic Zimmer bone cement is 2.1 mm. Increased prosthesis insertion rate increases the shear rate of penetrating bone cement. Shear rate does not influence the viscosity of rheoplectic bone cements, so increasing the velocity has no influence on the penetration of rheoplectic bone cement.

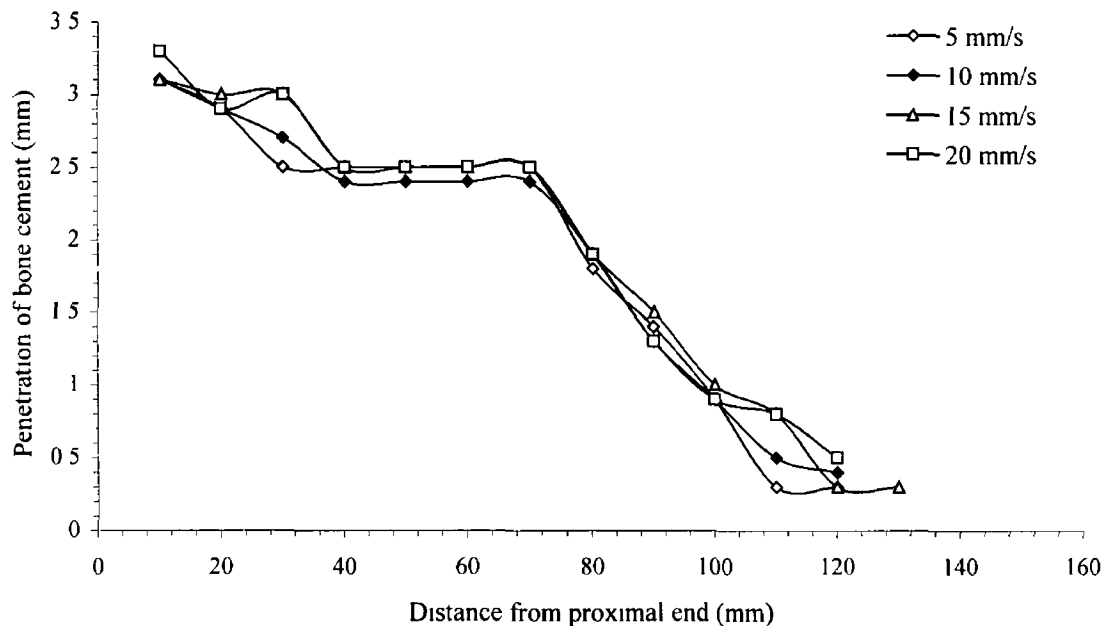


Figure 5-11 Penetration of rheopectic CMW3 bone cement through cancellous bone

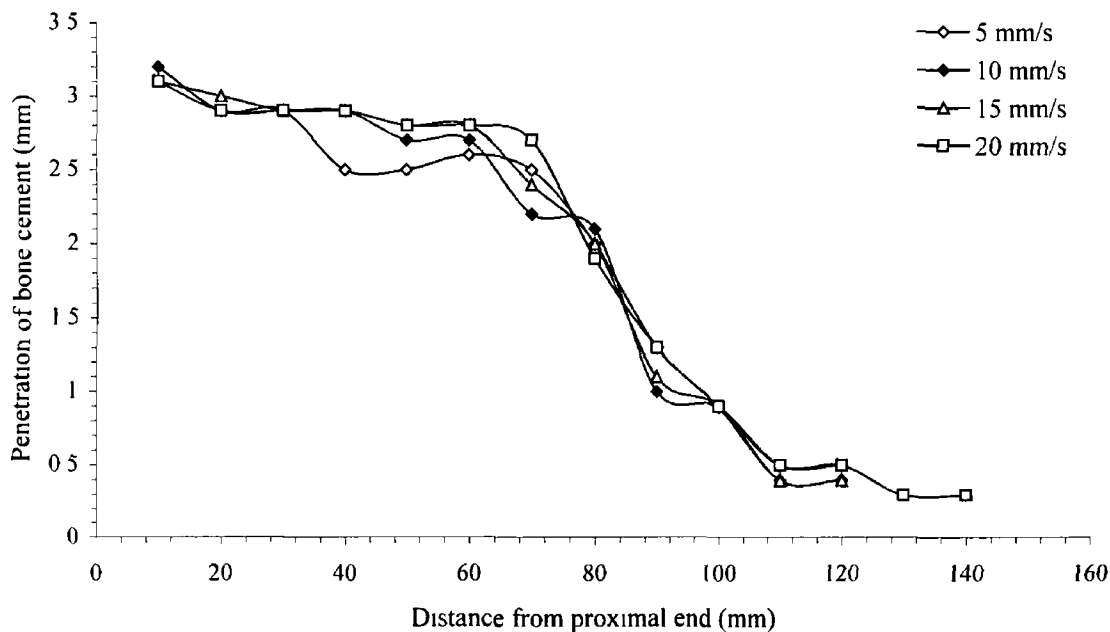


Figure 5-12 Penetration of rheopectic Zimmer bone cement through cancellous bone

Figure 5-13 and 5-14 show the **influence of time duration of applied pressure** on the penetration of bone cement for rheopectic behaviour of CMW3 and Zimmer respectively. The only variable is the duration of the applied pressure. Each type of rheopectic bone cement was simulated for three different time durations. In these simulations (six different simulation), pressure of 76 kPa was applied on the bone

cement at the proximal end for 1, 2 and 3 minutes duration 3 minutes after the start of the bone cement mixing Total simulation time was 12 minutes

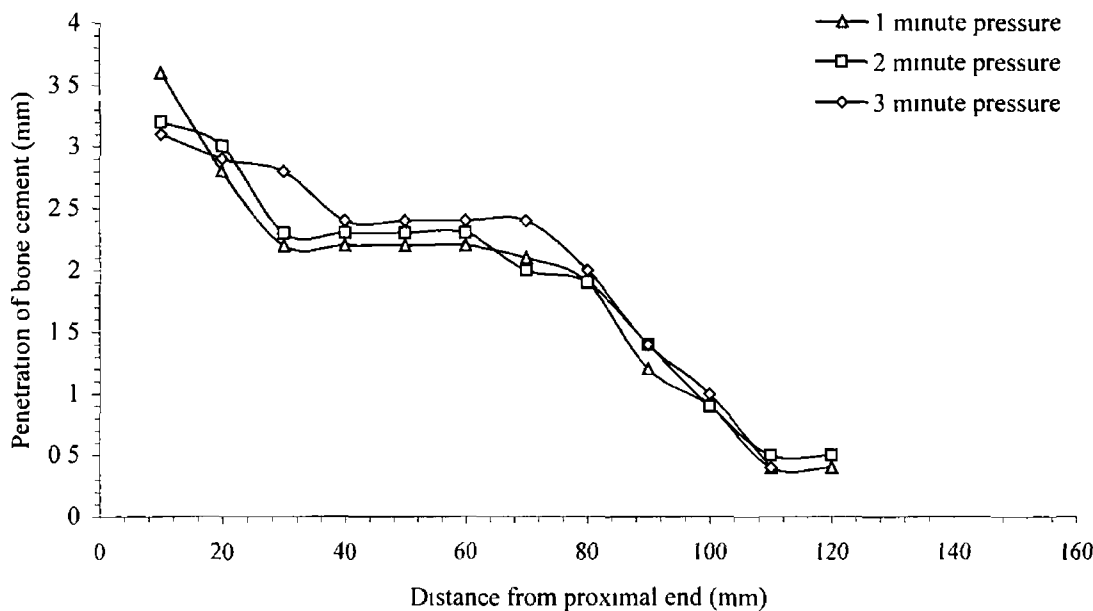


Figure 5-13 Penetration of rheopectic CMW3 bone cement through cancellous bone

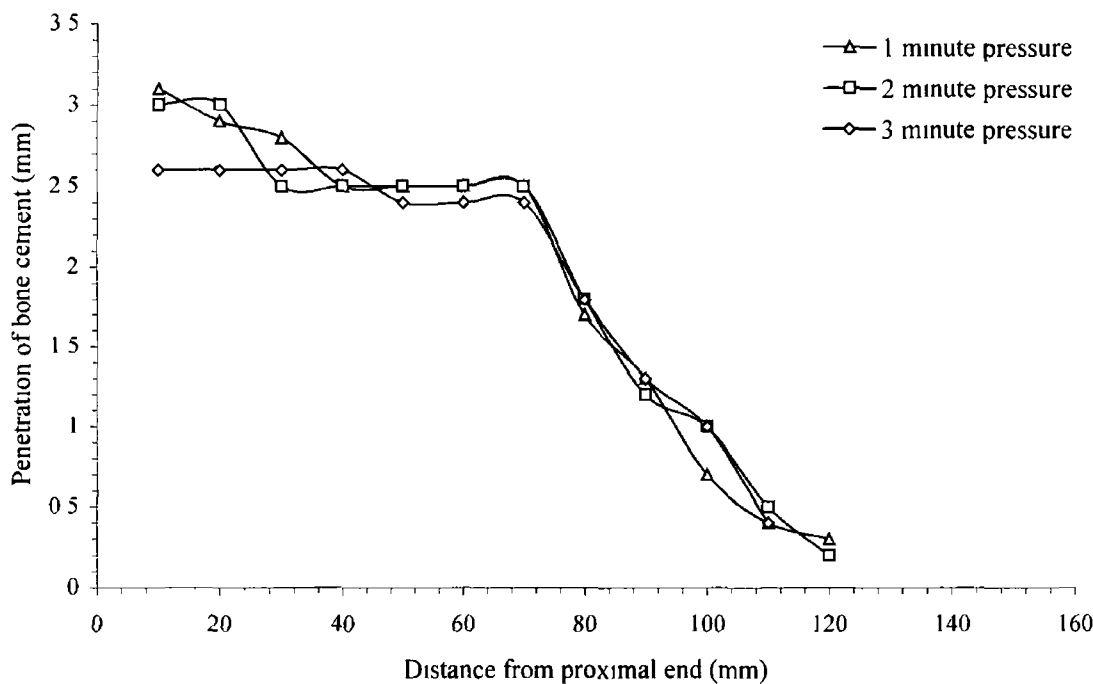


Figure 5-14 Penetration of rheopectic Zimmer bone cement through cancellous bone

Penetration of bone cement was plotted as a function of the distance from the proximal end of femur bone. A marginal increase of penetration is observed with increasing pressure duration. Rheopectic CMW3 (Figure 5-13) shows a marginal increase in the penetration in the location ranging from 20 to 70 mm from the proximal end.

5.2.1.2 Trends of penetration with respect to prosthesis insertion velocity

Figure 5-15 shows the penetration of bone cement through cancellous bone at 20 mm distance from the proximal end of femur bone as a function of the prosthesis insertion velocity. Each curve indicates a different bone cement. All the curves indicate that the penetration increases with increasing insertion velocity of prosthesis. The slope of the curve is greater for the pseudoplastic behaviour of Simplex P® and Zimmer bone cement. On the other hand, the slope of the curve is low for the rheopectic behaviour of Zimmer and CMW3 bone cement with respect to pseudoplastic bone cement. This indicates that the increase in penetration rate is greater for the pseudoplastic behaviour of Simplex P® and Zimmer bone cement.

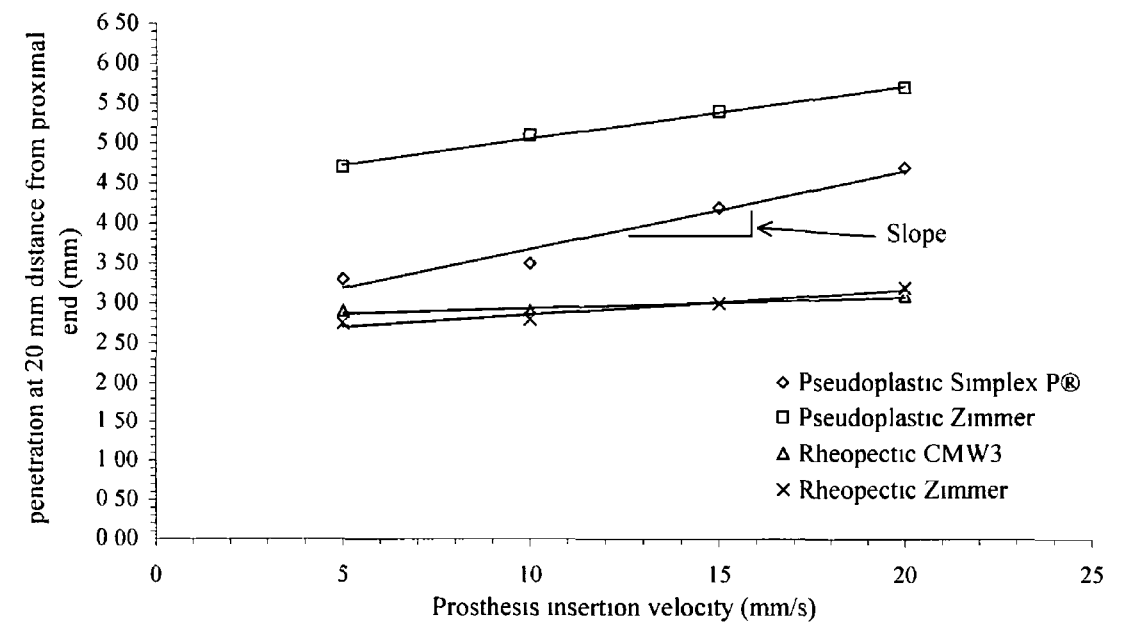


Figure 5-15 Penetration of bone cement through cancellous bone as a function of the prosthesis insertion velocity

The insertion rate of prosthesis decreases the viscosity of pseudoplastic bone cement due to the increasing shear rate [77] and this behaviour helps to increase the penetrate of

the bone cement through porous cancellous bone. On the other hand, insertion rate of prosthesis has no effect on the viscosity of the rheopectic bone cement and thus no effect on the rate of penetration of the bone cement through porous cancellous bone.

The pseudoplastic behaviour of bone cement is sensitive to the prosthesis insertion rate for the penetration of bone cement. A higher prosthesis insertion speed results in greater penetration of bone cement through cancellous bone.

The curve equations and R^2 values of Simplex P®, CMW3 and Zimmer bone cement here determined using regression analysis and the best fitting method. All equations and R^2 values are shown in table 5-2.

Table 5-2 Best fitting equation and R^2 values for pseudoplastic and rheopectic behaviour of bone cement

Bone cement	Best fitting equation	R^2 value
Pseudoplastic Simplex P®	$y = 0.098x + 2.7$	$R^2 = 0.96$
Rheopectic CMW3	$y = 0.014x + 2.8$	$R^2 = 0.89$
Rheopectic Zimmer	$y = 0.031x + 2.55$	$R^2 = 0.95$
Pseudoplastic Zimmer	$y = 0.066x + 4.4$	$R^2 = 0.99$

R^2 values show that the relation between the applied velocity and the average penetration are significant for all cases. These equations can be used to get the penetration at a certain prosthesis insertion velocity.

5.2.1.3 Maximum pressure developed in the bone cement

Figure 5-16 shows the maximum pressure developed in bone cement during pressurisation as a function of prosthesis insertion velocity. Each curve represents different bone cement. The slope of the curve is almost zero for the rheopectic behaviour of the Zimmer and CMW3 bone cement. This indicates that the maximum pressure developed in bone cement does not change with changing prosthesis insertion rate. On the other hand, the slope of the curve is negative and the magnitude is greater for the pseudoplastic behaviour of Simplex P® and Zimmer bone cement. This indicates

that maximum pressure decreases with increasing prosthesis insertion velocity for the pseudoplastic behaviour of Simplex P® and Zimmer bone cement

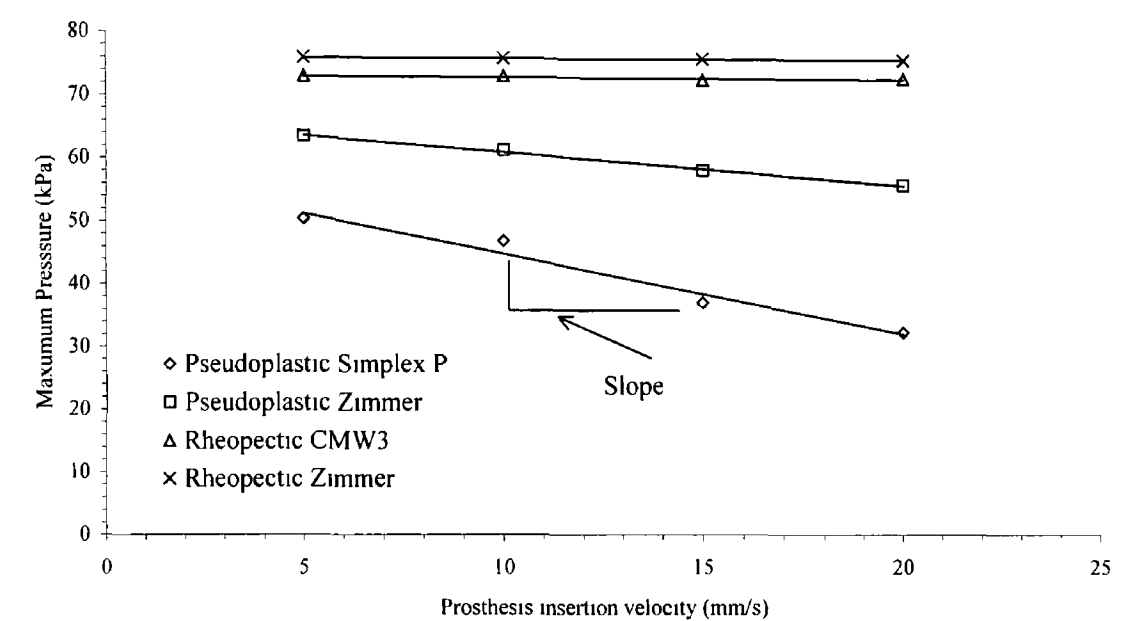


Figure 5-16 Maximum pressure as a function of prosthesis insertion velocity

Section 5 2 1 2 shows that the increasing prosthesis insertion rate increases the penetration of the bone cement due to the decreased viscosity of the pseudoplastic bone cement. The penetration of the bone cement is achieved through the application of pressure. The energy supplied by the increase in pressure is used to increase penetration. Thus pressure decreases with increases of penetration.

5 2 2 Effect of prosthesis insertion time duration

The duration of prosthesis insertion time is an important parameter also for total hip replacement surgery. The length of the femur varies depending on the height of human being. A long femur bone requires a long hip prosthesis and vice versa. The duration of the prosthesis insertion time depends on the length of the prosthesis. Long prosthesis requires a longer time to be inserted in to the prepared cavity of femur for particular insertion rate. Time durations of 0.5 minute, 1 minute and 1.5 minute were investigated to determine the penetration of bone cement.

The pseudoplastic behaviour of Simplex P®, Zimmer bone cement and rheopectic behaviour of CMW3, Zimmer bone cement were used to study the effect of time duration. Pressure of 76 kPa was applied on the bone cement at the proximal end for a duration of 2 minutes 3 minutes after the start of bone cement mixing. Later on, 5-20 mm/s prosthesis insertion velocity were applied for three different time durations, 0.5, 1 and 1.5 minute, 5 minutes after the start of bone cement mixing.

5.2.2.1 Penetration of bone cement through porous cancellous bone

Figure 5-17 shows the penetration of Simplex P® bone cement (Pseudoplastic behaviour) through porous cancellous bone as a function of the distance from the proximal end at a prosthesis insertion velocity of 5 mm/s. Three different curves denote the three different time durations for the prosthesis insertion. The penetration of the bone cement through the cancellous bone increases with increasing prosthesis insertion time duration for **pseudoplastic behaviour of Simplex P® bone cement**. This increasing trend is for a distance of from 10 mm to 30 mm and from 60 to 80 mm from proximal end. The penetration of the bone cement for times of 0.5 minute and 1 minute are the same for distances between 30 to 60 mm.

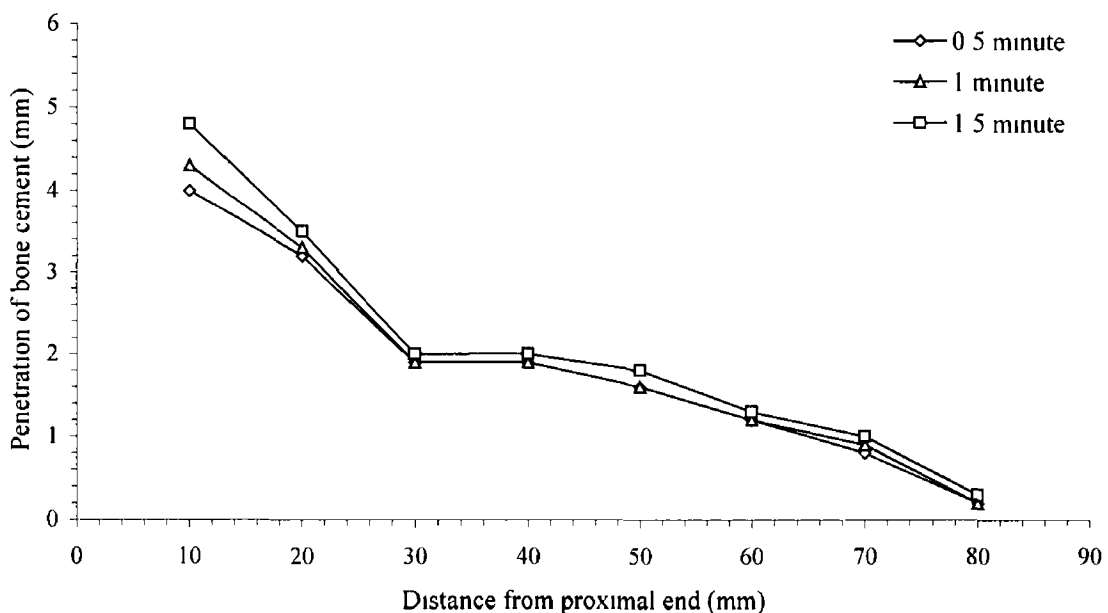


Figure 5-17 Penetration of pseudoplastic Simplex p® bone cement through cancellous bone at a prosthesis insertion velocity of 5 mm/s

Figures 5-18 to 5-20 show the penetration of pseudoplastic Simplex P® bone cement through porous cancellous bone as a function of the distance from the proximal end at insertion velocities of 10 mm/s, 15 mm/s and 20 mm/s respectively

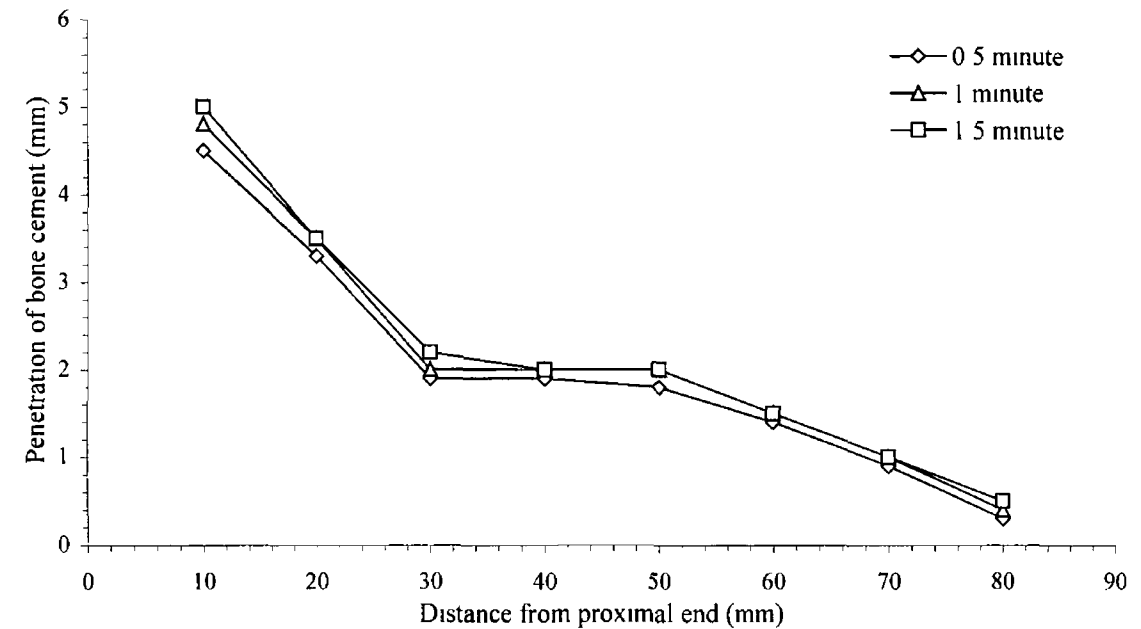


Figure 5-18 Penetration of pseudoplastic Simplex p® bone cement through cancellous bone a prosthesis insertion velocity of 10 mm/s

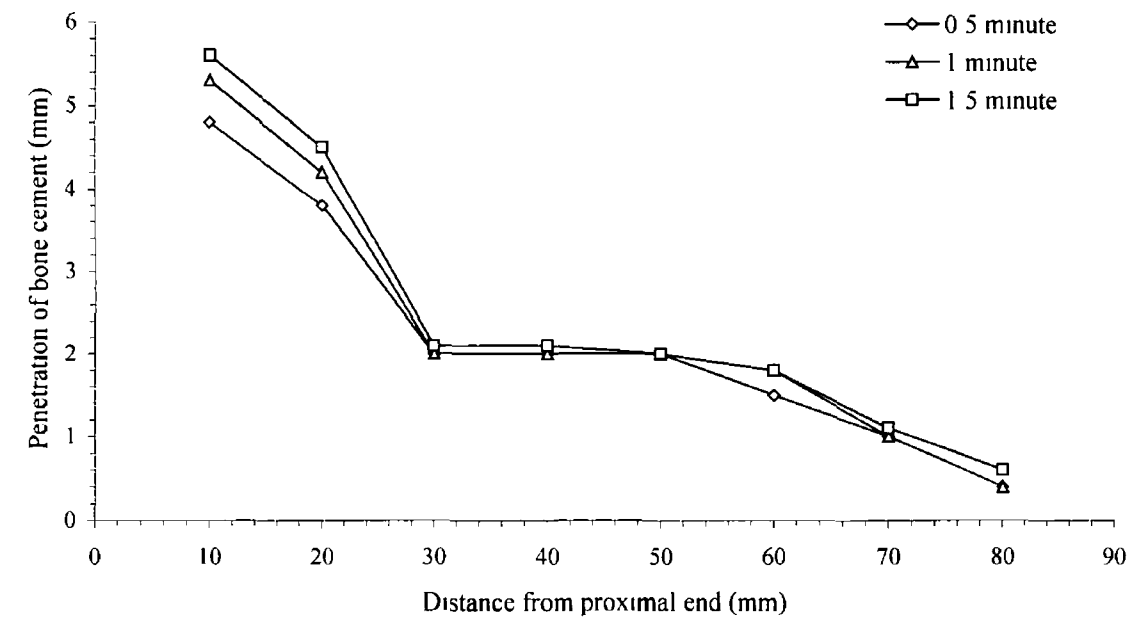


Figure 5-19 Penetration of pseudoplastic Simplex p® bone cement through cancellous bone at a prosthesis insertion velocity of 15 mm/s

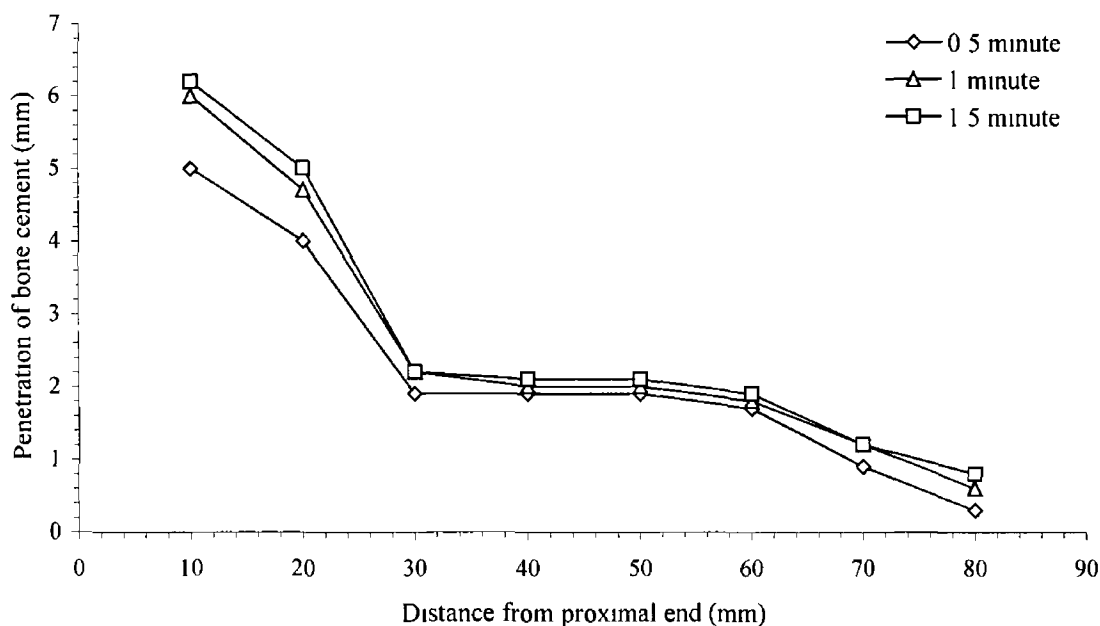


Figure 5-20 Penetration of pseudoplastic Simplex p® bone cement through cancellous bone a prosthesis insertion velocity of 20 mm/s

All figures show increased penetration with increasing prosthesis insertion time, although there are some variations such as figure 5-17. Moreover, it is common for all prosthesis insertion velocities that the increasing trend is more prominent at proximal end.

Figure 5-21 shows penetration of Zimmer bone cement (Pseudoplastic behaviour) through porous cancellous bone as a function of distance from proximal end at a prosthesis insertion velocity of 5 mm/s. The penetration result for a particular time duration of prosthesis insertion is denoted by a single curve in this figure. The penetration of bone cement through cancellous bone increases with increasing prosthesis insertion time for **pseudoplastic behaviour of Zimmer** bone cement. This increasing trend is observed up to a distance of 70 mm from the proximal end.

Figures 5-22 to 5-24 show the penetration of pseudoplastic Zimmer bone cement through porous cancellous bone as a function of distance from the proximal end at insertion velocities of 10 mm/s, 15 mm/s and 20 mm/s respectively. These figures denote that the penetration of bone cement increases due to increasing time duration of prosthesis

insertion This increasing trend is prominent for all prosthesis insertion rates through the length of the femoral cavity by pseudoplastic Zimmer bone cement

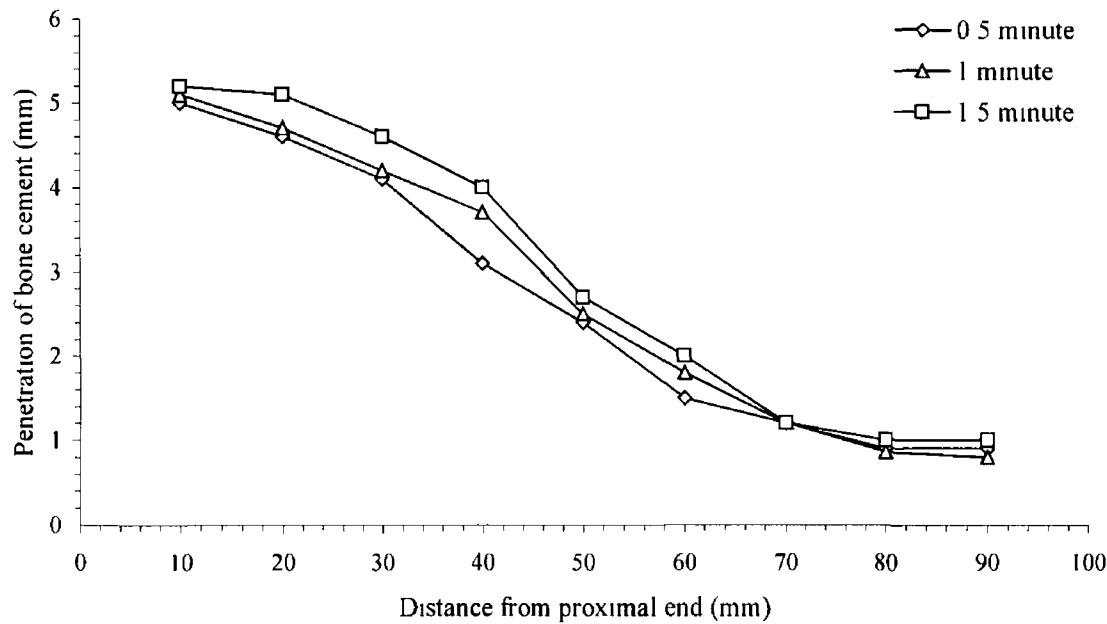


Figure 5-21 Penetration of pseudoplastic Zimmer bone cement through cancellous bone at a prosthesis insertion velocity of 5 mm/s

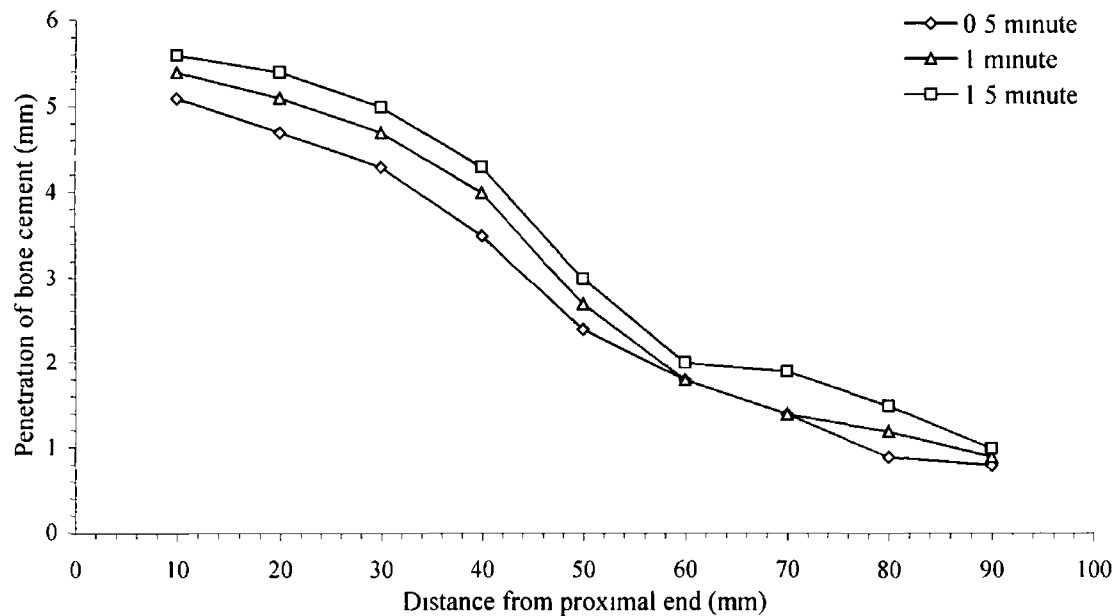


Figure 5-22 Penetration of pseudoplastic Zimmer bone cement through cancellous bone at a prosthesis insertion velocity of 10 mm/s

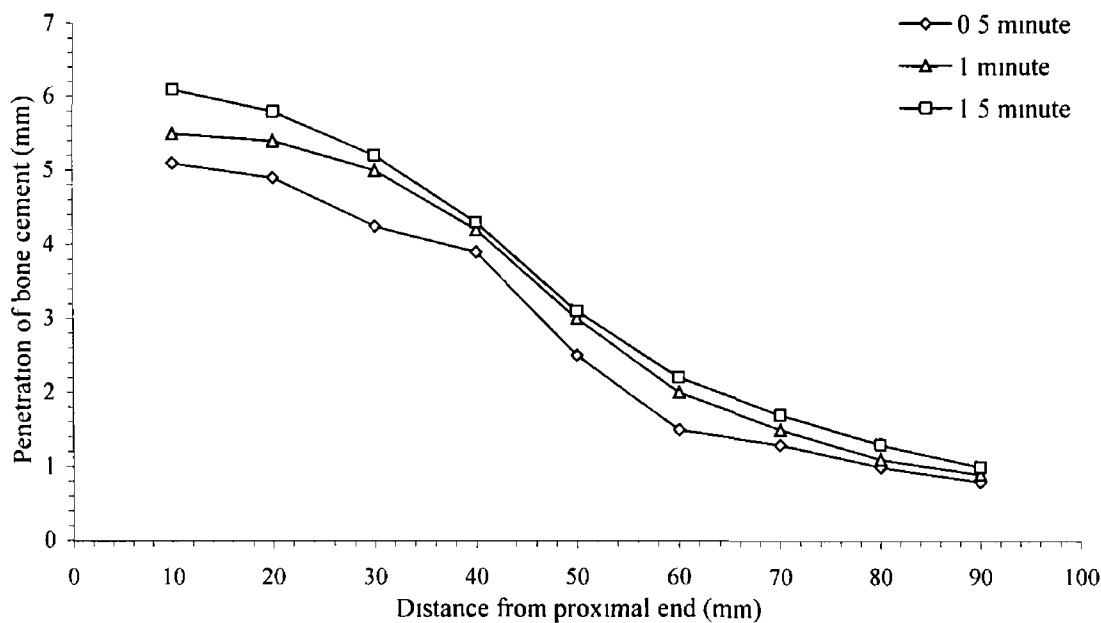


Figure 5-23 Penetration of pseudoplastic Zimmer bone cement through cancellous bone at a prosthesis insertion velocity of 15 mm/s

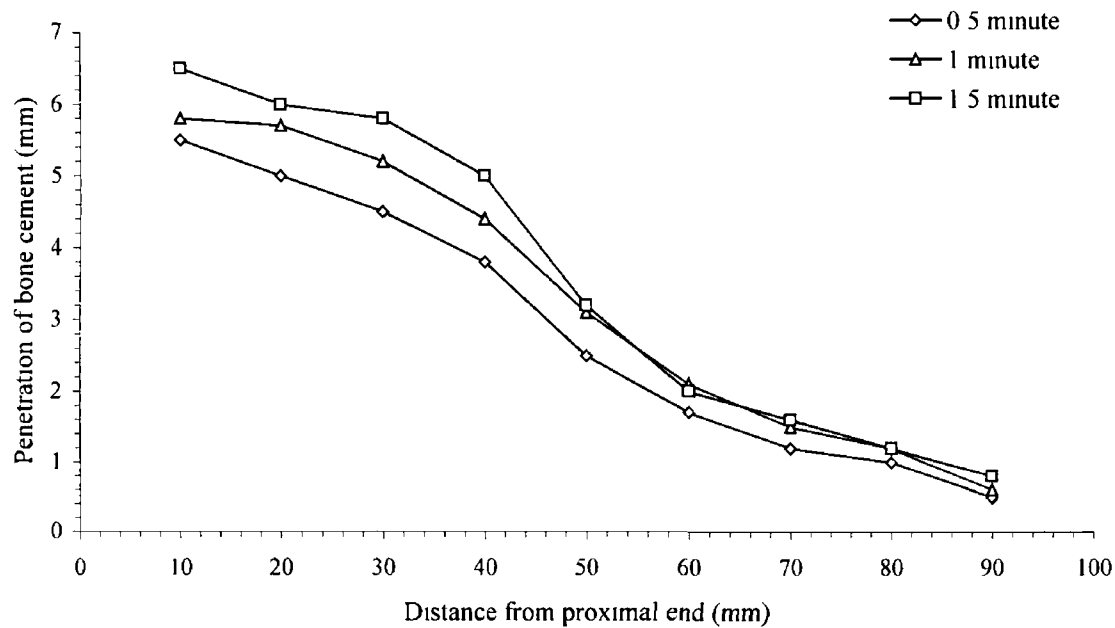


Figure 5-24 Penetration of pseudoplastic Zimmer bone cement through cancellous bone at a prosthesis insertion velocity of 20 mm/s

It can be observed from figures 5-21 to 5-24 that penetration of bone cement decreases gradually from the proximal end to distal end for the pseudoplastic behaviour of Zimmer bone cement

Figure 5-25 shows penetration of **rheoplectic CMW3** bone cement through porous cancellous bone as a function of distance from the proximal end at an insertion velocities of 5 mm/s. It can be noted that penetration increases with increasing prosthesis insertion time at a distance of 30 mm to 70 mm from proximal end

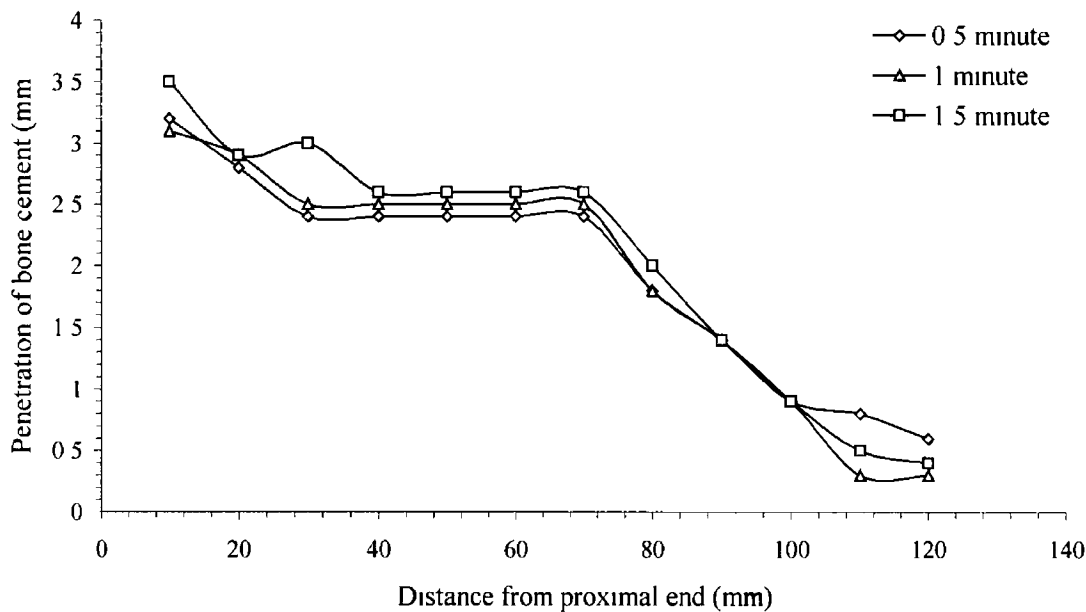


Figure 5-25 Penetration of rheoplectic CMW3 bone cement through cancellous bone at a prosthesis insertion velocity of 5 mm/s

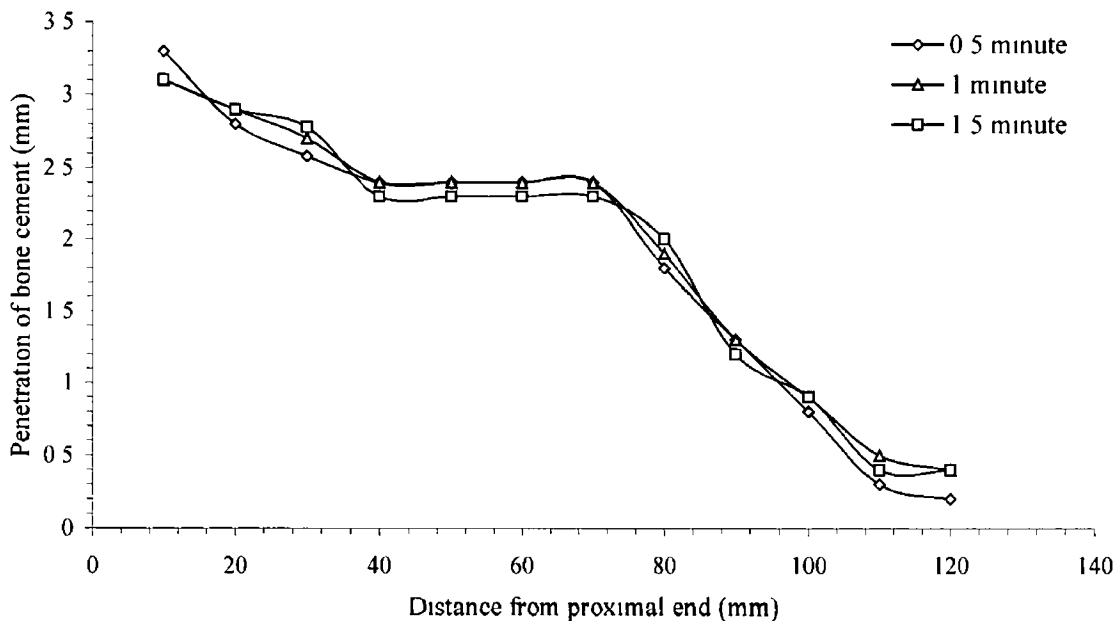


Figure 5-26 Penetration of rheoplectic CMW3 bone cement through cancellous bone at a prosthesis insertion velocity of 10 mm/s

Figures 5-26 to 5-28 show the penetration of rheopectic CMW3 bone cement through porous cancellous bone as a function of distance from proximal end at insertion velocities of 10 mm/s, 15 mm/s and 20 mm/s respectively. The penetration of bone cement decreases along the length of the femoral cavity. The prosthesis insertion time has an insignificant effect on the depth of bone cement penetration.

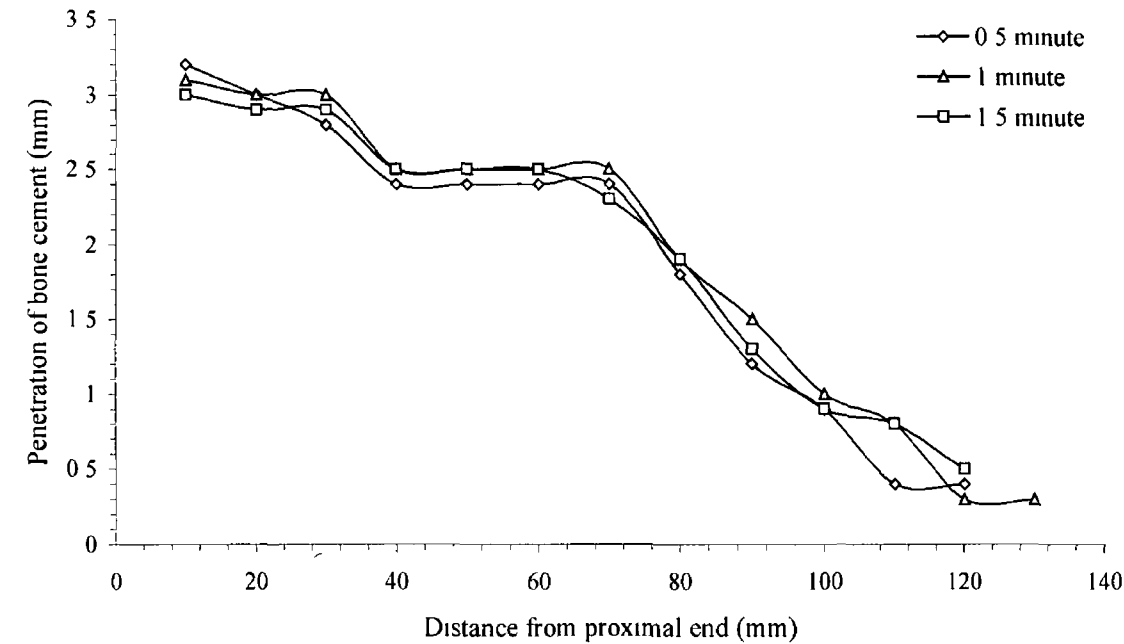


Figure 5-27 Penetration of rheopectic CMW3 bone cement through cancellous bone at a prosthesis insertion velocity of 15 mm/s

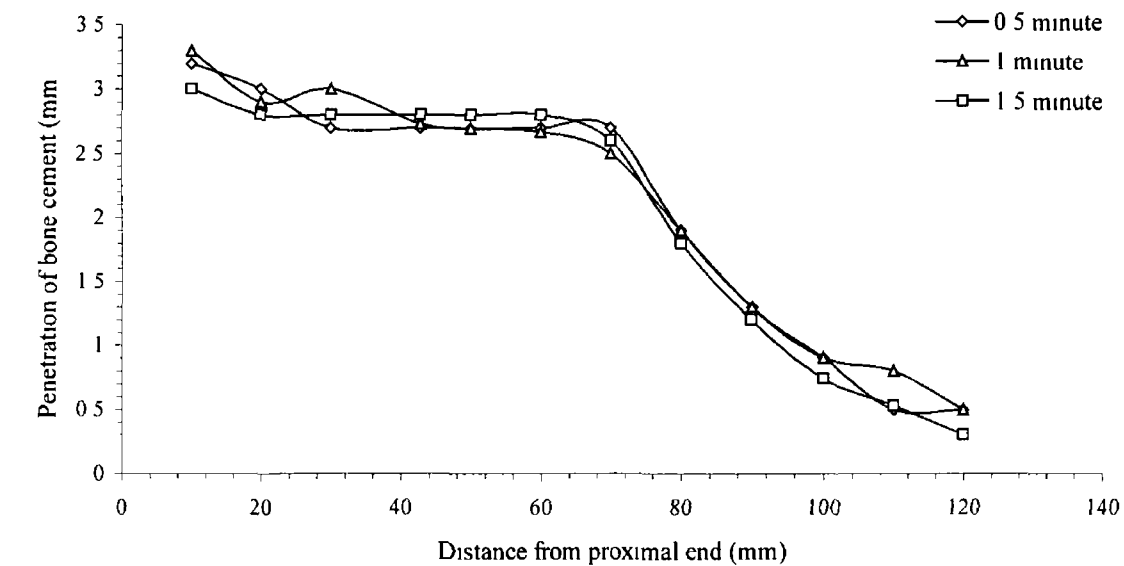


Figure 5-28 Penetration of rheopectic CMW3 bone cement through cancellous bone at a prosthesis insertion velocity of 20 mm/s

Figures 5-29 to 5-32 show the penetration of **rheopectic Zimmer** bone cement through porous cancellous bone as a function of distance from proximal end for four different insertion velocities (5 mm/s, 10 mm/s, 15 mm/s and 20 mm/s). The time taken for prosthesis insertion has an insignificant effect on the depth of bone cement penetration for prosthesis insertion rates of 5 mm/s (figures 5-29) and 10 mm/s (figures 5-30)

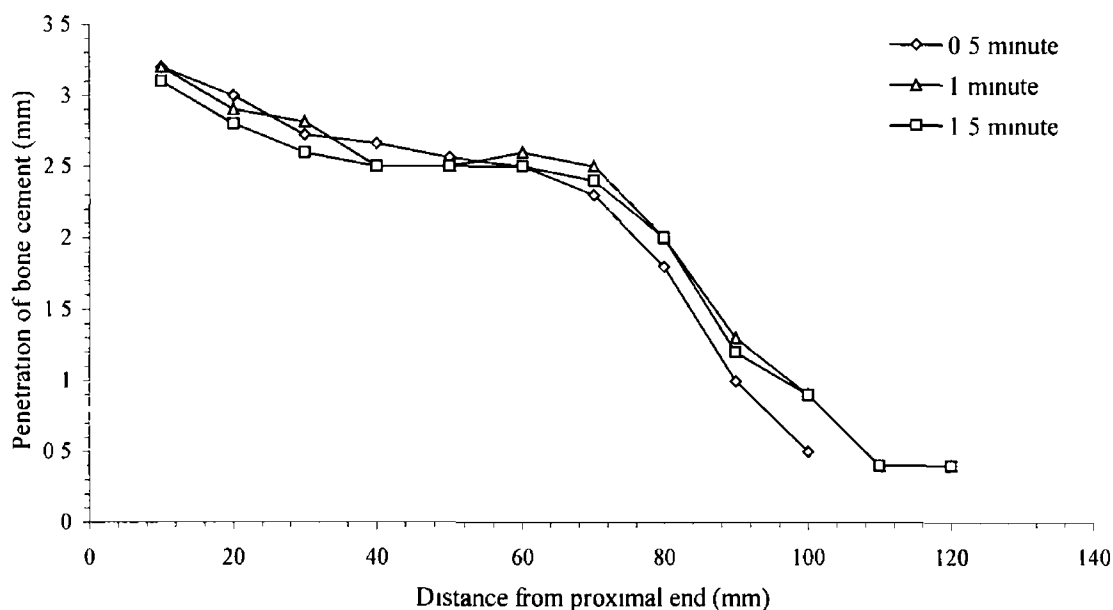


Figure 5-29 Penetration of rheopectic Zimmer bone cement through cancellous bone at a prosthesis insertion velocity of 5 mm/s

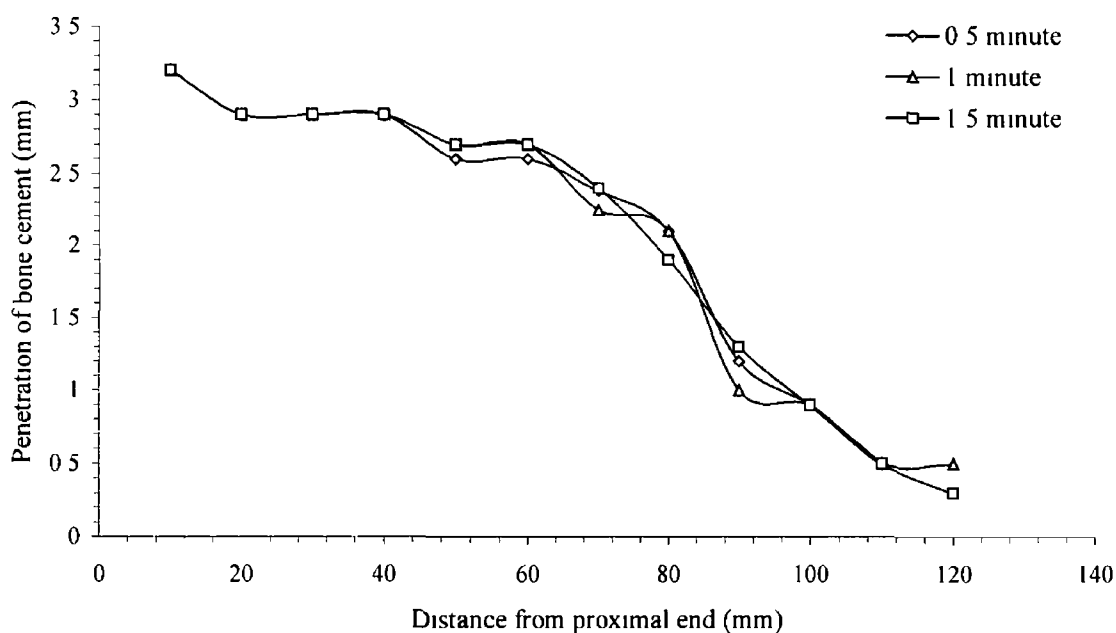


Figure 5-30 Penetration of rheopectic Zimmer bone cement through cancellous bone at a prosthesis insertion velocity of 10 mm/s

Bone cement penetration increases with increasing prosthesis insertion time at a distance of 40 to 60 mm in the femoral cavity for prosthesis insertion velocities of 15 mm/s (figure 5-31) and 20 mm/s (figure 5-32) In other locations the effect of duration of prosthesis insertion time have an insignificant effect on bone cement penetration

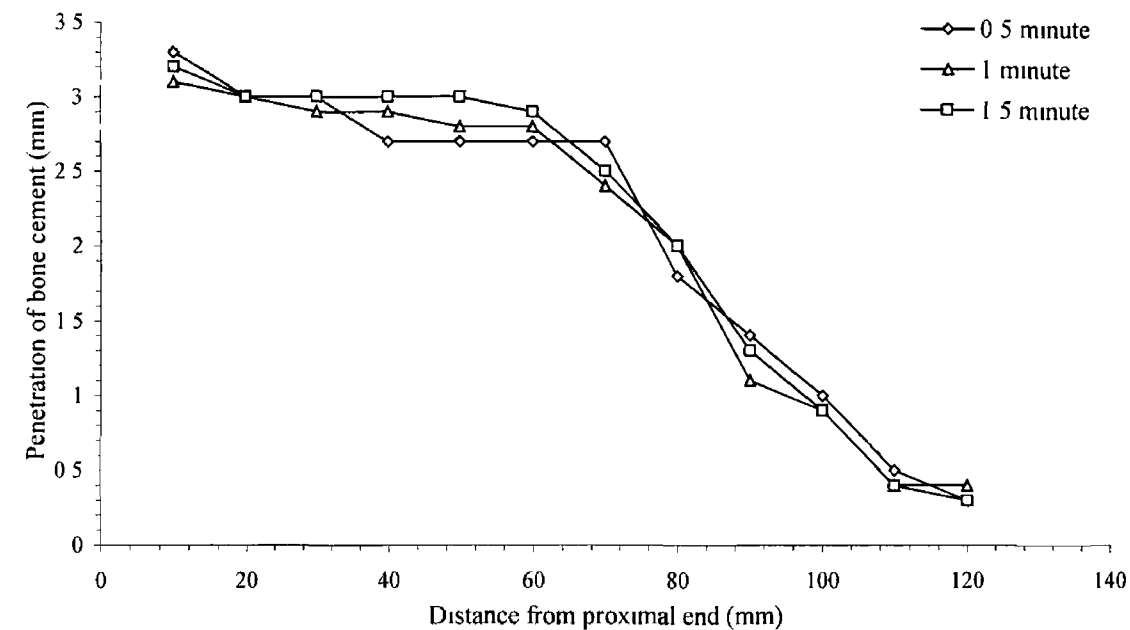


Figure 5-31 Penetration of rheopectic Zimmer bone cement through cancellous bone at a prosthesis insertion velocity of 15 mm/s

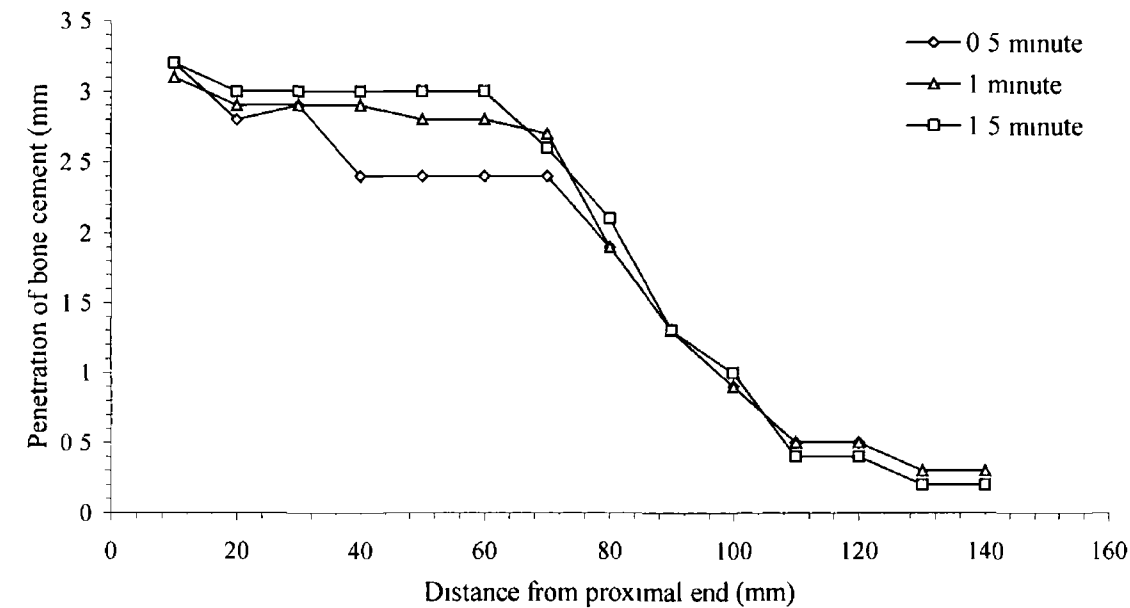


Figure 5-32 Penetration of rheopectic Zimmer bone cement through cancellous bone at a prosthesis insertion velocity of 20 mm/s

The penetration for pseudoplastic behaviour of Simplex P® and Zimmer bone cement increases with increasing prosthesis insertion time. On the other hand, there is an insignificant relationship between the penetration and the prosthesis insertion time for the rheoplectic behaviour of CMW3 and Zimmer bone cement.

5.2.2.2 Trends of penetration with respect to time taken for prosthesis insertion velocity

The penetration of the pseudoplastic Simplex P® bone cement at a distance of 20 mm from the proximal end as a function of time taken for prosthesis insertion is shown in figure 5-33. Each line represents this relationship for a particular prosthesis insertion velocity. The penetration increases with increasing prosthesis insertion times for all prosthesis insertion velocities. Penetration increases by 9%, 6%, 19% and 25% from duration of 0.5 to 1.5 minutes for prosthesis insertion velocities of 5 mm/s, 10 mm/s, 15 mm/s and 20 mm/s respectively. At a particular duration, penetration increases with prosthesis insertion velocities increasing from 5 mm/s to 20 mm/s. The increase of penetration is negligible from prosthesis insertion velocities of 5 mm/s to 10 mm/s.

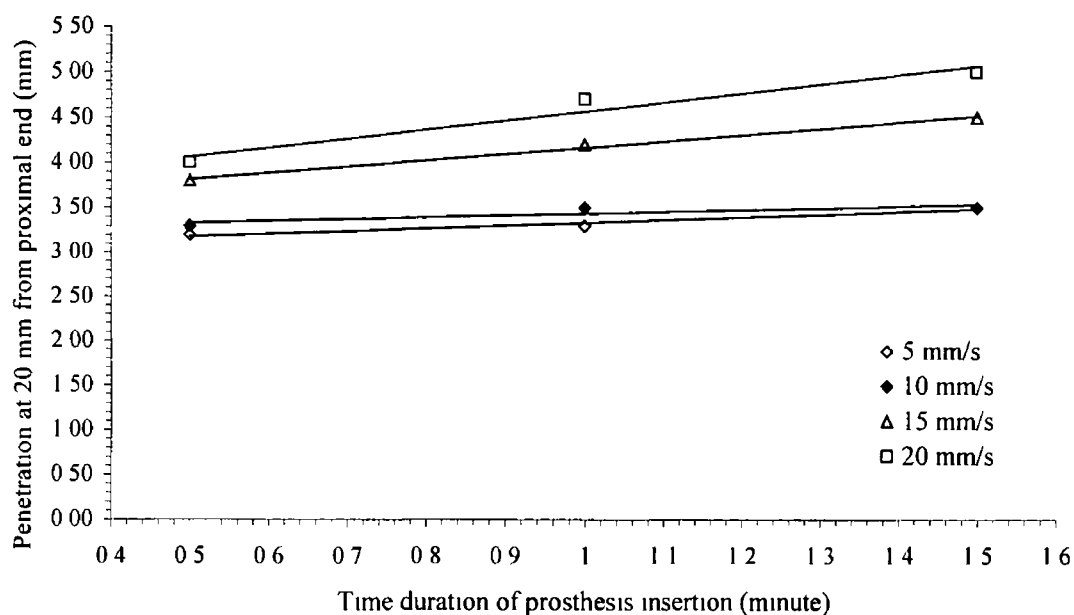


Figure 5-33 Penetration of pseudoplastic Simplex p® bone cement through cancellous bone as a function of time duration of prosthesis insertion

Figure 5-34 shows the penetration of pseudoplastic Zimmer bone cement at a distance of 20 mm from the proximal end as a function of the time taken for prosthesis insertion. This relationship is presented by a line for each prosthesis insertion velocity. Bone cement penetration increases as the time taken for prosthesis insertion increases from 0.5 to 1.5 minutes. Penetration increases by 11%, 15%, 18% and 20% for prosthesis insertion velocities of 5 mm/s, 10 mm/s, 15 mm/s and 20 mm/s respectively from prosthesis insertion time of 0.5 to 1.5 minutes. This figure also shows that penetration increases as the prosthesis insertion velocity is increased from 5 mm/s to 20 mm/s.

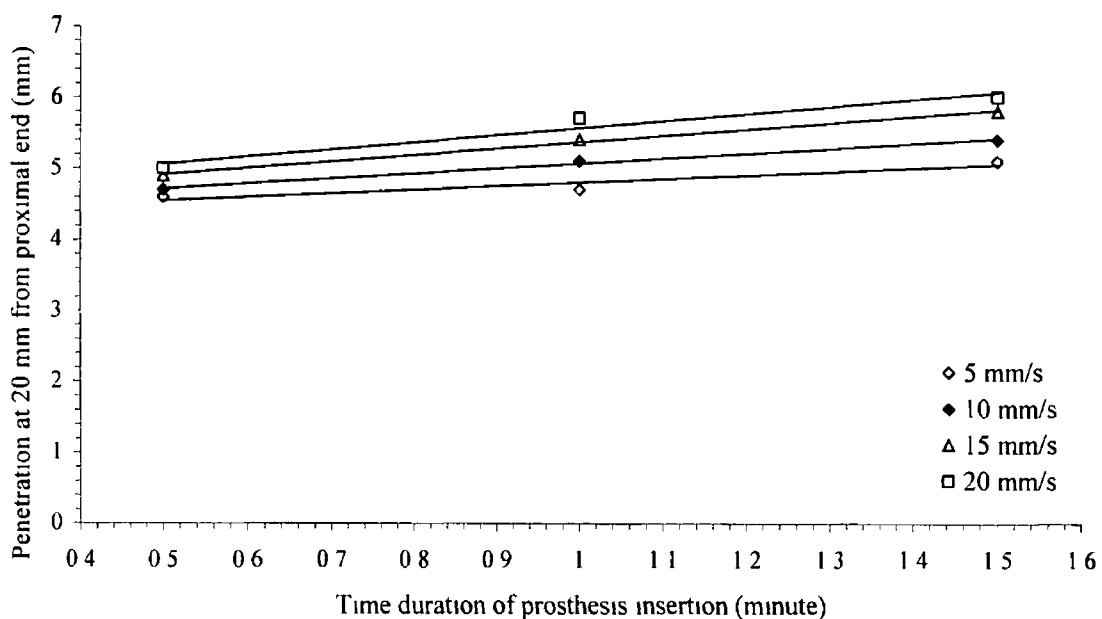


Figure 5-34 Penetration of pseudoplastic Zimmer bone cement through cancellous bone as a function of the time taken for prosthesis insertion

Figure 5-35 represents the penetration of rheopectic CMW3 bone cement at a distance of 20 mm from the proximal end as a function of time taken for prosthesis insertion. Bone cement penetration increases with increasing time duration of prosthesis insertion from 0.5 to 1.5 minutes. Penetration for four different prosthesis insertion velocities is represented by each line. Penetration increases by 7%, 4%, 3% and 7% for 5 mm/s, 10 mm/s, 15 mm/s and 20 mm/s prosthesis insertion velocity respectively from 0.5 to 1.5 minute time duration of prosthesis insertion. The increasing rate is low with respect to pseudoplastic behaviour of bone cements.

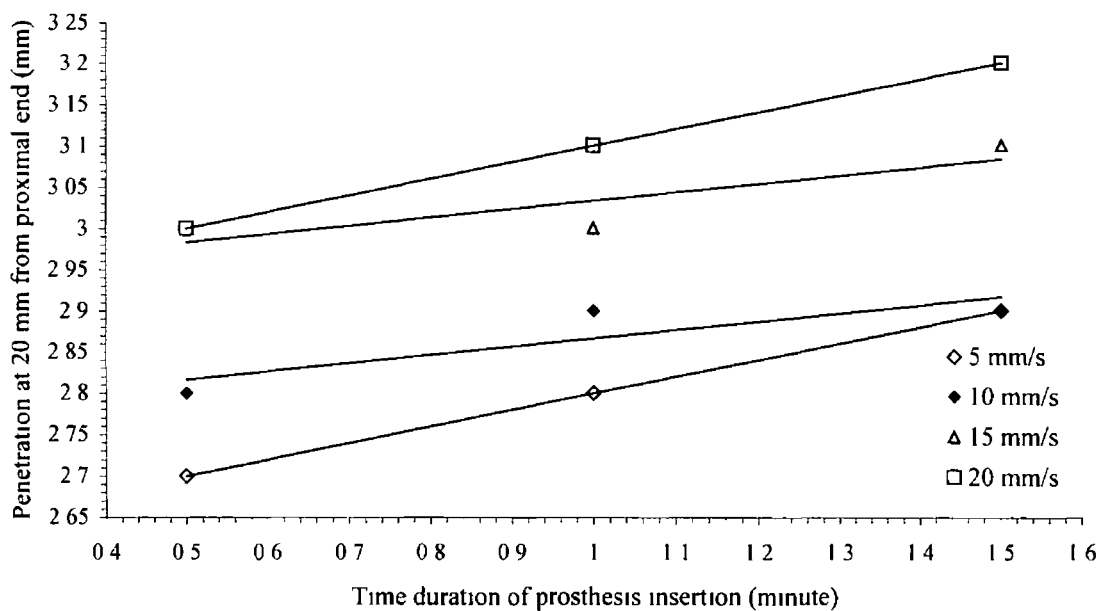


Figure 5-35 The penetration of rheopectic CMW3 bone cement through cancellous bone as a function of the time taken for prosthesis insertion

The penetration of rheopectic Zimmer bone cement at a distance of 20 mm from the proximal end as a function of prosthesis insertion time is represented in figure 5-36. The four lines in the figure represent this relationship for four different prosthesis insertion velocities.

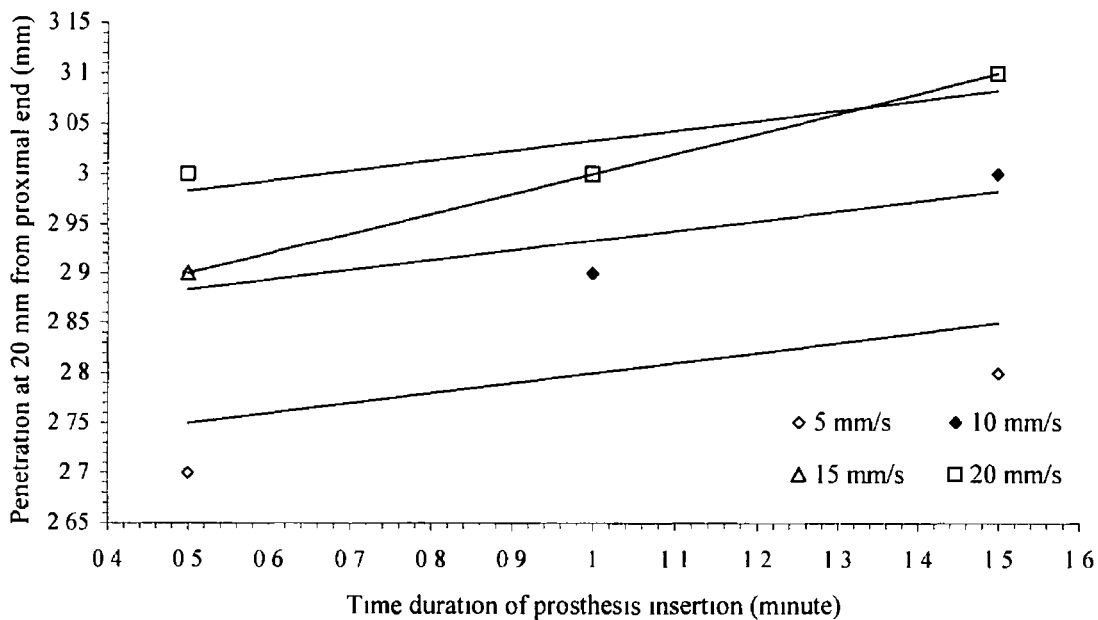


Figure 5-36 Penetration of rheopectic Zimmer bone cement through the cancellous bone as a function of the time taken for prosthesis insertion

The penetration of bone cement increases with prosthesis insertion times increasing from 0.5 to 1.5 minutes. The penetration increases by 4%, 3%, 7% and 3% for prosthesis insertion velocities of 5 mm/s, 10 mm/s, 15 mm/s and 20 mm/s respectively, for insertion time of 0.5 to 1.5 minutes. The increasing rate is also low like CMW3 bone cement with respect to the pseudoplastic behaviour of bone cements.

The above discussion points out that the increasing rate of penetration with increasing prosthesis insertion time is higher for the pseudoplastic behaviour of Simplex P® and Zimmer bone cement than the rheopectic behaviour of CMW3 and Zimmer bone cement.

5.2.2.3 Maximum pressure developed in the bone cement

The maximum pressure developed in the pseudoplastic Simplex P® bone cement is presented in figure 5-37, as a function of the time taken for prosthesis insertion. The maximum pressure is also presented for four different prosthesis insertion velocities, 5 mm/s, 10 mm/s, 15 mm/s and 20 mm/s. The maximum pressure decreases with increasing prosthesis insertion time. Maximum pressure decreases by 3%, 10%, 28% and 19% for prosthesis insertion velocities of 5 mm/s, 10 mm/s, 15 mm/s and 20 mm/s respectively for insertion times of 0.5 to 1.5 minutes.

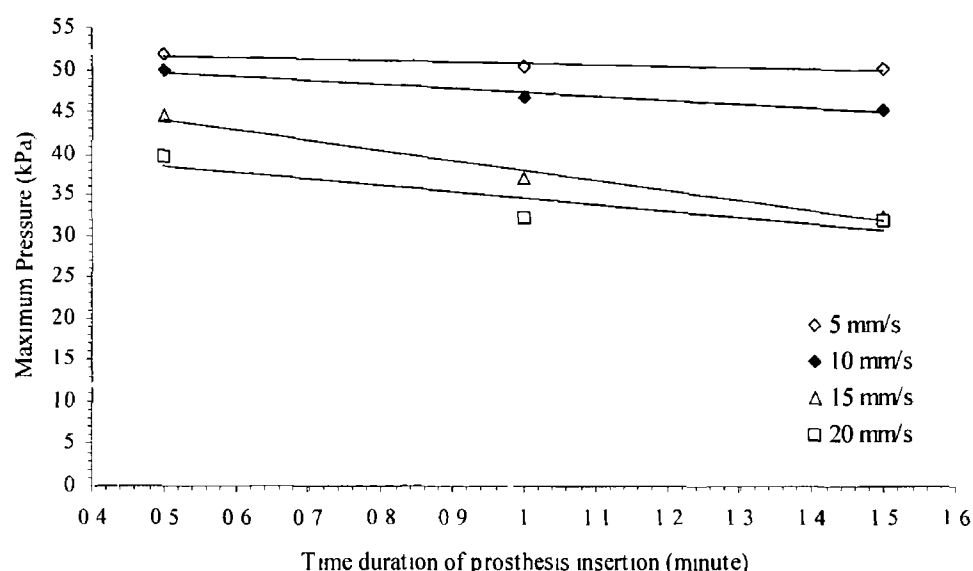


Figure 5-37 Maximum pressure as a function of prosthesis insertion duration time for pseudoplastic Simplex p® bone cement

The decreasing rate of maximum pressure increases with increasing prosthesis insertion velocity. The maximum pressure decreases with increasing prosthesis insertion velocity for all insertion times from 0.5 minute to 1.5 minutes.

Figure 5-38 shows the maximum pressure developed in pseudoplastic Zimmer bone cement as a function of the time taken for prosthesis insertion. Four different lines represent this relationship for the four different prosthesis insertion velocities. The maximum pressure developed in bone cement decreases with increasing prosthesis insertion time. The maximum pressure decreases by 5%, 11%, 12% and 15% for prosthesis insertion velocities of 5 mm/s, 10 mm/s, 15 mm/s and 20 mm/s respectively. The decreasing rate of maximum pressure increases with increasing prosthesis insertion velocity like pseudoplastic Simplex p® bone cement. The maximum pressure decreases with increasing prosthesis insertion velocity for all times from 0.5 minute to 1.5 minutes.

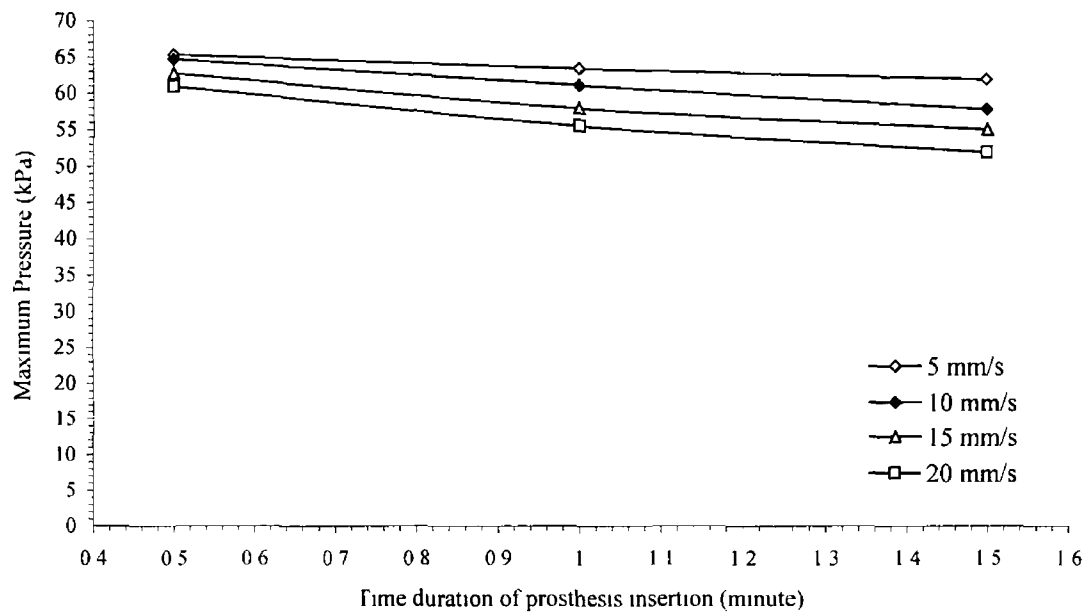


Figure 5-38 Maximum pressure as a function of prosthesis insertion time for pseudoplastic Zimmer bone cement

The maximum pressure developed in rheopectic CMW3 bone cement is shown in figure 5-39 as a function of the prosthesis insertion time. The maximum pressure is presented

for four different prosthesis insertion velocities, 5 mm/s, 10 mm/s, 15 mm/s and 20mm/s. The maximum pressure decreases with increasing prosthesis insertion time for all prosthesis insertion velocities. The maximum pressure decreases by 0.7%, 1%, 1% and 2% for prosthesis insertion velocities of 5 mm/s, 10 mm/s, 15 mm/s and 20 mm/s respectively for insertion time of 0.5 to 1.5 minutes. It is obvious that the rate at which the maximum pressure decreases is noticeably low for all prosthesis insertion velocities.

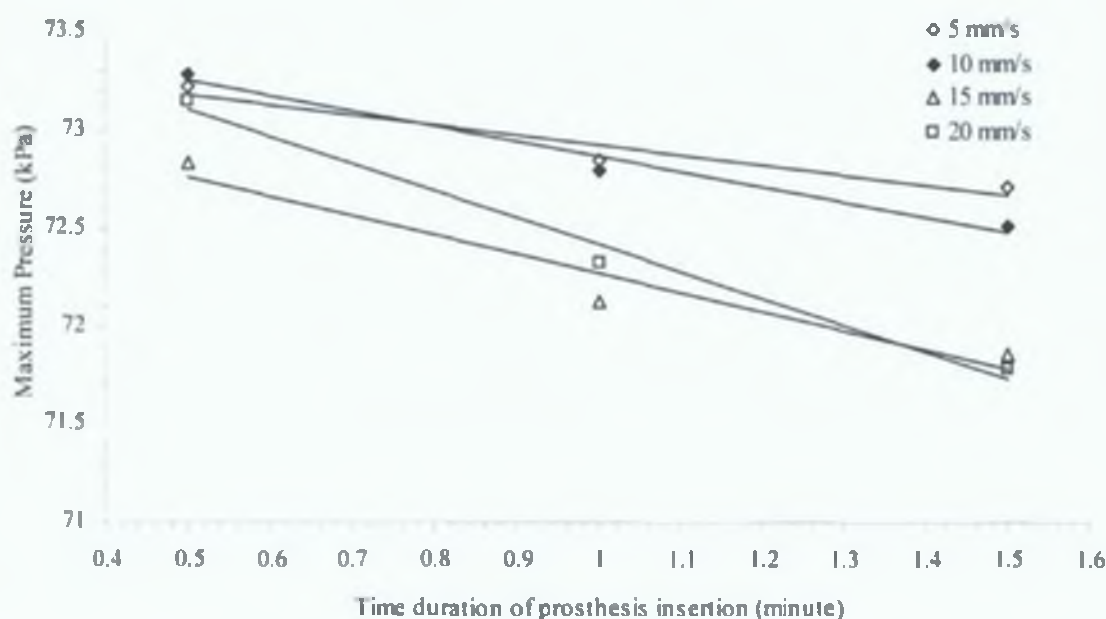


Figure 5-39: The maximum pressure as a function of the prosthesis insertion time for rheopectic CMW3 bone cement.

Figure 5-40 represents the maximum pressure developed in *rheopectic* Zimmer bone cement as a function of prosthesis insertion time. The four different lines show this relationship for four different prosthesis insertion velocities. The maximum pressure developed in bone cement decreases with increasing prosthesis insertion time. The maximum pressure decreases by 0.1%, 0.4%, 0.7% and 0.9% for prosthesis insertion velocities of 5 mm/s, 10 mm/s, 15 mm/s and 20 mm/s respectively. The rate with which the maximum pressure decreases, increases with increasing prosthesis insertion velocity. It is obvious that the rate with which it decreases is noticeably low for all prosthesis insertion velocities. The maximum pressure decreases with increasing prosthesis insertion velocity for times of 1 minute to 1.5 minutes.

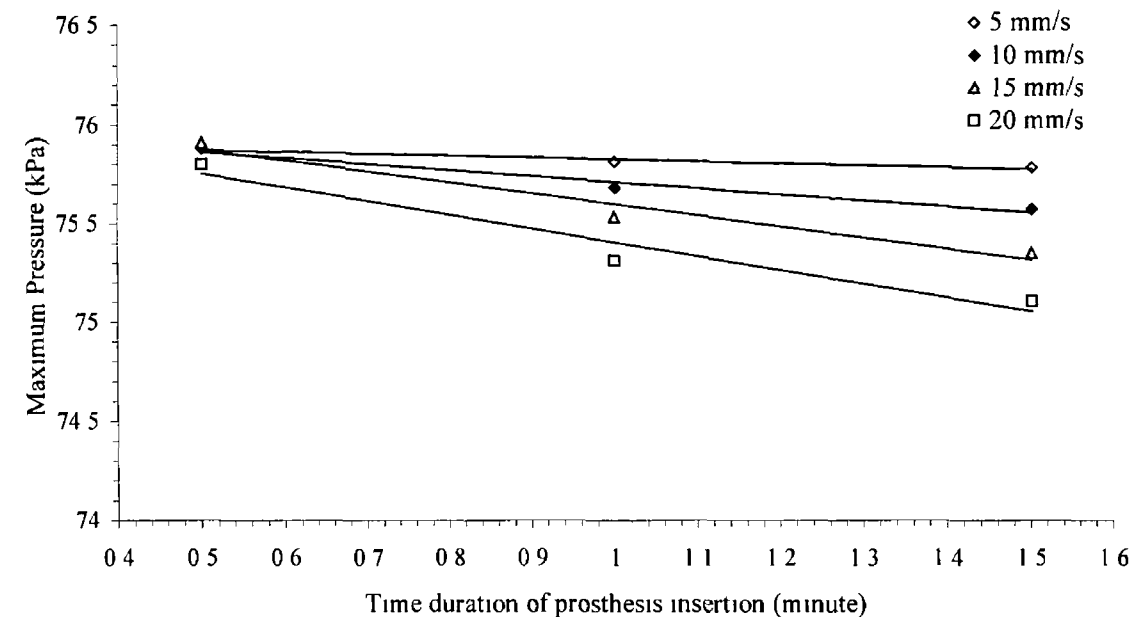


Figure 5-40 The maximum pressure as a function of prosthesis insertion time for rheopectic Zimmer bone cement

Observing the maximum pressure developed in the bone cement it can be said that the maximum pressure decreases with increasing prosthesis insertion time and prosthesis insertion velocity. This change is significant for the pseudoplastic behaviour of Simplex P® and Zimmer bone cement. On the other hand, there is no significant change in the maximum pressure with changing prosthesis insertion velocity or prosthesis insertion time.

5.2.3 Effect of bone cement thickness

Femur bone size depends on the height of the human being. Tall patients have long femur bones and vice versa. A long femur bone gives a larger cavity than a short femur bone. The amount of bone cement required varies according to the cavity size. The volume of the bone cement is an important parameter for total hip replacement surgery. The value can be represented as thickness in a 2D simulation. In this study, the pseudoplastic behaviour of Simplex P® and Zimmer bone cement has been used to study the effect of bone cement thickness variation. Two different thickness values (8 and 10 mm) were selected for this study. A pressure of 76 kPa was applied on bone cement at the proximal end for a duration of 2 minutes, 3 minutes after the start of

bone cement mixing. Later, prosthesis insertion velocities of 5 to 20 mm/s were applied for a duration of 1 minute, 5 minutes after the start of bone cement mixing.

5.2.3.1 Penetration of bone cement through porous cancellous bone

The depth of penetration is affected by the bone cement thickness for **pseudoplastic behaviour of Simplex P® bone cement**. Figure 5-41 shows the penetration of bone cement through cancellous bone as a function of distance from proximal end at prosthesis insertion velocity of 5 mm/s, 10 mm/s, 15 mm/s and 20 mm/s. Two different sets of curve represent the two different thickness of bone cement. The curve for the 8 mm bone cement thickness shows that penetration is 7 mm (thickness of the cancellous bone is also 7 mm) up to a distance of 30 mm from the proximal end for prosthesis insertion velocity of 5 mm/s, 10 mm/s and 15 mm/s. The penetration of Simplex P® bone cement is higher for bone cement thickness of 8 mm than 10 mm at all position of the femoral cavity.

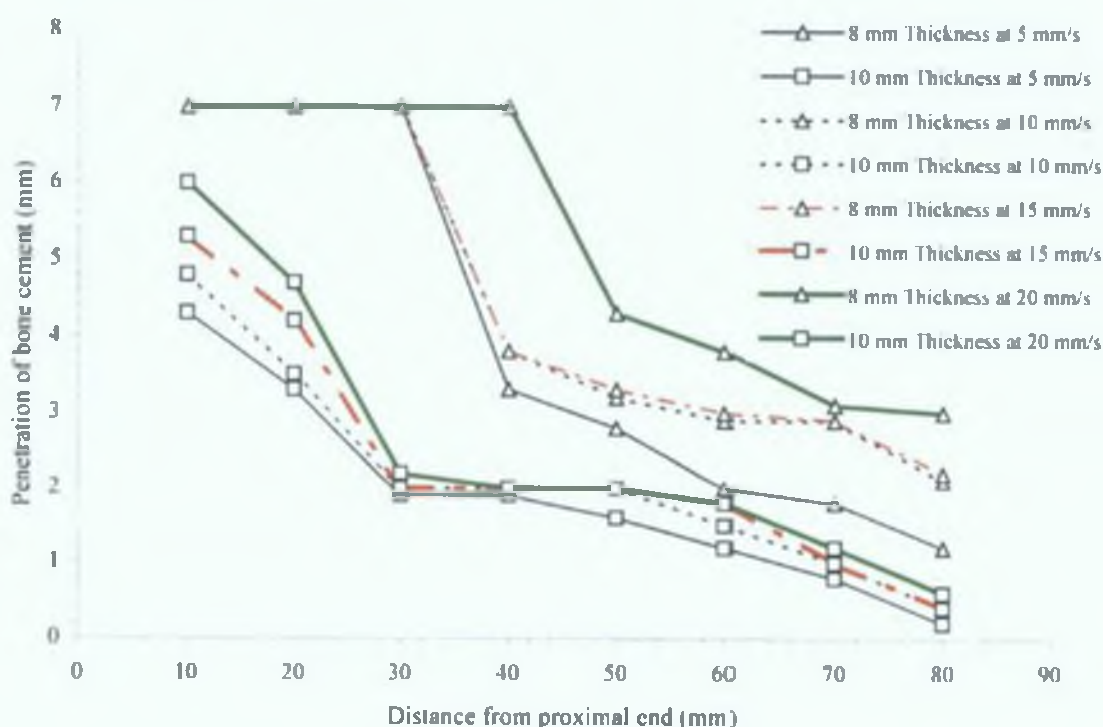


Figure 5-41: Penetration of pseudoplastic Simplex p® bone cement through two different cancellous bone thickness at different prosthesis insertion velocity.

The bone cement thickness also affects the depth of penetration of **pseudoplastic Zimmer bone cement**. The penetration of bone cement through cancellous bone as a

function of distance from the proximal end at prosthesis insertion velocities of 5 mm/s, 10 mm/s, 15 mm/s and 20 mm/s are presented in figure 5-42.

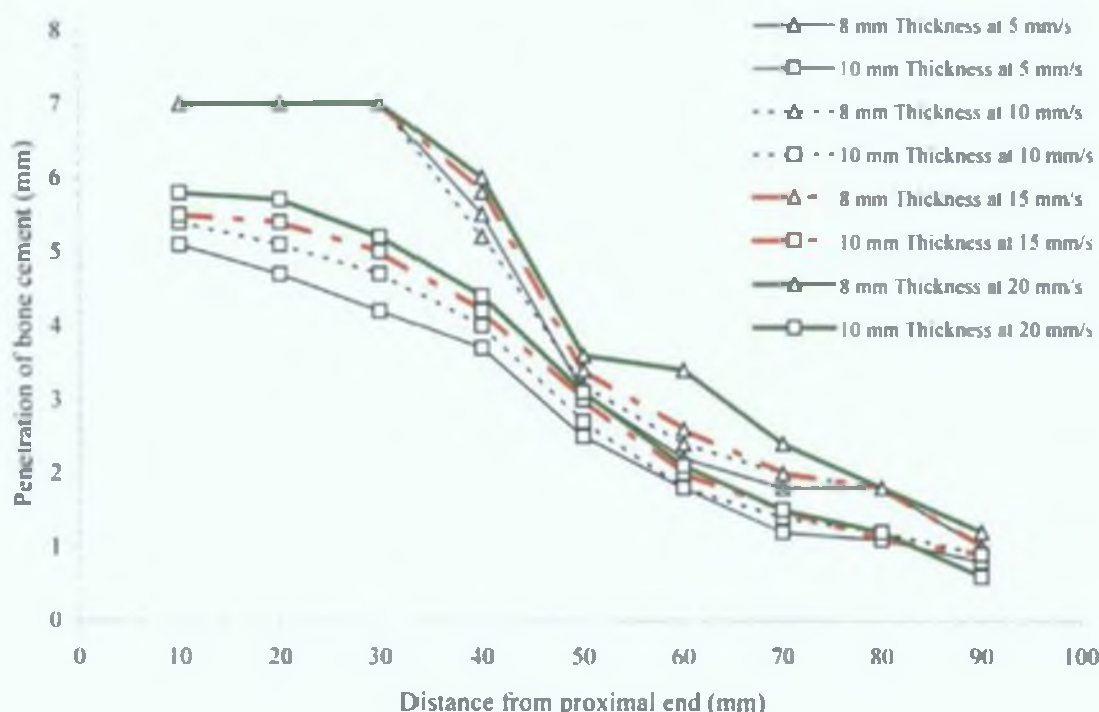


Figure 5-42: Penetration of pseudoplastic Zimmer bone cement through two different cancellous bone thickness at different prosthesis insertion velocity.

The penetration of Zimmer bone cement is higher for bone cement thickness of 8 mm than 10 mm at all femoral cavity positions. The curve for a bone cement thickness of 8 mm shows that the penetration is 7 mm (thickness of the cancellous bone is 7 mm) up to a distance of 30 mm from the proximal end.

5.2.3.2 Trends of penetration with respect to bone cement thickness

The penetration of bone cement at a distance of 40 mm from the proximal end with respect to bone cement thickness at prosthesis insertion velocity of 5 mm/s, 10 mm/s, 15 mm/s and 20 mm/s is presented in figure 5-43. Four lines present this relationship for the pseudoplastic behaviour of Simplex P® and another four lines present same relation for Zimmer bone cement. Bone cement penetration increases with decreasing bone cement thickness from 10 mm to 8 mm for the pseudoplastic behaviour of Simplex P® and Zimmer bone cement.

The penetration of pseudoplastic Zimmer bone cement is higher than the penetration of Simplex P® bone cement for a bone cement thickness of 10 mm in all cases. The penetration is also higher for Zimmer bone cement with a bone cement thickness of 8 mm, but the exception is for prosthesis insertion velocity of 20 mm/s.

Less bone cement in the femur cavity results in more penetration due to the same amount (76 kPa) of pressure being applied on the proximal end. So the same amount of applied pressure will result in more bone cement penetration through cancellous bone in a short femur bone.

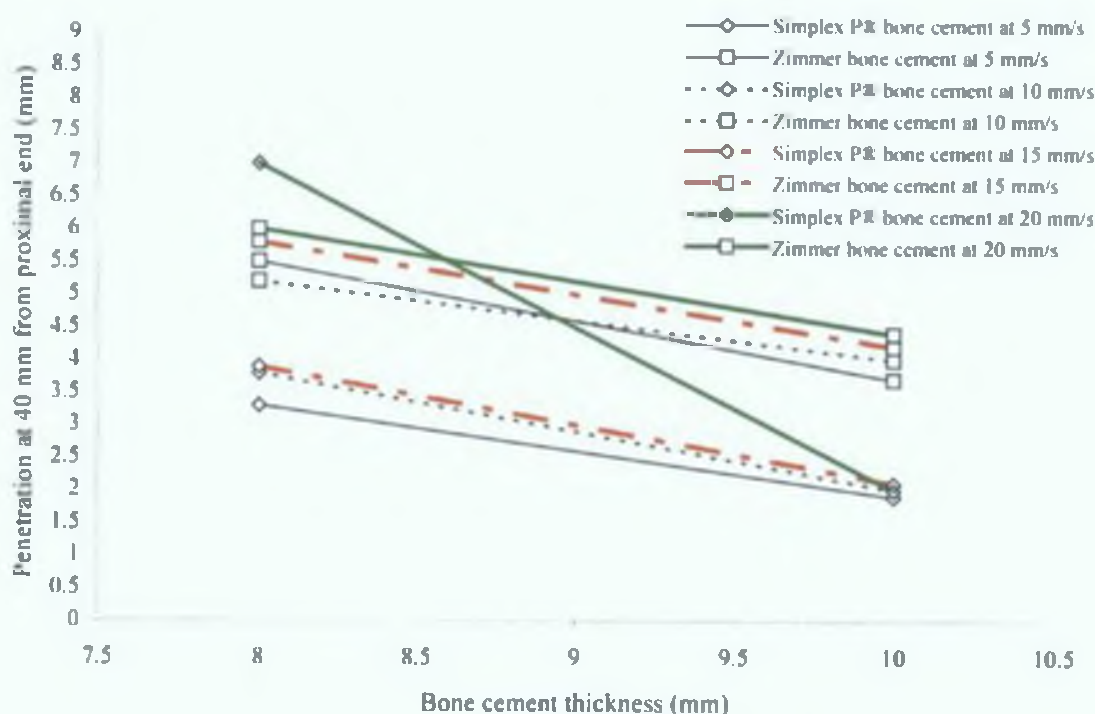


Figure 5-43: Penetration of bone cement through cancellous bone as a function of bone cement thickness at a prosthesis insertion velocity of 5 mm/s, 10 mm/s, 15 mm/s and 20 mm/s.

5.3 Comparison of the numerical results

The simulation results were compared in two ways.

- Conducting two experiments with similar boundary conditions using CMW3 bone cement.
- Using published data of previous researcher. [42, 109, 127]

5.3.1 Comparison experiments

Two different boundary conditions were compared using CMW3 bone cement.

First boundary condition: Pressure was applied on the inlet of the femur cavity for a duration of 1 minute, 3 minutes after the start of bone cement mixing. Then a prosthesis insertion velocity of 10 mm/s was applied for a duration of 1 minute.

Second boundary condition: Pressure was applied on the inlet of the femur cavity for a duration of 3 minutes, 3 minutes after the start of bone cement mixing. Then a prosthesis insertion velocity of 10 mm/s was applied for a duration of 1 minute.

The following figures, 5-44 to 5-48, show the sections of femur bone that have been treated using CMW3 bone cement, as mentioned in section 3.2 of Chapter 3. The pressure was applied on the inlet of the femur cavity for a duration of 3 minutes, 3 minutes after the start of bone cement mixing. Then a prosthesis insertion velocity of 10 mm/s was applied for a duration of 1 minute (Second comparison experiment).



Figure 5-44: First section from the proximal end.



Figure 5-45: Second section from the proximal end.



Figure 5-46: Third section from the proximal end.



Figure 5-47: Fourth section from the proximal end.



Figure 5-48: Fifth section from the proximal end.

The average penetration of bone cement at each section was calculated according to the method mentioned in section 3.2.2.2 of Chapter 3. The average penetrations of CMW3 bone cement measured from these experiments are listed in table 5-3. This table also presents the penetration determined using numerical analysis with the percentage of error. Error varies from 2.56% to 18.4%. The simulation was performed under definite condition. On the other hand, surgeons use their experience to apply pressure and velocity of prosthesis insertion in bone cement during total hip replacement surgery. The prosthesis insertion velocity is in the range of 3 to 12 mm/s [128]. Similarly in

comparison experiments pressure and velocity were applied without control device
This is the main source of error in the depth of penetration

Table 5-3 Numerical and experimental result with percentage of error for CMW3

A (mm)	B (mm)	C (mm)	Error (%)	D (mm)	E (mm)	Error (%)
10	3 9	4	2 56	3 1	3 8	18 4
20	3 2	3 3	3 13	2 9	3 3	12 12
30	2 9	3 2	10 34	2 9	3 1	6 45
40	2 7	-	-	2 9	3 0	3 3
50	2 7	-	-	2 7	-	-

Where,

A = Distance from proximal to distal end

B = Numerical penetration for the first boundary condition

C = Average experimental penetration for the first comparison condition

D = Numerical penetration for the second boundary condition

E = Average experimental penetration for the second comparison condition

5 3 2 Comparison using published data of previous researchers

Noble & Swarts [127] found that average penetration for Simplex P®, Zimmer and CMW3 were 5 4 mm, 5 1 mm and 2 72 mm respectively, in different conditions They used cancellous bone (from femoral condyles of cadaveric femurs) *in vitro* using a standard biological model under controlled conditions (22°C, 90 s following dough stage, 82% mean porosity, 35 kPa pressure) This simulation shows that average penetration for Simplex P®, Zimmer and CMW3 bone cement through cancellous bone are 4 25 mm, 5 15 mm and 2 95 mm, respectively Penetration up to a depth of 30 mm from proximal end of the femur was measured This is the region of cancellous bone in femur In this simulation, bone marrow viscosity of 0 067 pa-s and cancellous bone porosity of 85% was used Pressure of 76 kPa was applied on bone cement at the proximal end for a duration of 2 minutes, 3 minutes after the start of bone cement mixing Then prosthesis insertion velocity was applied for a duration of 1 minute

Comparison between work of Noble et al and this project shows that the error in percentage of the penetration for Simplex P®, Zimmer and CMW3 bone cement are 21%, 1% and 8% respectively. There errors are quite reasonable considering the variation of femur bone (porosity of bone) and experimental conditions.

Beaudoin et al [42] developed a numerical model to investigate the non-Newtonian flow of acrylic bone cement in a porous medium, cancellous bone. They found a final penetration depth of 5.6 mm for surgical simplex at applied pressure of 35 kPa. This study showed that average penetration for Simplex P® bone cement through cancellous bone is 4.25 mm. The percentage of error in bone cement penetration was 24%. Different boundary conditions in both simulations are the reason for this error.

Rey et al [109] found the penetration to be 2.72 mm and 5.40 mm for CMW3 and Simplex P® bone cement respectively. They used bovine cancellous bone and 140 kPa pressure was applied. The difference between the results of the current study and the results from Rey [109] can be related to the difference in the bone structure and the use of different boundary conditions.

Table 5-4 shows the average depth of penetration found in this study and the results published by other researchers with the percentage of error.

Table 5-4 Comparison of average depth of penetration with percentage error

Bone Cement	Average penetration (mm) and Percentage of Error (%)				
	Present study	Noble & Swarts		Beaudoin et al	
	Average penetration (mm)	Average penetration (mm)	Percentage of Error (%)	Average penetration (mm)	Percentage of Error (%)
Simplex P®	4.25	5.4	21	5.6	24
Zimmer	5.15	5.1	1	-	-
CMW3	2.95	2.72	8	-	-

5.4 Remarks on result

The results of the study underline the importance of the rheological model in estimating the penetration of bone cement through cancellous bone and the maximum pressure developed in the bone cement of the prepared canal during the insertion of the prosthesis

Although the material parameters were implemented for three bone cements, the model can be used for other bone cements and any non-Newtonian fluid. Therefore, for each material of interest, viscosity, shear rate and time relationships need to be identified through rheological testing and entered as a power law or in the USRVSC subroutine in FIDAP.

The rheological model of bone cement with porous media implemented in FIDAP is used to model interdigitation of cement through bone during total hip replacement. This model can be extended to model flow of bone cement through porous bone in total knee replacement and vertebroplasty.

Chapter six

Conclusions and recommendations

6 1 Findings of the study

It is believed that the model developed in the research work can benefit both the bioengineer and consultant surgeon. The model offers an added dimension for evaluating the functionality of the bone cement selection and the production process by determining the thermal and flow property of bone cement.

The concluding points of the study are as follows:

a Thermal property of bone cement

1. Maximum temperature of bone cement decreases with increasing vacuum level of cement mixing for Palacos R® and Simplex P® bone cements. The trend is reversed for CMW3 bone cements (Figure 5-4).
2. Setting time increases from the bone cement that is mixed at atmospheric pressure to cement mixed at 0.4 bar vacuum pressure. Further decreasing the mixing pressure to -0.7 bar decreases the setting time of bone cements. All bone cements that have been used in this experiment have minimum setting times when mixed at maximum vacuum pressure (Figure 5-6).

b Simulation of flow property

3. Prosthesis insertion velocity influences the depth of penetration of bone cement into the bone and the maximum pressure developed in the bone cement during total hip replacement surgery. Insertion rates of 5-20 mm/s were investigated in this study.
 - a. Average penetration increases with increasing prosthesis insertion velocity for pseudoplastic behaviour of Simplex P® and Zimmer bone cement (Figure 5-15).
 - b. The maximum pressure developed in the bone cement is decreased significantly for the pseudoplastic behaviour of Simplex P® and Zimmer bone cement by increasing the insertion rate of prosthesis (Figure 5-16).

4. The duration of applied pressure prior to insertion of the prosthesis was found to have no significant effect on the penetration of bone cement through cancellous bone for the rheopectic behaviour of Zimmer and CMW3 bone cement (Figure 5-13 and figure 5-14).
5. The time taken for prosthesis insertion also has an effect on the penetration and maximum pressure developed in bone cement.
 - a. Penetration of bone cement increases with increasing prosthesis insertion time for pseudoplastic Simplex P® and Zimmer bone cement (Figure 5-33 to figure 5-36).
 - b. The maximum pressure developed in the bone cement decreases significantly with increasing prosthesis insertion time for pseudoplastic behaviour of Simplex p® and Zimmer bone cement (Figure 5-37 to figure 5-40).
6. The amount of bone cement in the cavity influences the penetration of bone cement. Decreasing the amount of bone cement increases the penetration through the cancellous bone for pseudoplastic Simplex P® and Zimmer bone cement (Figure 5-43).
7. The intermedullary pressure, which was found by running the simulations using FIDAP, on the interface of bone cement and cancellous bone is in the range of 32-76 kPa for an applied pressure of 76 kPa (Appendix B).

6.2 Recommendations for further work

1. In this study the pressure applied in the cavity was kept constant (76 kPa). The effect of varying (76-140 kPa) the pressure can be studied using this model.
2. The effect of bone porosity variation on the penetration can be studied using this model. This will give an idea of how human age can affect the bone cement penetration.
3. The effect of thermal and shrinkage [152] properties on the penetration of bone cement can be incorporated in this model.
4. A 3D simulation using THR could also be done. For this simulation FIDAP and Fluent software is recommended.

- 5 A more generic 2D model could be created that would also represent the THR and vertebroplasty. The availability of the built-in porous feature in the FIDAP and fluent simulation software can help to generate a model for this study.

6.3 Contributions of the work

The flow pattern of bone cement through cancellous bone was found by modelling the rheological properties of curing PMMA bone cement. The contribution of the work can be summarized into three main groups:

- 1 The flow pattern includes the effect of velocity on the penetration of bone cement and consequently it can be used to predict the penetration depth of bone cement for various prosthesis insertion velocities. It has been found that increased penetration of bone cement through cancellous bone can be achieved by increasing prosthesis insertion velocity.
- 2 The flow pattern also includes the effect of prosthesis insertion time and the amount of bone cement on the degree of penetration. It has been found that decreasing the amount of bone cement in the cavity increases the penetration of the bone cement.
- 3 The models show that Zimmer bone cement results in more penetration than Simplex P® bone cement for the same conditions. Considering this point, surgeons could use Simplex P® bone cement in cases where lower penetration is required, such as cases with a high risk of revision surgery.
- 4 Overall, a preclinical testing tool has been developed which can be used to determine the suitability of particular bone cements for total hip arthroplasty procedures to ensure adequate bone cement penetration.

References

- [1] Joint replacement institute, [online],
http://www.jri-oh.com/hipsurgery/Hip_Treatment.asp (accessed 15th December 2004).
- [2] Healthpages, [online],
<http://www.healthpages.org/AHP/LIBRARY/HLTHTOP/THR/INDEX.HTM> (accessed 23rd November 2004).
- [3] Anderson Orthopaedic Research Institute, [online],
<http://www.aori.org/thr/thrwhat.html> (accessed 22nd December 2004).
- [4] DePuy "CEMVAC Reliability" Printed in Sweden.
- [5] The Biomedical Engineering Hand Book (2nd Edition) Volume 1 Editor-in-chief J. D. Bronzino. Copublished by CRC press LLC, USA and Springer Verlag GmbH & Co. KG Germany, 2000.
- [6] P. Ducheyne "Prosthesis fixation for orthopedics." In: Encyclopedia of Medical Devices and Instrumentation, J.G. Webster, Ed. (N.Y.: Wiley-Interscience), 1988; pp: 2146-2154.
- [7] J. B. Park "Orthopedic Prosthesis Fixation." Annals Biomed. Eng., 1992; 20, pp: 583-594.
- [8] J. B. Park "Hip Joint Prosthesis Fixation-Problems and Possible Solutions." The Biomedical Engineering Hand Book (2nd Edition) Volume 1 Editor-in-chief Joseph D. Bronzino. Copublished by CRC press LLC, USA and Springer Verlag GmbH & Co. KG Germany, 2000.
- [9] "Wrought Stainless Steels" Page 843-871. In: Properties and Selection: Irons, Steels and High performance Alloys. ASM International Metal hand book. Volume-1 (Tenth Edition).
- [10] "Cobalt and Cobalt Alloys" Page 453. In: Properties and Selection: Nonferrous Alloys and Special purpose Materials. ASM International Metal hand book. Volume-2 (Tenth Edition).
- [11] J. R. Crandall, G. W. Hall, and W. D. Pilkey "Section 20.3 Bioengineering" of "Patent Law and Miscellaneous Topics" Edited by Ed. Frank Kreith "Mechanical Engineering Handbook" Boca Raton: CRC Press LLC, 1999.
- [12] M. Long, H.J. Rack "Review Titanium alloys in total joint replacement-a materials science perspective" Biomaterials, 1998; 19, pp: 1621-1639.

- [13] S Lampman "Wrought Titanium and Titanium Alloys" Page 620-621 In Properties and Selection Nonferrous Alloys and Special purpose Materials ASM International Metal hand book Volume-2 (Tenth Edition)
- [14] S H Teoh, Z G Tang and G W Hastings "Thermoplastic Polymers In Biomedical Applications Structures, Properties and processing " From Handbook of Biomaterial properties –Edited by Jonathan Black and Garth Hastings , Chapman & Hall , First edition 1998
- [15] R B Martin "Biomaterials" In Edited by S A Berger, W Goldsmith and E R Lewis "Introduction to Bioengineering" Oxford University Press First Published, 1996, pp 339-360
- [16] J Currey Cortical bone Handbook of Biomaterial properties Edited by Jonathan Black and Garth Hastings Chapman & Hall (First Edition 1998)
- [17] T Weston "Atlas of anatomy" Produced 2000 by MARSHALL CAVENDISH books an imprint of Times Media Private Limited
- [18] R Saxena and T S Keller "Computer Modeling for Evaluating Trabecular Bone Mechanics" From "Mechanical Testing of Bone and the Bone-Implant Interface" Edited by Yuehuei H An and Robert A Draughn, 2000, CRC Press LLC (Washington, D C)
- [19] R B Martin and D B Burr "Structure, Function and Adaptation of Compact Bone" Raven Press, New York, 1989, 1, 275
- [20] M B Schaffler, D B Burr and R G Frederickson "Morphology of the osteonal cement line in human bone", Anat Rec , 217, 223, 1987
- [21] G A Marotti "new theory of bone lamellation", Calcif Tissue Int , 53, S47, 1993
- [22] X E Guo "Mechanical Properties of Cortical Bone and Cancellous Bone Tissue" Edited by Stephen C Cowin "Bone Mechanics HandBook (2nd Edition), 2001
- [23] Y H An "Mechanical Properties of Bone" from "Mechanical Testing of Bone and the Bone-Implant Interface" Edited by Y H An and R A Draughn, 2000, CRC Press LLC (Washington, D C)
- [24] D T Reilly and A H Burstein "The elastic and ultimate properties of compact bone tissue " J Biomech , 1975, 8, pp 393-405
- [25] R B Ashman, S C Cowin, W C Van Buskirk, et al "A continuous wave technique for the measurement of the elastic properties of cortical bone " J Biomech , 1984, 17, pp 349-361
- [26] J C Lotz, T N Gerhart and W C Hayes "Mechanical properties of metaphyseal bone in the proximal femur " J Biomech , 1991, 24, pp 317-329

- [27] D J Downey, P A Simkin, R Taggart "The effect of compressive loading on intraosseous pressure in the femoral head in vitro " *Journal of Bone and Joint Surgery*, Jul 1988, 70, pp 871-877
- [28] J A Ochoa, A P Sanders, T W Kiesler, D A Heck, J P Toombs, K D Brandt, B M Hillberry "In vivo observations of hydraulic stiffening in the canine femoral head *Journal of Biomechanical Engineering*, 1997, 119, pp 103-108
- [29] M J Grimm, J L Williams "Measurements of permeability in human calcaneal trabecular bone " *Journal of Biomechanics*, 1997, 30 7, pp 743-745
- [30] F Linde, P Nørgaard, I Hvid, A Odgaard and K Søballe "Mechanical properties of trabecular bone Dependency on strain rate " *J Biomech*, 1991, 24, pp 803-809
- [31] B V Rietbergen and R Huiskes "Elastic Constants of Cancellous Bone" In *Bone Mechanics HandBook* (2nd Edition) Edited by S C Cowin, 2001
- [32] M J Grimm, J L Williams "Measurements of permeability in human calcaneal trabecular bone " *Journal of Biomechanics*, 1997, 30 7, pp 743-745
- [33] R B Ashman, J Y Rho, C H Turner "Anatomical variation of orthotropic elastic moduli of the proximal human tibia " *Journal of Biomechanics*, 1989, 22 8-9, pp 895-900
- [34] R Hodgkinson, JD Currey "The effect of variation in structure on the Young's modulus of cancellous bone a comparison of human and non-human material " *Proc Inst Mech Eng*, 1990, 204, pp 115-121
- [35] T M Keaveny "Cancellous bone" from "Handbook of Biomaterial properties" Edited by J Black and G Hastings, Chapman & Hall, First Edition 1998
- [36] Y P Arramon, E A Nauman "The Intrinsic permeability of Cancellous Bone" from "Bone Mechanics Hand Book" (2nd Edition)- Edited by Stephen C Cowin, 2001
- [37] Henry Gray, *Anatomy of human body*, [online],
<http://www.bartleby.com/107/illus244.html> (Accessed on October 27, 2004)
- [38] S S Kohles, J B Roberts, M L Upton, C G Wilson, L J Bonassar, A L Schlichting "Direct perfusion measurements of cancellous bone anisotropic permeability" *Journal of Biomechanics*, 2001, 34, pp 1197-1202
- [39] T H Lim, J H Hong "Poroelectric properties of bovine vertebral trabecular bone " *Journal of Orthopaedic Research*, 2000, 18 4, pp 671-677
- [40] E A Nauman, K E Fong, T M Keaveny "Dependence of intertrabecular permeability on flow direction and anatomic site " *Annals of Biomedical Engineering*, 1999, 27, pp 517-524

- [41] P W Hui, P C Leung, A Sher "Fluid conductance of cancellous bone graft as a predictor for graft-host interface healing" *Journal of Biomechanics*, 1996, 29 1, pp 123-132
- [42] A J Beaudoin, W M Mihalko and W R Krause "Finite Element Modelling of Polymethylmethacrylate Flow Through Cancellous Bone" *J of Biomechanics*, 1991, 24 2, pp 127-136
- [43] J B Park and R S Lakes "Biomaterials an introduction" 2nd ed, New York, Plenum Press, 1992
- [44] M Jasty, W J Maloney, C R Bragdon, D O O'Connor, T Haire and W H Harris "The initiation of failure in cemented femoral components of hip arthroplasties" *J Bone Joint Surg*, 1991, 73B, pp 551-558
- [45] J Charnley "Acrylic Cement In Orthopaedic Surgery" E & S Livingstone, Edinburgh and London 1970
- [46] Park, Goel and Keller "Hard Tissue Replacements" *The Biomedical Engineering Hand Book (Second Edition) Volume 1*
- [47] H Malchau, P Herberts "Prognosis of total hip replacement", Scientific Exhibition from The Swedish National Registry presented at AAOS annual meeting 1998
- [48] Amstutz et al "Loosening of total hip components Cause and prevention" In *The Hip (St Louis Mosby)*, 1976, pp 102-116
- [49] A M Ahmed, S Raab, J E Miller "Metal/cement interface strength in cement stem fixation" *Journal of Orthopaedic Research*, 1984, 2, pp 105-118
- [50] W Bard, J B Park, G H Kenner and A F Von Recum "Intramedullary fixation of artificial hip joints with bone cement precoated implants I Interfacial strengths" *J Biomed Mater Res*, Jul 1982, 16, pp 447-458
- [51] J B Park, W Bard, G H Kenner and A F Von Recum "Intramedullary fixation of artificial hip joints with bone cement precoated implants II Density and Histological study" *J Biomed Mater Res*, Jul 1982, 16, pp 459-469
- [52] J B Park, C S Malstrom and A F Von Recum "Intramedullary fixation of implants pre-coated with bone cement A preliminary study" *Biomater Med Devices Artif Organs*, 1978, 6, pp 361-373
- [53] S Raab, A M Ahmed and J W Provan "Thin film PMMA precoating for improved implant bone-cement fixation" *J Biomed Mater Res*, Sep 1982, 16, pp 679-704

- [54] J B Park, A F Von Recum and G E Gratzick "Pre-coated orthopedic implants with bone cement" *Biomater Med Devices Artif Organs*, 1979, 7, pp 41-53
- [55] D O O'Connor, D W Burke, R C Sedlacek and W H Harris "Peak cement strains in cemented femoral total hip" *Trans Orthop Res Soc*, 1991, 16, pp 220-229
- [56] J K Kim and J B Park "Reinforcement of bone cement around the prostheses by precoated wire coil a preliminary study" *Biomed Mater Eng*, 4, pp 369-380
- [57] M Halawa, A J C Lee, R S M Ling, S S Vangala "The shear strength of trabecular bone from the femur, and some factors affecting the shear strength of the cement-bone interface" *Arch Orthop Traumat Surg*, 1978, 92, pp 19-30
- [58] W R Krause, W Krug, J Miller "Strength of cement-bone interface" *Clin Orthop Rel Res*, 1982, 163, pp 290-299
- [59] W Macdonald, E Swarts and R Beaver "Penetration and Shear Strength of Cement-Bone Interfaces In Vivo" *Clinical Orthopaedics and Related Research*, Jan 1993, 286, pp 283-288
- [60] A F Mak, J L Lewis "Fracture mechanics of the PMMA-cancellous bone interface" *Adv Bioeng ASME*, 1980, pp 209-212
- [61] G H Heyse-Moore and R S M Ling "Current cement mixing techniques" In *Proceedings of a Symposium on Progress in Cemented Hip Surgical and Revision* (Ed R K Marti), Amsterdam, October 1982, pp 71-86 (Excerpta Medica)
- [62] B E McKoy, Y H An, and R J Friedman "Factors Affecting the strength of the Bone-Implant Interface" from "Mechanical Testing of Bone and the Bone-Implant Interface" Edited by Y H An and R A Draughn, 2000, CRC Press LLC (Washington, D C)
- [63] R Huiskes "Stress patterns, failure modes, and bone remodeling" In Fitzgerald Jr R, editor *Non-cemented total hip arthroplasty* New York Raven Press, 1988, pp 283-302
- [64] R Huiskes "Properties of the stem-cement interface and artificial hip joint failure" In Lewis JL, Galante JO, editors *The bone-implant interface Workshop report*, 1985, pp 86-101
- [65] R Huiskes, D Nunamaker "Local stress and bone adaptation around orthopedic implants" *Calcif Tissue Int*, 1984, 36, pp S110-117
- [66] F Erdogan, G D Gupta "The problem of an elastic stiffener bonded to a half plane" *J Appl Mech*, 1971, 38, pp 937-41

- [67] H A Lowenstam and S Weiner "On Biomineralization", Oxford University Press, (1989) New York
- [68] R M Rose, A S Litsky "Biomechanical considerations in the loosening of hip replacement prostheses" In Williams DF, editor Current perspectives on implantable devices, vol 1 London JAI Press, 1989, pp 1-45
- [69] D N Yetkinler "Viscoelastic behavior of acrylic bone cements" Doctoral Dissertation, Ohio State University, 1994
- [70] D N Yetkinler and A S Litsky "Viscoelastic behaviour of acrylic bone cements" Biomaterials, 1998, 19, pp 1551-1559
- [71] "Instruction manual for use" of Howmedica Surgical Simplex® P bone cement Howmedica international S de R L Raheen Business Park, Limerick, Ireland
- [72] J M Yang "Polymerization of acrylic bone cement using differential scanning calorimetry" Biomaterials 1997, 18 19, pp 1293-1298
- [73] K D Kuhn "Bone Cements Up to Date Composition of Physical and Chemical properties of Commercial Materials", Berlin, Springer, 2000
- [74] "Instruction manual for use" of Zimmer bone cement Schering-Plough Europe Brussels, Belgium
- [75] DePuy CMW "Instruction Leaflet" For the personal Attention of the surgeon Lancashire, England
- [76] J R Cooper, D Dowson, J Fisher, B Jobbins "Ceramic bearing surfaces in total artificial joints resistance to third body wear damage from bone cement particles" J Med Eng Technol, Mar-Apr 1991, 15, pp 63-67
- [77] C M Schoenfeld, "The Rheology and monomer release of unset methyl methacrylate for bone cements" PhD thesis, North Western University, Illinois, 1974
- [78] G Lewis "Properties of acrylic bone cement state of the art review" J Biomed Mater Res (Appl Biomater) 1997, 38, pp 155-182
- [79] N J Dunne and J F Orr "Influence of mixing techniques on the physical properties of acrylic bone cement" Biomaterials, July 2001, 22 13, pp 819-1826
- [80] DePuy "The Science of Cement Critical Issues" Cat No 4010-035, 2001
- [81] B Gallez and N Beghein "Noninvasive in vivo EPR monitoring of the methyl methacrylate polymerization during the bone cement formation" Biomaterials, 2002, 23, pp 4701-4704
- [82] J A Brydson Chapter 2 "The Chemical Nature of Plastics" Plastics Materials 5th edition Butterworth Heinemann

- [83] P J Prendergast “ Bone Prostheses and Implants” from Bone Mechanics HandBook (2nd Edition) Edited by S C Cowin, 2001
- [84] Summit medica, [online],
<http://www.summit-medical.co.uk/product/pressuriser.html> (Accessed November 23, 2005)
- [85] E Ebramzadeh, A Sarmiento, H A McKellop, A Llinas, W Gogan “The cement mantle in total hip arthroplasty Analysis of long-term radiographic results ” J Bone Joint Surg Am, Jan 1994, 76, pp 77-87
- [86] Data from DePuy company
- [87] DePuy CMW “CMW bone cement An in depth view ” Cat No 4010-080
- [88] DePuy “Surgical Technique Utilising Modern Cementing Techniques” Cat No 4010-030 2001
- [89] M Baleani, R Fognani, A Toni “The influence of stem insertion rate on the porosity of the cement mantle of hip joint replacements” Proceedings Of The Institution Of Mechanical Engineers Part H, Journal Of Engineering In Medicine, 2003, 217 3, pp 199-205
- [90] J B Benjamin, G A Gie, A J C Lee, R S M Line, R G Volz “Cementing technique and effects of bleeding” Journal of Bone and Joint Surgery, Aug 1987, 69, pp 220-4
- [91] R S Majkowski, G C Bannister, A W Miles “The effect of bleeding on cement/bone interface An experimental study” Clinical Orthopaedic and Related Research, Feb 1994, pp 293-297
- [92] L E Nielsen ‘Polymer rheology’ Marcel Dekker, INC New York and Basel
- [93] H G Elias ‘An introduction to Plastics’ VCH (Heinheim NY Basel Cambridge Tokyo)
- [94] J Charnley “Acrylic Cement in Orthopaedic Surgery” 1970 (E&S Livingstone, Edinburgh)
- [95] W R Krause, J Miller and P Ng “The viscosity of acrylic bone cements” Journal of Biomedical Materials Research, 1982, 16, pp 219-243
- [96] S C Weber and W L Barger “A comparison of the Mechanical Properties of Simplex, Zimmer and Zimmer Low Viscosity Bone Cements” Biomat , Med Dev , Art Org , 1983, 11 1, pp 3-12

- [97] N. J. Dunne and J. F. Orr "Flow characteristics of curing polymethylmethacrylate bone cement." *Proceedings Of The Institution Of Mechanical Engineers, Part H, Journal Of Engineering In Medicine*, 1998; 212:3, pp: 199-207.
- [98] H. A. Barnes, J. F. Hutton, K. Walters "An introduction to rheology." Amsterdam: Elsevier, 1989.
- [99] J. Ferguson, Z. Kemplowski "Applied Fluid Rheology." London: Elsevier, 1991.
- [100] F.A. Holland, R. Bragg 'Fluid flow for Chemical Engineers' Second Edition (Edward Arnold).
- [101] R. I. Tanner 'Engineering Rheology', Oxford University Press, New York (1985).
- [102] M. J. Funk, A. S. Litsky "Effect of cement modulus on the shear properties of the bone-cement interface". *Biomaterials*, 1998; 19, pp: 1561-1567.
- [103] K. Walter 'Rheometry'. Chapman and Hall, London (1975).
- [104] A. J. Giacomin and J. M. Dealy 'Large-Amplitude Oscillatory Shear' Edited by A.A Collyer 'Techniques in Rheological Measurement' (First edition 1993). Chapman & Hall.
- [105] Tutor gig. [online]
<http://www.tutorgig.com/encyclopedia/getdefn.jsp?keywords=Permeability> (Accessed on April 2, 2004).
- [106] M. J. Askew, J. W. Steege, J. L. Lewis, J. R. Ranieri, R. L. Wixson "Effect of cement pressure and bone strength on polymethylmethacrylate fixation." *J Orthop Res*, 1984; 1:4, pp: 412-420.
- [107] R. S. Majowski, A. W. Miles, G. C. Bannister, J. Perkins and J. S. Taylor "Bone surface preparation in cemented joint replacement." *J. Bone Jt Surg.*, 1993, 75B, pp: 459-463.
- [108] M. J. Askew, J. W. Steege, J. L. Lewis, R. L. Ranieri "Effect of cement pressure and bone cement strength in polymethyl methacrylate fixation" *J. of Orthopaedic Research*, 1984; 1: 4, pp: 412-420.
- [109] R. M. Rey, G. D. Paiement, W. M. McGann, M. Jasty, T. P. Harrigan, D. W. Burke, W. H. Harris "A study of intrusion characteristics of low viscosity cement Simplex-P and Palacos cements in a bovine cancellous bone model." *Clinical Orthopaedics and Related Research*, Feb 1987; pp: 272-278.
- [110] R. Kusleika and S. I. Stupp "Mechanical strength of PMMA cement-human bone interfaces." *J. Biomed. Mater. Res.*, 1983, 17, pp: 441-458.

- [111] R. S. Majowski, G. C. Bannister, and A. W. Miles "The effect of bleeding on the cement-bone interface." *Clin. Orthop. Rel. Res.*, 1994, 299, pp: 293-297.
- [112] K. L. Markolf and H. C. Amstutz "Penetration and Flow of Acrylic Bone Cement" *Clinical Orthopaedics and Related Research*, Nov-Dec 1976; 121, pp: 99-102.
- [113] S. A. Maher and B. A. O. McCormack "Quantification of interdigitation at bone cement/cancellous bone interfaces in cemented femoral reconstructions" *Proc Instn Mech Engrs*, 1999; 213:H, pp: 347-354.
- [114] F. R. DiMaio "The Science of Bone Cement: A Historical Review." *Orthopedics* December 2002; 25:12, pp: 1399-1409.
- [115] N. M. Kurdy, J. P. Hodgkinson and R. Haynes "Acrylic bone-cement. Influence of mixer design and unmixed powder." *J Arthroplasty* Oct 1996; 11, pp: 813-819.
- [116] S. Smeds, D. Goertzen, I. Ivarsson "Influence of temperature and vacuum mixing on bone cement properties." *Clin Orthop* Jan 1997, pp: 326-334.
- [117] S. He, C. Scott and P. Higham "Mixing of acrylic bone cement: effect of oxygen on setting properties" *Biomaterials* 2003; 24, pp: 5045-5048.
- [118] L. Lidgren, B. Bodelind, J. Moller "Bone cement improved by vacuum mixing and chilling." *Acta Orthop Scand* 1987; 58, pp: 27-32.
- [119] D. Hansen, J. S. Jensen "Prechilling and vacuum mixing not suitable for all bone cements." *J Arthroplasty* 1990; 5, pp: 287-90.
- [120] N.J. Dunne and J.F. Orr. "Thermal characteristics of curing acrylic bone cement." *ITBM-RBM* 2001; 22, pp: 88-97.
- [121] F. F. Oldfield and H. K. Yasuda "ESR study of MMA polymerization by a peroxide/amine system: bone cement formation." *J Biomed Mater Res*, Mar 1999; 44, pp: 436-45.
- [122] J. L. Ferracane and E. H. Greener "Rheology of Acrylic Bone Cements" *Biomat., Med. Dev., Art. Org.*, 1981; 9:3, pp: 213-224.
- [123] A. Nzihou, L. Attias, P. Sharrock and A. Ricard "A rheological, thermal and mechanical study of bone cement-from a suspension to a solid biomaterial" *Powder Technology*, 1998; 99, p: 60-69.
- [124] D.F. Farrar and J. Rose "Rheological properties of PMMA bone cements during curing" *Biomaterials*, 2001; 22, pp: 3005-3013.
- [125] G. Lewis and M. Carroll "Rheological Properties of Acrylic Bone Cement During Curing and Role of the Size of the Powder Particles" *Journal of Biomedical Materials Research, Applied Biomaterials*, 2002; 63:2.

- [126] A W McCaskie, M R Barnes, E Lin, W M Harper and P J Gregg "Cement Pressurisation During Hip Replacement" *The Journal of Bone and Joint Surgery*, May 1997, 79-B 3, pp 379-384
- [127] P C Noble & E Swarts "Penetration of Acrylic Bone Cements into Cancellous Bone" *Acta Orthop scand* 1983, 54, pp 566-573
- [128] F Canabal and B Katz "A computational fluid dynamics simulation of PMMA cement flow upon insertion of a femoral stem into a bone cavity during a total hip prosthesis procedure" *Advances in Bioengineering, ASME* 1994, 28, pp 165-166
- [129] N J Dunne, J F Orr and D J Heylings "Measurement of Intermedullary Cement Pressure" *Innovation and Technology in Biology and Medicine*, 1998, 19 5, p 347-359
- [130] N J Dunne, J F Orr "Development of a computer model to predict pressure generation around hip replacement stems" *Proceedings Of The Institution Of Mechanical Engineers Part H, Journal Of Engineering In Medicine*, 2000, 214 6, pp 645-658
- [131] N J Dunne "Evaluation of static and dynamic properties of polymethyl methacrylate bone cements and their effects on implant fixation" PhD thesis, The Queen's University of Belfast, 1996
- [132] S Breusch, C Heisel, J Muller, T Borchers and H Mau "Influence of cement viscosity on cement interdigitation and venous fat content under in vivo conditions A bilateral study of 13 sheep" *Acta Orthop Scand*, 2002, 73 4, pp 409-415
- [133] M Bohner, B Gasser, G Baroud, P Heini "Theoretical and experimental model to describe the injection of a polymethylmethacrylate cement into a porous structure" *Biomaterials*, 2003, 24, pp 2721-2730
- [134] G Baroud, J Z Wu, M Bohner, S Sponagel, T Steffen "How to determine the permeability for cement infiltration of osteoporotic cancellous bone" *Medical Engineering & Physics*, 2003, 25, pp 283-288
- [135] G Baroud and F B Yahia "A finite element rheological model for polymethylmethacrylate flow analysis of the cement delivery in vertebroplasty" *Proceedings Of The Institution Of Mechanical Engineers, Journal Of Engineering In Medicine*, 2004, 218 H, pp 331-338
- [136] Pico technology limited, [online], <http://www.picotech.com/> (Accessed November 10, 2002)
- [137] ASTM Specification F 451-95 Standard specification for acrylic bone cement

- [138] International Standard ISO 5833:1992(E). Implants for Surgery-Acrylic Resin Cements.
- [139] "Introduction to ANSYS" Release 5.3, July 24, 1996.
- [140] V. Adams and A. Askenazi "Building Better Products with Finite Element Analysis", First edition, 1999, OnWord press USA.
- [141] S. Moaveni "Finite element analysis : theory and application with ANSYS" Upper Saddle River, NJ : Prentice Hall, 1999.
- [142] J. D. Bryant, T. David, P. H. Gaskell, S. King, G. Lond "Rheology of bovine bone marrow" Proc Inst Mech Eng. H. 1989; 203:2, pp: 71-75.
- [143] "Online Manual of ANSYS 6.1" -Release 6.1 UP20020321.
- [144] A. Bettencourt, A. Calado, J. Amaral, F.M. Vale, J.M.T. Rico, J. Monteiro, M. Castro "The influence of vacuum mixing on methylmethacrylate liberation from acrylic cement powder" International Journal of Pharmaceutics, 2001; 219, pp: 89-93.
- [145] Tekno Surgical Ltd. Unit A4 Centrepont Business Park, Oak Road, Dublin 12. Supplier of Howmedica Osteonics in Dublin. Contact date start from 2nd March 2004.
- [146] C STEM Triple Taper Stabilized Hip. [online]
http://www.jnigateway.com/home.jhtml?loc=USENG&page=viewContent&contentId=09008b98800547a2&nodekey=/Prod_Info/Company/DePuy_Orthopaedics/Joint_Reconstruction_Components/Hip_Primary&parentId=fc0de00100000503 (Accessed on 7th January, 2004).
- [147] C-STEM Impaction Bone Grafting Technique. [online]
http://www.jnigateway.com/home.jhtml?loc=USENG&page=viewContent&contentId=09008b98800547a2&nodekey=/Prod_Info/Company/DePuy_Orthopaedics/Joint_Reconstruction_Components/Hip_Primary&parentId=fc0de00100000503 (Accessed on 7th January, 2004).
- [148] Endurance and Luster Total Hip System Surgical Technique. [online]
http://www.jnigateway.com/home.jhtml?loc=USENG&page=viewContent&contentId=fc0de00100000173&parentId=fc0de00100000173&specialty=Orthopaedics&category=Hip&subcategory=Primary_Prostheses (Accessed on 7th January, 2004).
- [149] Fluent's Online Support Resources. [online],
http://www.fluentusers.com/fidap/doc/doc_f.htm (Accessed on August 20, 2004. Registration required to access the site).

- [150] Fluent's Online Support Resources. Theory manual. [online].
http://www.fluentusers.com/fidap/doc/ori/html/theory/th07_06.htm#th0706 (Accessed on March 15, 2006. Registration required to access the site).
- [151] Fluent's Online Support Resources. Theory manual. [online].
http://www.fluentusers.com/fidap/doc/ori/html/theory/th07_01-02.htm (Accessed on March 15, 2006. Registration required to access the site).
- [152] J. L. Gilbert, J. M. Hasenwinkel, R. L. Wixson and E. P. Lautenschlager "A theoretical and experimental analysis of polymerization shrinkage of bone cement: A potential major source of porosity" J Biomed Mater Res. 2000, 52:1. pp: 210-218.

Appendix A

Simulation softwares

In order to simulate the model in this study it was necessary to select software that is capable of dealing with porous and fluid media together. The fluid element selected should have the capability to add shear-rate and time dependent viscosity.

A.1 Ansys

Ansys is a general purpose simulation software. Element 141 (2D) and Element 142 (3D) have been used for VOF (Volume of fluid) feature to calculate the free surface movement of fluid. The VOF feature is restricted to 2D models in this software [143].

- a) At the beginning of the study, a model of porous cancellous bone was created by creating holes in the geometry (2D and 3D). The model failed due to two reasons. Firstly, there were difficulties when meshing the model. Also, the CFD elements and other elements, such as solid, can not be used together [143]. CFD elements can only be used with other element for fluid solid interaction (FSI) analysis. Moreover, there should be equal number of interfaces (line for 2D and plane for 3D) in the fluid and solid boundary. But it is quite impossible to divide the fluid interface according to number of solid interfaces.
- b) Using FSI, bone cement was represented by Fluid 141 and cancellous bone by plane 41. Porosity of cancellous bone was assigned by selecting elements of the particular location and setting to air property. This approach was failed due to a convergence error.
- c) Finally, a built in feature called the distributed resistance was used in the fluid region to define the porosity of cancellous bone. This feature mathematically applies the resistance term in the continuity equations to create the porous effect. In this approach, solid properties of cancellous bone can't be applied, due to the single-phase limitation of CFD.

elements [143] In this study, penetration of bone cement through the porous cancellous bone was calculated using this approach The simulation was performed by changing the applied pressure from 76 kPa to 126 kPa for the rheopectic and pseudoplastic behaviour of bone cement This shows that the penetration is less than 1 mm for all bone cements

A 2 Fluent

Fluent is a computational fluid dynamics (CFD) simulation software It has the capability to include fluid, solid and porous entities The porous entity is modeled as a special type of fluid entity Only the porosity of the porous entity can be specified The depth of penetration of bone cement through cancellous bone using fluent did not match the experimental values

A 3 MSC Marc

MSC Mark is a general purpose simulation software Solid, soil and fluid elements can be incorporated using the software Non-Newtonian fluid properties in shear-rate dependent viscosity can be included There are, however, no porous elements in the software

A.4 Abaqus

Abaqus is a general purpose simulation software It has no fluid elements It has the capability to add poro fluid element in which permeability can be included The unit of the permeability is in the form of soil mechanics Beside this only linear viscosity can be included using this software

Appendix B

Time step and mesh density convergence

A convergence test was performed in this Finite Element analysis to determine the optimum mesh density and time step.

B.1 Time step convergence

Four different time steps (0.005 sec, 0.001 sec, 0.0008 sec and 0.0005 sec) were used to check the time step convergence for the pseudoplastic behaviour of bone cement. One set of simulations for the pseudoplastic simplex P® bone cement (figure B-1) was performed to determine the converged time step. A pressure of 76 kPa was applied for a duration of 2 minutes, 3 minutes after the start of bone cement mixing followed by application of prosthesis insertion velocity of 5 mm/s for duration of 1 minute.

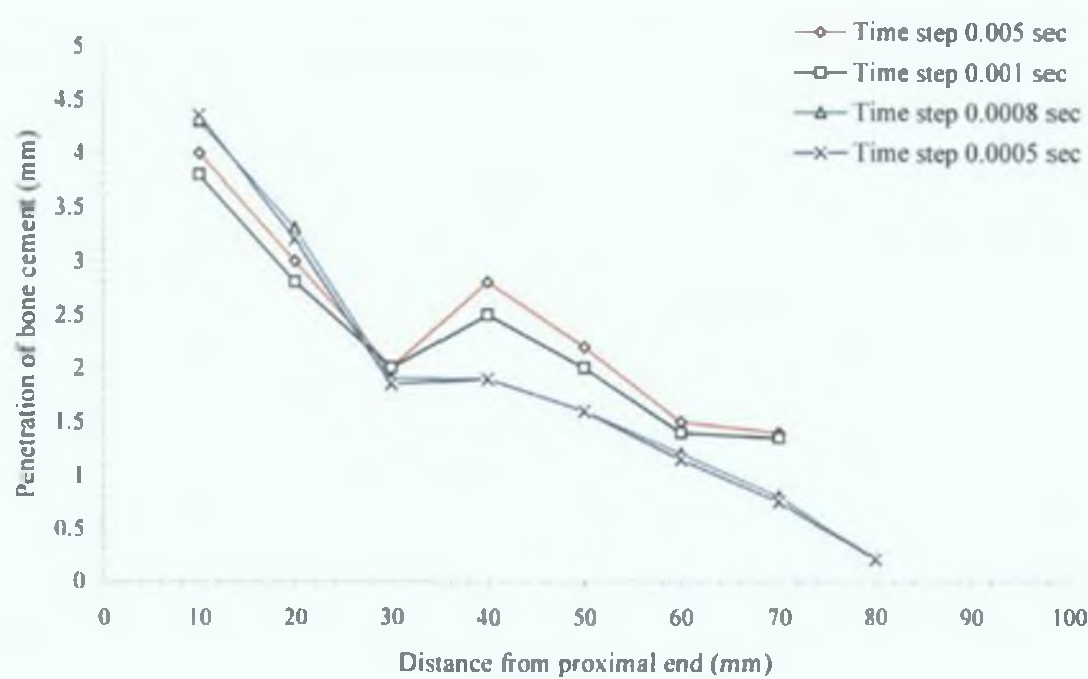


Figure B-1: Time step convergence of pseudoplastic Simplex P® bone cement penetration at prosthesis insertion velocity of 5 mm/s for four different time steps.

Figure B-1 shows that both the 0.0008 sec and the 0.0005 sec time steps converge the penetration of bone cement. The solution time required for .0008 sec time step is less

than 0.0005 sec time step. Considering this point the 0.0008 sec time step was used for the simulation of pseudoplastic bone cement.

Three different time steps (0.005 sec, 0.001 sec and 0.0008 sec) were used to check the time step convergence for the rheopectic behaviour of bone cement. One set of simulations for the rheopectic CMW3 bone cement (figure B-2) was performed to determine the converged time step. The boundary condition was same as for pseudoplastic behaviour of bone cement.

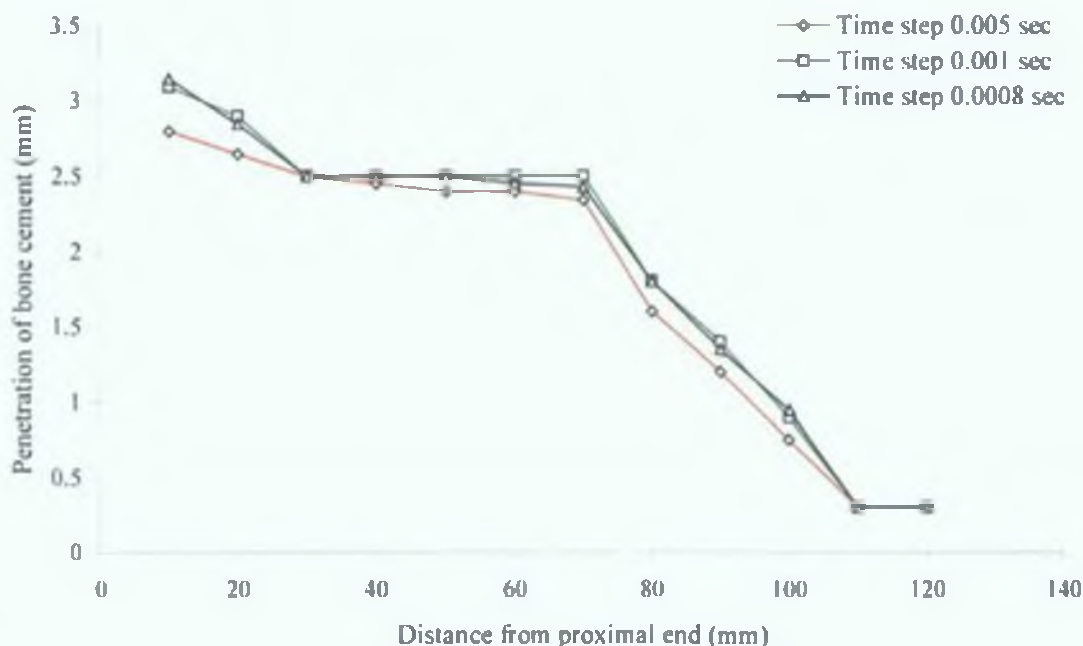


Figure B-2: Time step convergence of rheopectic CMW3 bone cement penetration at 5 mm/s prosthesis insertion velocity for three different time steps.

Figure B-2 shows that both the 0.001 sec and the 0.0008 sec time steps converge the penetration of bone cement. Considering the requirement for a quick solution time, 0.001 sec time step was used for the simulation of rheopectic bone cement.

B.2 Mesh density convergence

The mesh density convergence was checked for the pseudoplastic and rheopectic behaviour of bone cement at converged time step of 0.0008 sec and 0.001 sec respectively. Similar boundary condition was used to determine the converged mesh density for pseudoplastic Simplex P® (figure B-3) and rheopectic CMW3 bone cement (figure B-4). In both case, the results from element number 3030 and 3450 are almost

identical. A total number of 3030 elements was used in all simulation in this study due to the solution time considerations.

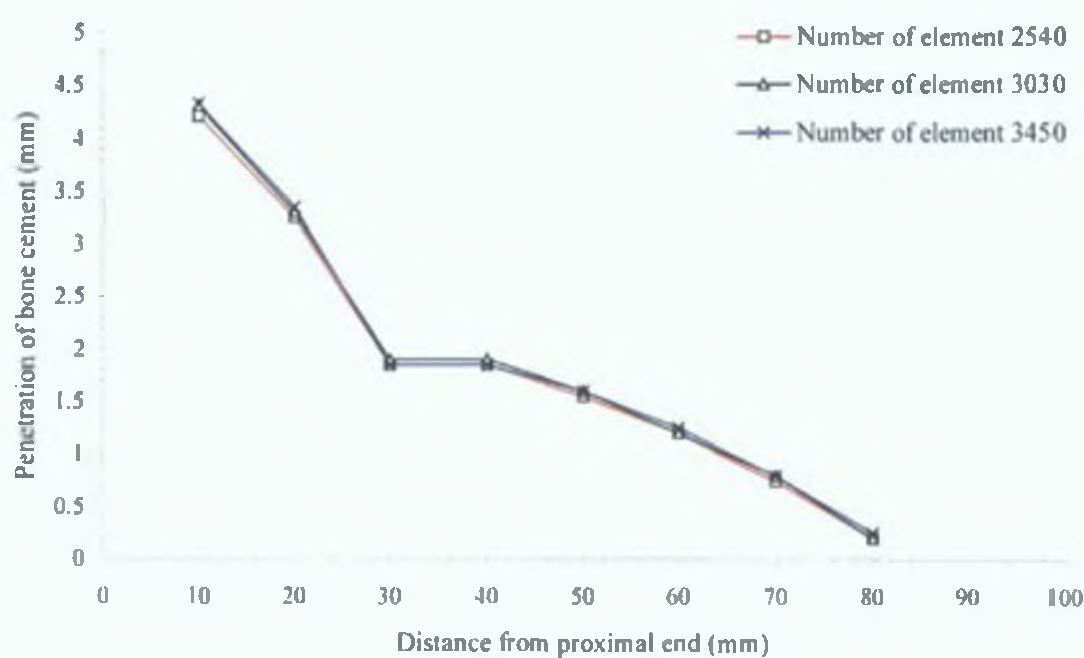


Figure B-3: Mesh density convergence of pseudoplastic Simplex P® bone cement penetration at a prosthesis insertion velocity of 5 mm/s for a time step of 0.0008 sec.

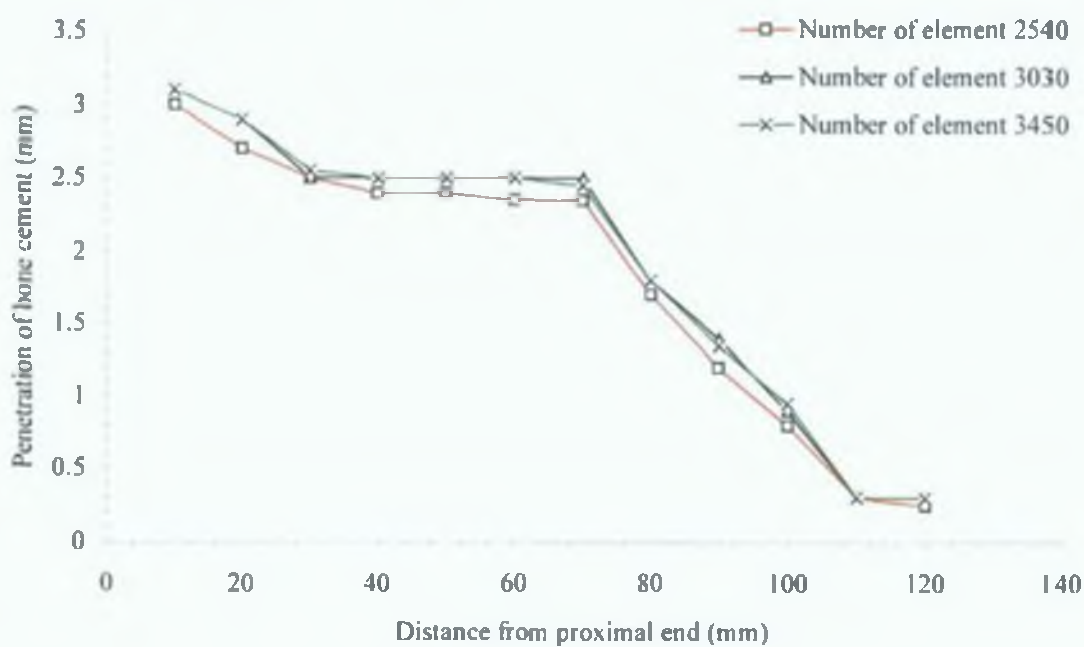


Figure B-4: Mesh density convergence of rheoplectic CMW3 bone cement penetration at a prosthesis insertion velocity 5 mm/s for a time step of 0.001 sec.

Appendix C

This appendix contains figures showing pressure distribution, units in Pa, in bone cement with a free surface, at the end of 12 minute simulation. Bone marrow viscosity was 0.067 Pa.s [142] and the porosity of cancellous bone was 85% [129] for all cases.

The results are grouped in four categories.

1. **Variation of prosthesis insertion velocity**

a. **Simplex p® bone cement:** Pseudoplastic behaviour of bone cement.

Common boundary condition: A pressure of 76 kPa was applied on the inlet from 3 to 5 minutes.



Figure C-1: Prosthesis insertion velocity of 5 mm/s from 5 to 6 minutes.



Figure C-2: Prosthesis insertion velocity of 10 mm/s from 5 to 6 minutes.



Figure C-3: Prosthesis insertion velocity of 15 mm/s from 5 to 6 minutes.



Figure C-4: Prosthesis insertion velocity of 20 mm/s from 5 to 6 minutes.

b. Zimmer bone cement: Pseudoplastic behavior of bone cement.

Common boundary condition: A pressure of 76 kPa was applied on the inlet from 3 to 5 minutes.



Figure C-5: Prosthesis insertion velocity of 5 mm/s from 5 to 6 minutes.



Figure C-6: Prosthesis insertion velocity of 10 mm/s from 5 to 6 minutes.



Figure C-7: Prosthesis insertion velocity of 15 mm/s from 5 to 6 minutes.



Figure C-8: Prosthesis insertion velocity of 20 mm/s from 5 to 6 minutes.

c. CMW3 bone cement: Rheopectic behavior of bone cement.



Figure C-9: A pressure of 76 kPa was applied on inlet from 3 to 4 minutes.



Figure C-10: A pressure of 76 kPa was applied on inlet from 3 to 5 minutes.



Figure C-11: A pressure of 76 kPa was applied on inlet from 3 to 6 minutes.

d. **CMW3 bone cement:** Rheopectic behavior of bone cement.

Common boundary condition: A pressure of 76 kPa was applied on inlet from 3 to 5 minutes.



Figure C-12: Prosthesis insertion velocity of 5 mm/s from 5 to 6 minutes.



Figure C-13: Prosthesis insertion velocity of 10 mm/s from 5 to 6 minutes.



Figure C-14: Prosthesis insertion velocity of 15 mm/s from 5 to 6 minutes.



Figure C-15: Prosthesis insertion velocity of 20 mm/s from 5 to 6 minutes.

e. **Zimmer bone cement:** Rheopectic behavior of bone cement.



Figure C-16: A pressure of 76 kPa was applied on inlet from 3 to 4 minutes.



Figure C-17: A pressure of 76 kPa was applied on inlet from 3 to 5 minutes.



Figure C-18: A pressure of 76 kPa was applied on inlet from 3 to 6 minutes.

f. **Zimmer bone cement:** Rheopectic behavior of bone cement.

Common boundary condition: A pressure of 76 kPa was applied on inlet from 3 to 5 minutes.



Figure C-19: Prosthesis insertion velocity of 5 mm/s from 5 to 6 minutes.



Figure C-20: Prosthesis insertion velocity of 10 mm/s from 5 to 6 minutes.



Figure C-21: Prosthesis insertion velocity of 15 mm/s from 5 to 6 minutes.



Figure C-22: Prosthesis insertion velocity of 20 mm/s from 5 to 6 minutes.

2. Variation of prosthesis insertion velocity time duration
- a. Simplex p® bone cement: Pseudoplastic behavior of bone cement.
- Common boundary condition: A pressure of 76 kPa was applied on inlet from 3 to 5 minutes.



Figure C-23: Prosthesis insertion velocity of 5 mm/s from 5 to 5.5 minutes.



Figure C-24: Prosthesis insertion velocity of 5 mm/s from 5 to 6.5 minutes.



Figure C-25: Prosthesis insertion velocity of 10 mm/s from 5 to 5.5 minutes.



Figure C-26: Prosthesis insertion velocity of 10 mm/s from 5 to 6.5 minutes.



Figure C-27: Prosthesis insertion velocity of 15 mm/s from 5 to 5.5 minutes.



Figure C-28: Prosthesis insertion velocity of 15 mm/s from 5 to 6.5 minutes.



Figure C-29: Prosthesis insertion velocity of 20 mm/s from 5 to 5.5 minutes.



Figure C-30: Prosthesis insertion velocity of 20 mm/s from 5 to 6.5 minutes.

b. CMW3 bone cement: Rheopectic behavior of bone cement.

Common boundary condition: A pressure of 76 kPa was applied on inlet from 3 to 5 minutes.



Figure C-31: Prosthesis insertion velocity of 5 mm/s from 5 to 5.5 minutes.



Figure C-32: Prosthesis insertion velocity of 5 mm/s from 5 to 6.5 minutes.



Figure C-33: Prosthesis insertion velocity of 10 mm/s from 5 to 5.5 minutes.



Figure C-34: Prosthesis insertion velocity of 10 mm/s from 5 to 6.5 minutes.



Figure C-35: Prosthesis insertion velocity of 15 mm/s from 5 to 5.5 minutes.



Figure C-36: Prosthesis insertion velocity of 15 mm/s from 5 to 6.5 minutes.



Figure C-37: Prosthesis insertion velocity of 20 mm/s from 5 to 5.5 minutes.



Figure C-38: Prosthesis insertion velocity of 20 mm/s from 5 to 6.5 minutes.

c. **Zimmer bone cement:** Rheopectic behavior of bone cement.

Common boundary condition: A pressure of 76 kPa was applied on inlet from 3 to 5 minutes.



Figure C-39: Prosthesis insertion velocity of 5 mm/s from 5 to 5.5 minutes.



Figure C-40: Prosthesis insertion velocity of 5 mm/s from 5 to 6.5 minutes.



Figure C-41: Prosthesis insertion velocity of 10 mm/s from 5 to 5.5 minutes.



Figure C-42: Prosthesis insertion velocity of 10 mm/s from 5 to 6.5 minutes.



Figure C-43: Prosthesis insertion velocity of 15 mm/s from 5 to 5.5 minutes.



Figure C-44: Prosthesis insertion velocity of 15 mm/s from 5 to 6.5 minutes.



Figure C-45: Prosthesis insertion velocity of 20 mm/s from 5 to 5.5 minutes.



Figure C-46: Prosthesis insertion velocity of 20 mm/s from 5 to 6.5 minutes.

d. Zimmer bone cement: Pseudoplastic behavior of bone cement.

Common boundary condition: A pressure of 76 kPa was applied on inlet from 3 to 5 minutes.



Figure C-47: Prosthesis insertion velocity of 5 mm/s from 5 to 5.5 minutes.



Figure C-48: Prosthesis insertion velocity of 5 mm/s from 5 to 6.5 minutes.



Figure C-49: Prosthesis insertion velocity of 10 mm/s from 5 to 5.5 minutes.



Figure C-50: Prosthesis insertion velocity of 10 mm/s from 5 to 6.5 minutes.



Figure C-51: Prosthesis insertion velocity of 15 mm/s from 5 to 5.5 minutes.



Figure C-52: Prosthesis insertion velocity of 15 mm/s from 5 to 6.5 minutes.



Figure C-53: Prosthesis insertion velocity of 20 mm/s from 5 to 5.5 minutes.



Figure C-54: Prosthesis insertion velocity of 20 mm/s from 5 to 6.5 minutes.

3. **Variation of bone cement thickness:** The bone cement thickness for the group was 8 mm. All other groups had a bone cement thickness of 10 mm.
- a. **Simplex p® bone cement:** Pseudoplastic behavior of bone cement.
- Common boundary condition: A pressure of 76 kPa was applied on inlet from 3 to 5 minutes.



Figure C-55: Prosthesis insertion velocity of 5 mm/s from 5 to 6 minutes.



Figure C-56: Prosthesis insertion velocity of 10 mm/s from 5 to 6 minutes.



Figure C-57: Prosthesis insertion velocity of 15 mm/s from 5 to 6 minutes.



Figure C-58: Prosthesis insertion velocity of 20 mm/s from 5 to 6 minutes.

b. Zimmer bone cement: Pseudoplastic behavior of bone cement.

Common boundary condition: A pressure of 76 kPa was applied on inlet from 3 to 5 minutes.



Figure C-59: Prosthesis insertion velocity of 5 mm/s from 5 to 6 minutes.



Figure C-60: Prosthesis insertion velocity of 10 mm/s from 5 to 6 minutes.



Figure C-61: Prosthesis insertion velocity of 15 mm/s from 5 to 6 minutes.



Figure C-62: Prosthesis insertion velocity of 20 mm/s from 5 to 6 minutes.

4. **Variation of applied pressure duration time for validation:** The bone cement thickness for this group was 8 mm. All other groups had a bone cement thickness of 10 mm.

a. **CMW3 bone cement:** Rheopectic behavior of bone cement.



Figure C-63: A pressure of 76 kPa was applied on inlet from 3 to 4 minute and prosthesis insertion velocity was 10 mm/s from 4 to 5 minutes.



Figure C-64: A pressure of 76 kPa was applied on inlet from 3 to 5 minute and prosthesis insertion velocity was 10 mm/s from 5 to 6 minutes.



Figure C-65: A pressure of 76 kPa was applied on inlet from 3 to 6 minute and prosthesis insertion velocity was 10 mm/s from 6 to 7 minutes.

Appendix D

Example of input (log) files for the simulation

D.1 Journal file for GAMBIT pre-processor

```
/ Journal File for GAMBIT 2 0 4
/ File opened for write Mon Jul 28 21 09 07 2003
/Modified by Mohammad Mafizur Rahman

solver select "FIDAP"

/geometry
vertex create coordinates 0 0 0
vertex create coordinates 0 15 0 0
vertex create coordinates 0 15 0 01 0
vertex create coordinates 0 0 01 0
vertex create coordinates 0 15 0 017 0
vertex create coordinates 0 0 017 0
edge create straight "vertex 1" "vertex 2"
edge create straight "vertex 2" "vertex 3"
edge create straight "vertex 3" "vertex 4"
edge create straight "vertex 4" "vertex 1"
edge create straight "vertex 3" "vertex 5"
edge create straight "vertex 5" "vertex 6"
edge create straight "vertex 6" "vertex 4"
face create wireframe "edge 1" "edge 2" "edge 3" "edge 4" real
face create wireframe "edge 3" "edge 5" "edge 6" "edge 7" real
window modify shade

/meshing

/Edge division
```

```
edge mesh "edge 1" "edge 3" "edge 6" successive ratio 1 1 intervals 100
edge mesh "edge 2" "edge 4" "edge 5" "edge 7" successive ratio 1 1 intervals 8
```

```
/Face Mesh creation
```

```
face mesh "face 1" "face 2" map size 1
```

```
/BOUNDARY ENTITIES
```

```
physics create "axis" btype "PLOT" edge "edge 1"
physics create "inlet" btype "PLOT" edge "edge 4"
physics create "outlet" btype "PLOT" edge "edge 2"
physics create "left" btype "PLOT" edge "edge 7"
physics create "top" btype "PLOT" edge "edge 6"
physics create "right" btype "PLOT" edge "edge 5"
physics create "part" btype "PLOT" edge "edge 3"
```

```
/CONTINUUM ENTITIES
```

```
physics create "bonec" ctype "FLUID" face "face 1"
physics create "cance" ctype "POROUS" face "face 2"
```

```
/Element Type
```

```
default set "MESH NODES QUAD" numeric 4
```

D 2 Input (FIPREP) file for FIDAP simulation software

a Sample file for Pseudoplastic viscosity behaviour

```
/ *****
/ Disclaimer This file was written by GAMBIT and contains
/ all the continuum and boundary entities and coordinate systems
/ defined in GAMBIT Additionally, some frequently used FIPREP
/ commands are added Modify/Add/Uncommment any necessary commands
/ Refer to FIPREP documentation for complete listing of commands
/ *****
/ Modified by Mohammad Mafizur Rahman
```



```

/ *****
/      CONVERSION OF NEUTRAL FILE TO FIDAP Database
/
FICONV( NEUTRAL )
INPUT( FILE="1 FDNEUT" )
OUTPUT( DELETE )
END
/
TITLE
Finite Element Modelling of Rheological and Penetration characteristics of curing
PMMA bone Cement in total hip replacement
/
FIPREP
/
/      PROBLEM SETUP
/
PROBLEM (AXI-SYMMETRIC, NONLINEAR, TRANSIENT)
EXECUTION( NEWJOB )
PRINTOUT(NBLOCKS=4)
1 10 1
10 700 10
700 20000 100
20000 200000 1000
DATAPRINT( CONTROL )
FILLING( FILL, COUR = 0 1, SUBC)
/
/      CONTINUUM ENTITIES
/
ENTITY ( NAME = "bonec", FLUI, MDENS = "mbonecfd", MVIS = "mbonecfv" )

/**For a porous entity, both fluid and solid matrix properties are required**

```

```
ENTITY ( NAME = "cance", POROUS, MDENS= "mcancefd", MVISC= "mcancefv",
MSDENS="mcancesd", MPOISSON = "mcancesp", MYMODULUS = "mcancesy",
MAPERM = "mcancespa")
```

```
/
```

```
/    BOUNDARY ENTITIES
```

```
/
```

```
ENTITY ( NAME = "axis", PLOT )
```

```
ENTITY ( NAME = "inlet", PLOT )
```

```
ENTITY ( NAME = "outlet", PLOT )
```

```
ENTITY ( NAME = "left", PLOT )
```

```
ENTITY ( NAME = "top", PLOT )
```

```
ENTITY ( NAME = "right", PLOT )
```

```
ENTITY ( NAME = "part", PLOT )
```

```
/
```

```
/
```

```
/    SOLUTION PARAMETERS
```

```
/
```

```
SOLUTION( SEGREGATED = 1000, VELCONV = .001, SCHARGE = 0.0)
```

```
PRESSURE( MIXED=1E-10, DISCONTINUOUS )
```

```
TIME( BACKWARD, NSTEPS =200000, DT=1e-3,TSTART=0, TEND=720,
```

```
DTMAX= 1, INCMAX= 1.2, WINDOW = 0.7 )
```

```
POSTPROCESS(NBLOCKS=4)
```

```
1 10 1
```

```
10 700 10
```

```
700 20000 100
```

```
20000 200000 1000
```

```
/
```

```
/    MATERIAL PROPERTIES
```

```
/
```

```
/*Material Properties of Fluid Bone Cement****
```

```
/*Set label must be unique and must same as property type of Entity command****
```

```
/
```

```
/Simplex P
```

```

DENSITY( SET = "mbonecfd", CONSTANT = 1290 )
VISCOSITY( SET = "mbonecfv", POWERLAW )
265 15,1 48,0 65,50
/
/****Material Properties of Porous Bone****
/
/Property of Fluid Part
/
DENSITY( SET = "mcancefd", CONSTANT = 1 )
VISCOSITY( SET = "mcancefv", CONSTANT = 0.067 )
/
/Property of Solid Part
/
DENSITY( SET = "mcancesd", CONSTANT = 300 )
YOUNGMODULUS( SET = "mcancesy", CONS = 389000000 )
POISSONCOEFFICIENT( SET = "mcancesp", CONS = 0.4 )
PERMEABILITY( SET = "mcancespa", ACOE, CONS = 100, x=1.0e-9, y=1.0e-9,
z=1.0e-9, POROSITY = 0.85 )
/
/      INITIAL AND BOUNDARY CONDITIONS FOR FILLING
/
ICNODE(FILL,CONSTANT=1,ENTITY="bonec")

/The following boundary condition on the fill fraction is
/specified to indicate that fluid (not void) enters the mesh
/from the inlet
BCNODE(FILL,CONSTANT=1,ENTITY="inlet")
/INITIAL AND BOUNDARY CONDITIONS FOR VELOCITY AND
/DISPLACEMENT
/
ICNODE(VELOCITY,STOKES)
TMFUNCTION (SET = 1,NPOINTS = 7)

```

```

0 0,0 000000001 180 0,0 000000001 299 999999,0 000000001 300 0,0 01 360 0,0 01
360 000001,0 000000001 720 0,0 000000001
BCNODE( UY, CONSTANT = 1, ENTITY = "axis", FACTOR=1, CURVE=1 )
TMFUNCTION (SET = 2,NPOINTS = 7)
0 0,1 0 179 999999,1 0 180 0,76000 0 299 999999,76000 0 300 0,1 0 600 0,1 0
720 0,1 0
BCFLUX( X, CONSTANT = 1, ENTITY = "inlet", FACTOR=1, CURVE=2 )
BCNODE( VELOCITY, ZERO, ENTITY = "left" )
BCNODE( VELOCITY, ZERO, ENTITY = "top" )
BCNODE( VELOCITY, ZERO, ENTITY = "right" )
BCNODE( UX, ZERO, ENTITY = "outlet" )
END
/
CREATE( FIPREP,DELETE )
PARAMETER( LIST )
CREATE( FISOLV )
/RUN( FISOLV, FOREGROUND )

```

b Sample file for rheopectic viscosity behaviour

```

/ *****
/ Disclaimer This file was written by GAMBIT and contains
/ all the continuum and boundary entities and coordinate systems
/ defined in GAMBIT Additionally, some frequently used FIPREP
/ commands are added Modify/Add/Uncommment any necessary commands
/ Refer to FIPREP documentation for complete listing of commands
/ *****
/ Modified by Mohammad Mafizur Rahman
/ *****
/
/      CONVERSION OF NEUTRAL FILE TO FIDAP Database
/
FICONV( NEUTRAL )

```

```

INPUT( FILE="1 FDNEUT" )
OUTPUT( DELETE )
END
/
TITLE
Modelling of Rheological Properties of Curing Bone Cement
/
FIPREP
/
/      PROBLEM SETUP
/

PROBLEM (AXI-SYMMETRIC, NONLINEAR, TRANSIENT)
NONN, STRU, REME )
EXECUTION( NEWJOB )
PRINTOUT(NBLOCKS=4)
1 10 1
10 700 10
700 20000 100
20000 200000 1000
DATAPRINT( CONTROL )
FILLING( FILL, COUR = 0 1, SUBC)
/
/      CONTINUUM ENTITIES
/

ENTITY ( NAME = "bonec", FLUI, MDENS = "mbonecfd", MVISC = "mbonecfv" )

/**For a porous entity, both fluid and solid matrix properties are required**
ENTITY ( NAME = "cance", POROUS, MDENS= "mcancefd", MVISC= "mcancefv",
MSDENS="mcancesd", MPOISSON = "mcancesp", MYMODULUS = "mcancesy",
MAPERM = "mcancespa")
/
/      BOUNDARY ENTITIES

```

```

/
ENTITY ( NAME = "axis", PLOT )
ENTITY ( NAME = "inlet", PLOT )
ENTITY ( NAME = "outlet", PLOT )
ENTITY ( NAME = "left", PLOT )
ENTITY ( NAME = "top", PLOT )
ENTITY ( NAME = "right", PLOT )
ENTITY ( NAME = "part", PLOT )
/
/      SOLUTION PARAMETERS
/
SOLUTION( SEGREGATED = 1000, VELCONV = .001, SCHARGE = 0.0)
PRESSURE( MIXED=1E-10, DISCONTINUOUS )
TIME( BACKWARD, NSTEPS =200000, DT=1e-3,TSTART=0, TEND=720,
DTMAX= 1, INCMAX= 1.2, WINDOW = 0.7 )
POSTPROCESS(NBLOCKS=4)
1 10 1
10 700 10
700 20000 100
20000 200000 1000
/
/
/      MATERIAL PROPERTIES
/
/****Material Properties of Fluid Bone Cement****
/**** Set label must be unique and must same as property type of Entity command****
/
/Zimmer bone cement
DENSITY( SET = "mbonecfd", CONSTANT = 1230 )
VISCOSITY( SET = "mbonecfv", SUBROUTINE )
/
/****Material Properties of Porous Bone****
/

```

/Property of Fluid Part

/

DENSITY(SET = "mcancefd", CONSTANT = 1)

VISCOSITY(SET = "mcancefv", CONSTANT = 0.067)

/

/Property of Solid Part

/

DENSITY(SET = "mcancesd", CONSTANT = 300)

YOUNGMODULUS(SET = "mcancesy", CONS = 389000000)

POISSONCOEFFICIENT(SET = "mcancesp", CONS = 0.4)

PERMEABILITY(SET = "mcancespa", ACOE, CONS = 100, x=1.0e-9, y=1.0e-9,
z=1.0e-9, POROSITY = 0.85)

/

/ INITIAL AND BOUNDARY CONDITIONS FOR FILLING

/

ICNODE(FILL,CONSTANT=1,ENTITY="bonec")

/The following boundary condition on the fill fraction is

/specified to indicate that fluid (not void) enters the mesh

/from the inlet

BCNODE(FILL,CONSTANT=1,ENTITY="inlet")

/

INITIAL AND BOUNDARY CONDITIONS FOR VELOCITY AND
DISPLACEMENT

/

ICNODE(VELOCITY,STOKES)

TMFUNCTION (SET = 1,NPOINTS = 7)

0.0,0.000000001 180 0.0,0.000000001 299 999999,0.000000001 300 0.0,0.01 360 0.0,0.01
361 0.0,0.000000001 720 0.0,0.000000001

BCNODE(UY, CONSTANT = 1, ENTITY = "axis", FACTOR=1, CURVE=1)

TMFUNCTION (SET = 2,NPOINTS = 7)

```
0 0,1 0 179 999999,1 0 180 0,76000 0 299 999999,76000 0 300 0,1 0 600 0,1 0
720 0,1 0
```

```
BCFLUX( X, CONSTANT = 1, ENTITY = "inlet", FACTOR=1, CURVE=2 )
```

```
BCNODE( VELOCITY, ZERO, ENTITY = "left" )
```

```
BCNODE( VELOCITY, ZERO, ENTITY = "top" )
```

```
BCNODE( VELOCITY, ZERO, ENTITY = "right" )
```

```
BCNODE( UX, ZERO, ENTITY = "outlet" )
```

```
END
```

```
/
```

```
CREATE( FIPREP,DELETE )
```

```
PARAMETER( LIST )
```

```
CREATE( FISOLV )
```

```
/RUN( FISOLV, FOREGROUND )
```

c Part of subroutine to add rheopectic viscosity

```
SUBROUTINE USRVSC (NELT,NE,NG,VISC,VARI,DVARI,NDFCD,LDOFU,SHP,
```

```
1          DSDX,XYZL,PROP,TIME,NPTS,ndp,MNDP,IERR)
```

```
C
```

```
C  USER DEFINED VISCOSITY
```

```
C
```

```
C  NELT = GLOBAL ELEMENT NUMBER
```

```
C  NE   = LOCAL ELEMENT NUMBER
```

```
C  NG   = GROUP NUMBER
```

```
C  VISC = VISCOSITY
```

```
C  VARI = ARRAY OF SOLUTION VARIABLES AT INTEGRATION POINTS
```

```
C  DVARI = GRADIENTS OF SOLUTION VARIABLES AT INTEGRATION
POINTS
```

```
C  LDOFU = pointer array for accessing vari and dvari information
```

```
C  XYZL = X,Y,Z COORDINATES
```

```
C  SHP   = ELEMENT SHAPE FUNCTIONS
```

```
C  DSDX  = SHAPE FUNCTION DERIVATIVES IN THE X,Y,Z DIRECTION
```



```
C  PROP = USER DEFINED PARAMETERS
C  MNDP = FIRST DIMENSION OF SHAPE FUNCTION MATRICES
C  TIME = TIME
C  NPTS = NUMBER OF POINTS
C
#include "IMPLCT COM"
#include "PARUSR COM"
    DIMENSION VISC(NPTS)
    DIMENSION
SHP(NPTS,MNDP),DSDX(NPTS,NDFCD,MNDP),XYZL(NPTS,NDFCD)
    DIMENSION PROP(*),VARI(NPTS,*),DVARI(NPTS,NDFCD,*),LDOFU(*)
    ZRO = 0 D0
C
C    VISCOSITY OF CMW3 FROM PUBLISHED WORK
C
    VISC=0.0092*TIME*TIME-3.1643*TIME+291.71

    RETURN
END
```

Appendix E

List of data tables

Properties of cancellous bone

Bone marrow viscosity is 0.067 Pa s and the porosity of bone is 85%

E 1 Effect of prosthesis insertion velocity

Bone cement thickness = 10 mm

Prosthesis inserted from 5 to 6 minutes

Table E-1 Penetration for pseudoplastic behaviour of Simplex p® bone cement

<i>Distance from proximal to distal end (mm)</i>	<i>Penetration for prosthesis insertion velocity 5 mm/s (mm)</i>	<i>Penetration for prosthesis insertion velocity 10 mm/s (mm)</i>	<i>Penetration for prosthesis insertion velocity 15 mm/s (mm)</i>	<i>Penetration for prosthesis insertion velocity 20 mm/s (mm)</i>
10	4.3	4.8	5.3	6
20	3.3	3.5	4.2	4.7
30	1.9	2	2	2.2
40	1.9	2	2	2
50	1.6	2	2	2
60	1.2	1.5	1.8	1.8
70	0.8	1	1	1.2
80	0.2	0.4	0.4	0.6

Table E-2 Penetration for rheopectic behaviour of CMW3 bone cement

<i>Distance from proximal to distal end (mm)</i>	<i>Penetration for prosthesis insertion velocity 5 mm/s (mm)</i>	<i>Penetration for prosthesis insertion velocity 10 mm/s (mm)</i>	<i>Penetration for prosthesis insertion velocity 15 mm/s (mm)</i>	<i>Penetration for prosthesis insertion velocity 20 mm/s (mm)</i>
10	3.1	3.1	3.1	3.3
20	2.9	2.9	3	2.9
30	2.5	2.7	3	3
40	2.5	2.4	2.5	2.5
50	2.5	2.4	2.5	2.5
60	2.5	2.4	2.5	2.5
70	2.5	2.4	2.5	2.5
80	1.8	1.9	1.9	1.9
90	1.4	1.3	1.5	1.3
100	0.9	0.9	1	0.9
110	0.3	0.5	0.8	0.8
120	0.3	0.4	0.3	0.5
130	-	-	0.3	-

Table E-3 Penetration for rheopectic behaviour of Zimmer bone cement

<i>Distance from proximal to distal end (mm)</i>	<i>Penetration for prosthesis insertion velocity 5 mm/s (mm)</i>	<i>Penetration for prosthesis insertion velocity 10 mm/s (mm)</i>	<i>Penetration for prosthesis insertion velocity 15 mm/s (mm)</i>	<i>Penetration for prosthesis insertion velocity 20 mm/s (mm)</i>
10	3 2	3 2	3 1	3 1
20	2 9	2 9	3	2 9
30	2 9	2 9	2 9	2 9
40	2 5	2 9	2 9	2 9
50	2 5	2 7	2 8	2 8
60	2 6	2 7	2 8	2 8
70	2 5	2 2	2 4	2 7
80	2	2 1	2	1 9
90	1 3	1	1 1	1 3
100	0 9	0 9	0 9	0 9
110	0 4	0 5	0 4	0 5
120	0 4	0 5	0 4	0 5
130	-	-	-	0 3
140	-	-	-	0 3

Table E-4 Penetration for pseudoplastic behaviour of Zimmer bone cement

<i>Distance from proximal to distal end (mm)</i>	<i>Penetration for prosthesis insertion velocity 5 mm/s (mm)</i>	<i>Penetration for prosthesis insertion velocity 10 mm/s (mm)</i>	<i>Penetration for prosthesis insertion velocity 15 mm/s (mm)</i>	<i>Penetration for prosthesis insertion velocity 20 mm/s (mm)</i>
10	5 1	5 4	5 5	5 8
20	4 7	5 1	5 4	5 7
30	4 2	4 7	5	5 2
40	3 7	4	4 2	4 4
50	2 5	2 7	3	3 1
60	1 8	1 8	2	2 1
70	1 2	1 4	1 5	1 5
80	1 1	1 2	1 1	1 2
90	0 8	0 9	0 9	0 6

Table E-5: Penetration for rheopectic behaviour of CMW3 bone cement

<i>Distance from proximal to distal end (mm)</i>	<i>Penetration for only pressure applied from 3 to 4 min (mm)</i>	<i>Penetration for only pressure applied from 3 to 5 min (mm)</i>	<i>Penetration for only pressure applied from 3 to 6 min (mm)</i>
10	3.6	3.2	3.1
20	2.8	3	2.9
30	2.2	2.3	2.8
40	2.2	2.3	2.4
50	2.2	2.3	2.4
60	2.2	2.3	2.4
70	2.1	2	2.4
80	1.9	1.9	2
90	1.2	1.4	1.4
100	0.9	0.9	1
110	0.4	0.5	0.4
120	0.4	0.5	-

Table E-6: Penetration for rheopectic behaviour of Zimmer bone cement

<i>Distance from proximal to distal end (mm)</i>	<i>Penetration for only pressure applied from 3 to 4 min (mm)</i>	<i>Penetration for only pressure applied from 3 to 5 min (mm)</i>	<i>Penetration for only pressure applied from 3 to 6 min (mm)</i>
10	3.1	3	2.6
20	2.9	3	2.6
30	2.8	2.5	2.6
40	2.5	2.5	2.6
50	2.5	2.5	2.4
60	2.5	2.5	2.4
70	2.5	2.5	2.4
80	1.7	1.8	1.8
90	1.3	1.2	1.3
100	0.7	1	1
110	0.4	0.5	0.4
120	0.3	0.2	-

E.2 Effect of prosthesis insertion time duration

Bone cement thickness = 10 mm

Table E-7: Penetration for pseudoplastic behaviour of Simplex p® bone cement

Distance from proximal to distal end (mm)	Penetration for prosthesis insertion velocity 5 mm/s (mm)		Penetration for prosthesis insertion velocity 10 mm/s (mm)		Penetration for prosthesis insertion velocity 15 mm/s (mm)		Penetration for prosthesis insertion velocity 20 mm/s (mm)	
	0.5 min	1.5 min	0.5 min	1.5 min	0.5 min	1.5 min	0.5 min	1.5 min
10	4	4.8	4.5	5	4.8	5.6	5	6.2
20	3.2	3.5	3.3	3.5	3.8	4.5	4	5
30	1.9	2	1.9	2.2	2	1.9	1.9	2.2
40	1.9	2	1.9	2	2	2.1	1.9	2.1
50	1.6	1.8	1.8	2	2	2	1.9	2.1
60	1.2	1.3	1.4	1.5	1.5	1.8	1.7	1.9
70	0.8	1	0.9	1	1	1.1	0.9	1.2
80	0.2	0.3	0.3	0.5	0.4	0.6	0.3	0.8

Table E-8: Maximum pressure developed in pseudoplastic Simplex P® bone cement.

Time duration of prosthesis insertion velocity (min)	Maximum pressure for different velocity (Pa)			
	5 mm/s	10 mm/s	15 mm/s	20 mm/s
0.5	51830	49980	44470	39550
1	50360	46770	36960	32170
1.5	50230	45240	32250	31880

Table E-9: Penetration for rheopectic behaviour of CMW3 bone cement

Distance from proximal to distal end (mm)	Penetration for prosthesis insertion velocity 5 mm/s (mm)		Penetration for prosthesis insertion velocity 10 mm/s (mm)		Penetration for prosthesis insertion velocity 15 mm/s (mm)		Penetration for prosthesis insertion velocity 20 mm/s (mm)	
	0.5 min	1.5 min	0.5 min	1.5 min	0.5 min	1.5 min	0.5 min	1.5 min
10	3.2	3.5	3.3	3.1	3.2	3	3.2	3
20	2.8	2.9	2.8	2.9	3	2.9	3	2.8
30	2.4	3	2.4	2.9	2.8	2.9	2.7	2.8
40	2.4	2.6	2.4	2.3	2.4	2.5	2.7	2.8
50	2.4	2.6	2.4	2.3	2.4	2.5	2.7	2.8
60	2.4	2.6	2.4	2.3	2.4	2.5	2.7	2.8
70	2.4	2.6	2.4	2.3	2.4	2.3	2.7	2.6
80	1.8	2	1.8	2	1.8	1.9	1.9	1.8
90	1.4	1.4	1.3	1.2	1.2	1.3	1.3	1.2
100	0.9	0.9	0.8	0.9	0.9	0.9	0.9	0.6
110	0.8	0.5	0.3	0.4	0.4	0.8	0.5	0.3
120	0.6	0.4	0.2	0.4	0.4	0.5	0.5	0.3

Table E-10 Maximum pressure developed in rheopectic CMW3 bone cement for different prosthesis insertion times

<i>Prosthesis insertion time (min)</i>	<i>Maximum pressure for different velocity (Pa)</i>			
	<i>5 mm/s</i>	<i>10 mm/s</i>	<i>15 mm/s</i>	<i>20 mm/s</i>
0 5	73220	73280	72830	73150
1	72840	72790	72130	72320
1 5	72710	72510	71850	71780

Table E-11 Penetration for rheopectic behaviour of Zimmer bone cement

<i>Distance from proximal to distal end (mm)</i>	<i>Penetration for prosthesis insertion velocity 5 mm/s (mm)</i>		<i>Penetration for prosthesis insertion velocity 10 mm/s (mm)</i>		<i>Penetration for prosthesis insertion velocity 15 mm/s (mm)</i>		<i>Penetration for prosthesis insertion velocity 20 mm/s (mm)</i>	
	<i>0 5 min</i>	<i>1 5 min</i>	<i>0 5 min</i>	<i>1 5 min</i>	<i>0 5 min</i>	<i>1 5 mm</i>	<i>0 5 min</i>	<i>1 5 min</i>
10	3 2	3 1	3 2	3 2	3 3	3 2	3 2	3 2
20	3	2 8	2 9	2 9	3	3	2 8	3
30	2 9	2 6	2 9	2 9	3	3	2 9	3
40	2 9	2 5	2 9	2 9	2 7	3	2 4	3
50	2 9	2 5	2 6	2 7	2 7	3	2 4	3
60	2 5	2 5	2 6	2 7	2 7	2 9	2 4	3
70	2 3	2 4	2 6	2 4	2 7	2 5	2 4	2 6
80	1 8	2	2 1	1 9	1 8	2	1 9	2 1
90	1	1 2	1 2	1 3	1 4	1 3	1 3	1 3
100	0 5	0 9	0 9	0 9	1	0 9	0 9	1
110	-	0 4	0 5	0 5	0 5	0 4	0 5	0 4
120	-	0 4	-	0 3	0 3	0 3	0 5	0 4
130	-	-	-	-	-	-	-	0 2
140	-	-	-	-	-	-	-	0 2

Table E-12 Maximum pressure developed in rheopectic Zimmer bone cement at different time duration of different prosthesis insertion velocity

<i>Prosthesis insertion time (min)</i>	<i>Maximum pressure for different velocity (Pa)</i>			
	<i>5 mm/s</i>	<i>10 mm/s</i>	<i>15 mm/s</i>	<i>20 mm/s</i>
0 5	75880	75880	75910	75800
1	75810	75680	75530	75310
1 5	75780	75570	75350	75100

Table E-13 Penetration for pseudoplastic behaviour of Zimmer bone cement

<i>Distance from proximal to distal end (mm)</i>	<i>Penetration for prosthesis insertion velocity 5 mm/s (mm)</i>		<i>Penetration for prosthesis insertion velocity 10 mm/s (mm)</i>		<i>Penetration for prosthesis insertion velocity 15 mm/s (mm)</i>		<i>Penetration for prosthesis insertion velocity 20 mm/s (mm)</i>	
	0 5 min	1 5 min	0 5 min	1 5 min	0 5 min	1 5 min	0 5 min	1 5 min
10	5	5 2	5 1	5 6	5 1	6 1	5 5	6 5
20	4 6	5 1	4 7	5 4	4 9	5 8	5	6
30	4 1	4 6	4 3	5	4 2	5 2	4 5	5 8
40	3 1	4	3 5	4 3	3 9	4 3	3 8	5
50	2 4	2 7	2 4	3	2 5	3 1	2 5	3 2
60	1 5	2	1 8	2	1 5	2 2	1 7	2
70	1 2	1 2	1 4	1 9	1 3	1 7	1 2	1 6
80	0 9	1	0 9	1 5	1	1 3	1	1 2
90	0 9	1	0 8	1	0 8	1	0 5	0 8

Table E-14 Maximum pressure developed in pseudoplastic Zimmer bone at different time duration of different prosthesis insertion velocity

<i>Prosthesis insertion time (min)</i>	<i>Maximum pressure for different velocity (Pa)</i>			
	<i>5 mm/s</i>	<i>10 mm/s</i>	<i>15 mm/s</i>	<i>20 mm/s</i>
0 5	65360	64700	62770	60980
1	63390	61100	57880	55510
1 5	61910	57810	55040	51910

E.3 Effect of bone cement thickness

Bone cement thickness = 8 mm

Prosthesis inserted from 5 to 6 min

Table E-15 Penetration for pseudoplastic behaviour of Simplex p® bone cement

<i>Distance from proximal to distal end (mm)</i>	<i>Penetration for prosthesis insertion velocity 5 mm/s (mm)</i>	<i>Penetration for prosthesis insertion velocity 10 mm/s (mm)</i>	<i>Penetration for prosthesis insertion velocity 15 mm/s (mm)</i>	<i>Penetration for prosthesis insertion velocity 20 mm/s (mm)</i>
10	7	7	7	7
20	7	7	7	7
30	7	7	7	7
40	3 3	3 8	3 8	7
50	2 8	3 2	3 3	4 3
60	2	2 9	3	3 8
70	1 8	2 9	2 9	3 1
80	1 2	2 1	2 2	3

Table E-16 Penetration for pseudoplastic behaviour of Zimmer bone cement

<i>Distance from proximal to distal end (mm)</i>	<i>Penetration for prosthesis insertion velocity 5 mm/s (mm)</i>	<i>Penetration for prosthesis insertion velocity 10 mm/s (mm)</i>	<i>Penetration for prosthesis insertion velocity 15 mm/s (mm)</i>	<i>Penetration for prosthesis insertion velocity 20 mm/s (mm)</i>
10	7	7	7	7
20	7	7	7	7
30	7	7	7	7
40	5 5	5 2	5 8	6
50	3 1	3 2	3 4	3 6
60	2 2	2 4	2 6	3 4
70	1 8	2	2	2 4
80	1 8	1 8	1 8	1 8
90	1	1	1	1 2

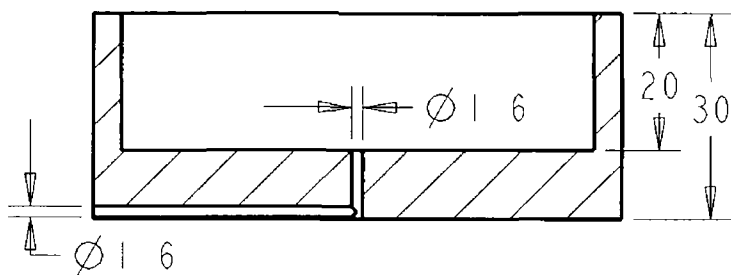
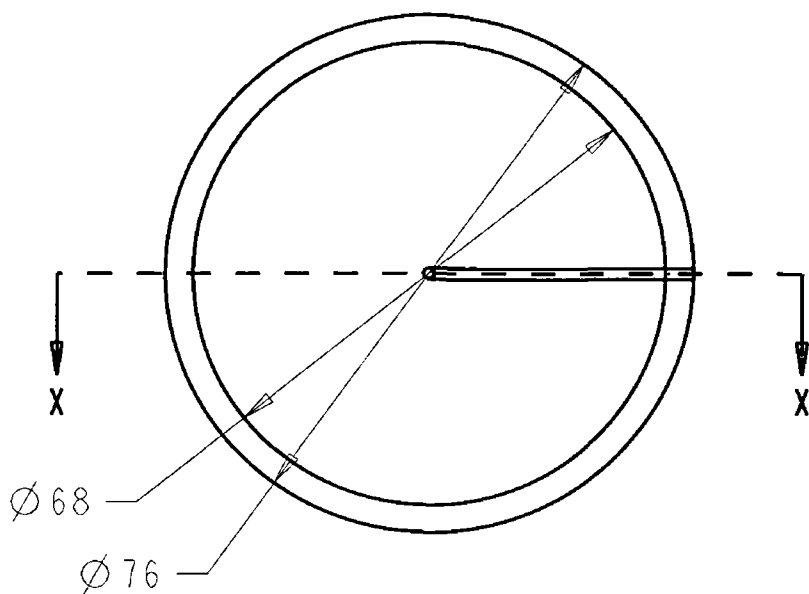
Appendix F

List of Publications

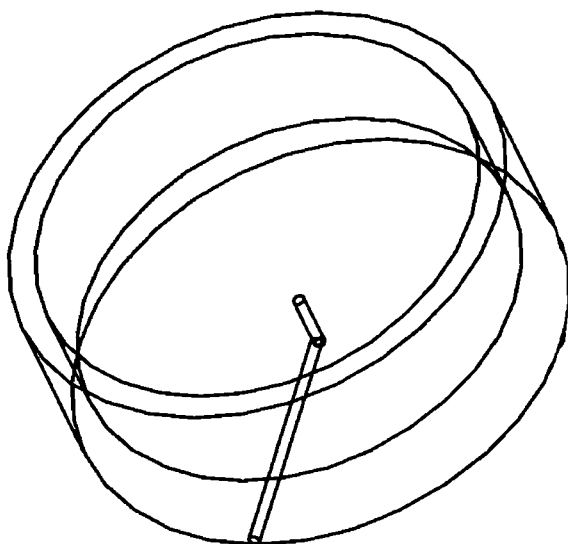
Conference paper

- 1 M M Rahman, A G Olabi and M S J Hashmi “Thermal properties of curing acrylic bone cement mixed at different vacuum level” ICEM12- 12th International Conference on Experimental Mechanics, 29 August - 2 September, 2004 Politecnico di Bari, Italy Page in abstract volume 82-83
- 2 M M Rahman, A G Olabi and M S J Hashmi “Finite element modelling of rheological property of curing PMMA bone cement analysis of cement flow in total hip replacement” accepted for the conference of AMPT 2006, Jul 30-Aug 3, 2006, Las Vegas, USA

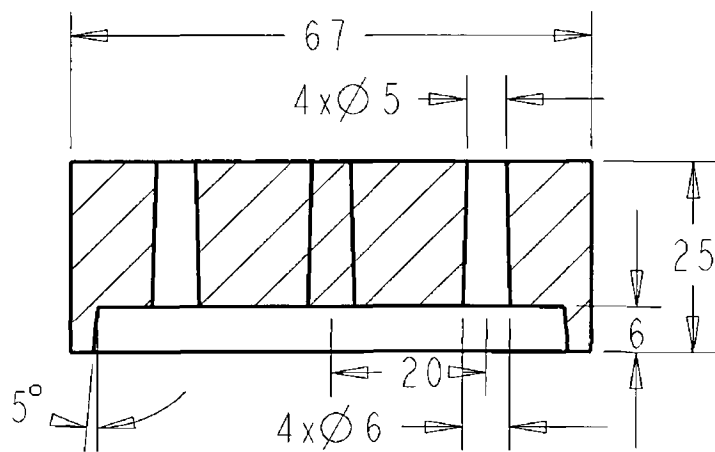
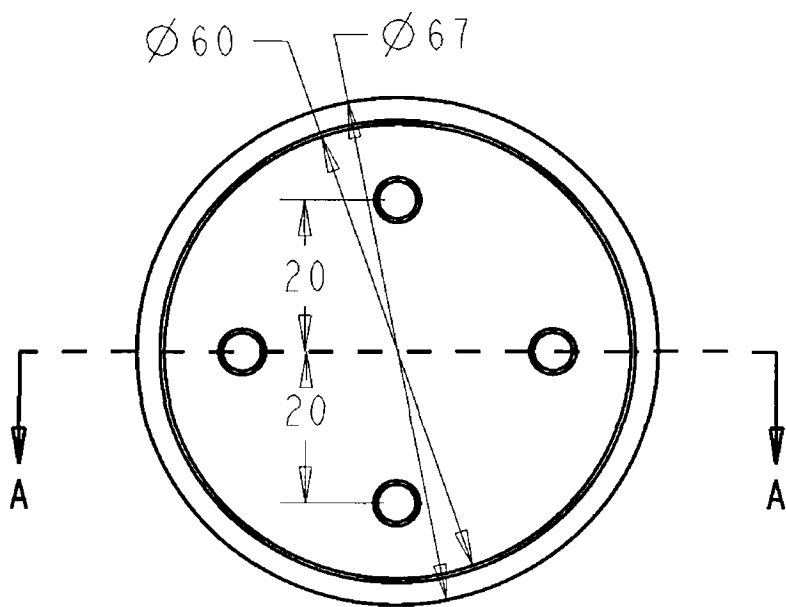
Appendix G



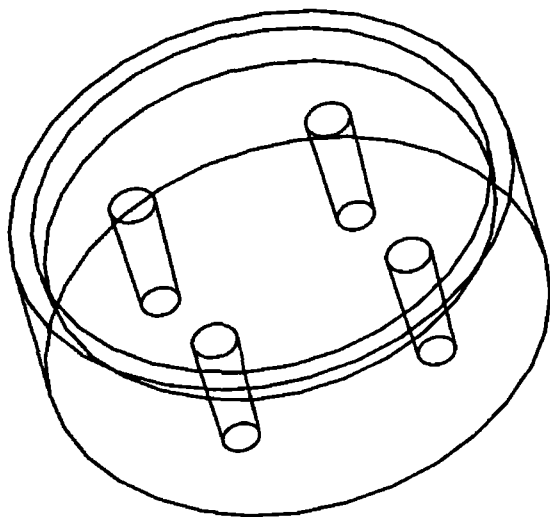
SECTION X-X
SCALE 1 000



Designer	Mafizur Rahman	Scale	1 : 000
Material	polytetrafluoroethylene	Date	01/09/2005
Standard	ASTM F 451	Note	
Part Name	Exothermic Heat Mold	Dublin City University School of Mechanical & Manufacturing Engineering	
Project	PhD		
Part No	01		



SECTION A-A
SCALE 1 000



Designer	Mafizur Rahman	Scale	1 000
Material	polytetrafluoroethylene	Date	01/09/2005
Standard	ASTM F 451	Note	
Part Name	Exothermic Heat Mold	Dublin City University School of Mechanical & Manufacturing Engineering	
Project	PhD		
Part No	02		